

**Attachment 10**

**Holtec Report HI-2043149 (Non-Proprietary)**

**Note Regarding Pagination:**

The documents included in this enclosure are controlled by the page-count indicated in the Table of Contents below. To preserve the integrity of the documents as suitable for use by the NRC Staff, the header and pagination notations (such as appears on this page) are not used on every page of Attachment 10.

**Table of Contents**

| <b><u>Description</u></b>     | <b><u>Pages</u></b> |
|-------------------------------|---------------------|
| Table of Contents (this page) | 1                   |
| HI-2043149 (Non-Proprietary)  | <u>209</u>          |
| Total pages this attachment   | 210                 |



Holtec Center, 555 Lincoln Drive West, Marlton, NJ 08053

Telephone (856) 797-0900

Fax (856) 797-0909

**BORAFLEX REMEDY**

at

**TURKEY POINT NUCLEAR PLANT**

for

***FPL***

**HOLTEC PROJECT NO. 1322**

**HOLTEC REPORT: HI-2043149**

**REPORT CATEGORY: A**

**REPORT CLASS: SAFETY RELATED**

**COMPANY PRIVATE**

This document contains proprietary information which is the property of Holtec International and its Client. The proprietary information in the text has been denoted by backshading or by the addition of a "Holtec Proprietary" note in instances where entire pages contain proprietary information. This document is to be used only in connection with the performance of work by Holtec International or its designated subcontractors. Reproduction, publication or presentation, in whole or in part, for any other purpose by any party other than the Client is expressly forbidden.

# HOLTEC INTERNATIONAL

DOCUMENT NUMBER: HI-2043149

PROJECT NUMBER: 1322

## DOCUMENT ISSUANCE AND REVISION STATUS

DOCUMENT NAME: BORAFLEX REMEDY AT TURKEY POINT  
HI-2043149

DOCUMENT CATEGORY:  GENERIC  PROJECT SPECIFIC

| No. | Document Portion†† | REVISION No. <u>3</u> |               |        | REVISION No. _____ |               |       | REVISION No. _____ |               |       |
|-----|--------------------|-----------------------|---------------|--------|--------------------|---------------|-------|--------------------|---------------|-------|
|     |                    | Author's Initials     | Date Approved | VIR #  | Author's Initials  | Date Approved | VIR # | Author's Initials  | Date Approved | VIR # |
| 1.  | Chap 1             | EB                    | 9/23/05       | 37662  |                    |               |       |                    |               |       |
| 2.  | Chap 2             | EB                    | 9/23/05       | 637220 |                    |               |       |                    |               |       |
| 3.  | Chap 3             | EB                    | 9/23/05       | 368707 |                    |               |       |                    |               |       |
| 4.  | Chap 4             | SPA                   | 9/26/05       | 625024 |                    |               |       |                    |               |       |
| 5.  | Chap 5             | ER                    | 9/23/05       | 348717 |                    |               |       |                    |               |       |
| 6.  | Chap 6             | CB                    | 9/23/05       | 392372 |                    |               |       |                    |               |       |
| 7.  | Chap 7             | CB                    | 9/23/05       | 889472 |                    |               |       |                    |               |       |
| 8.  | Chap 8             | EB                    | 9/23/05       | 91875  |                    |               |       |                    |               |       |
| 9.  | Chap 9             | EB                    | 9/23/05       | 679937 |                    |               |       |                    |               |       |
| 10. | Chap 10            | EB                    | 9/23/05       | 61623  |                    |               |       |                    |               |       |

†† Chapter or section number.

# HOLTEC INTERNATIONAL

DOCUMENT NUMBER: HI-2043149

PROJECT NUMBER: 1322

## DOCUMENT CATEGORIZATION

In accordance with the Holtec Quality Assurance Manual and associated Holtec Quality Procedures (HQPs), this document is categorized as a:

- Calculation Package<sup>3</sup> (Per HQP 3.2)       Technical Report (Per HQP 3.2)(Such as a Licensing Report)
- Design Criterion Document (Per HQP 3.4)       Design Specification (Per HQP 3.4)
- Other (Specify):

## DOCUMENT FORMATTING

The formatting of the contents of this document is in accordance with the instructions of HQP 3.2 or 3.4 except as noted below:

## DECLARATION OF PROPRIETARY STATUS

- Nonproprietary       Holtec Proprietary       Privileged Intellectual Property (PIP)

Documents labeled Privileged Intellectual Property contain extremely valuable intellectual/commercial property of Holtec International. They cannot be released to external organizations or entities without explicit approval of a company corporate officer. The recipient of Holtec's proprietary or Top Secret document bears full and undivided responsibility to safeguard it against loss or duplication.

### Notes:

1. This document has been subjected to review, verification and approval process set forth in the Holtec Quality Assurance Procedures Manual. Password controlled signatures of Holtec personnel who participated in the preparation, review, and QA validation of this document are saved in the N-drive of the company's network. The Validation Identifier Record (VIR) number is a random number that is generated by the computer after the specific revision of this document has undergone the required review and approval process, and the appropriate Holtec personnel have recorded their password-controlled electronic concurrence to the document.
2. A revision to this document will be ordered by the Project Manager and carried out if any of its contents is materially affected during evolution of this project. The determination as to the need for revision will be made by the Project Manager with input from others, as deemed necessary by him.
3. Revisions to this document may be made by adding supplements to the document and replacing the "Table of Contents", this page and the "Revision Log".

| <b>SUMMARY OF REVISIONS</b>   |                  |
|---|------------------|
| <b>Revision 3 contains the following pages:</b>                           |                  |
| COVER PAGE  | 1 page           |
| DOCUMENT ISSUANCE AND REVISION STATUS                                     | 2 pages          |
| SUMMARY OF REVISIONS  | 1 page           |
| TABLE OF CONTENTS   | 5 pages          |
| 1.0 INTRODUCTION  | 6 pages          |
| 2.0 RACK MODIFICATION DESCRIPTION, PRINCIPAL DESIGN CRITERIA & REFERENCES | 12 pages         |
| 3.0 MATERIAL CONSIDERATIONS   | 8 pages          |
| 4.0 CRITICALITY SAFETY ANALYSES   | 94 pages         |
| 5.0 THERMAL-HYDRAULIC CONSIDERATIONS                                      | 11 pages         |
| 6.0 EXISTING RACK STRUCTURAL/SEISMIC CONSIDERATIONS                       | 47 pages         |
| 7.0 STRUCTURAL INTEGRITY CONSIDERATIONS FOR THE FUEL POOL STRUCTURE       | 3 pages          |
| 8.0 RADIOLOGICAL EVALUATION   | 6 pages          |
| 9.0 INSTALLATION AND OPERATION  | 6 pages          |
| 10.0 ENVIRONMENTAL AND COST / BENEFIT ASSESSMENT                          | 7 pages          |
| <b>TOTAL</b>  | <b>209 pages</b> |

Revision 1 incorporates client editorial comments in Sections 1, 2, 3, 4, 7, 8, 9, and 10.

Revision 2 incorporates client editorial comments in all Sections.

Revision 3 incorporates client editorial comments in all Sections.

|          |  |      |
|----------|--|------|
| 1.0      | INTRODUCTION .....   | 1-1  |
| 1.1      | References.....  | 1-4  |
| 2.0      | RACK MODIFICATION DESCRIPTION, PRINCIPAL DESIGN<br>CRITERIA & REFERENCES ..... | 2-1  |
| 2.1      | Introduction.....  | 2-1  |
| 2.2      | Summary of Principal Design Criteria.....                                      | 2-1  |
| 2.3      | Applicable Codes and Standards .....   | 2-4  |
| 2.4      | Quality Assurance Program .....  | 2-5  |
| 2.5      | Metamic Insert Mechanical Design .....   | 2-7  |
| 3.0      | MATERIAL CONSIDERATIONS .....  | 3-1  |
| 3.1      | Introduction.....  | 3-1  |
| 3.2      | Materials Used in Insert.....  | 3-1  |
| 3.3      | Neutron Absorbing Material .....   | 3-1  |
| 3.3.1    | Metamic Insert Assembly .....  | 3-1  |
| 3.3.2    | Characteristics of Metamic .....   | 3-2  |
| 3.4      | Compatibility with Environment .....   | 3-4  |
| 3.5      | Potential for Abrasion .....   | 3-4  |
| 3.6      | References.....  | 3-7  |
| 4.0      | CRITICALITY SAFETY ANALYSES .....  | 4-1  |
| 4.1      | Introduction and Summary .....   | 4-1  |
| 4.2      | Acceptance Criteria.....   | 4-7  |
| 4.3      | Assumptions.....   | 4-8  |
| 4.4      | Design and Input Data .....  | 4-12 |
| 4.4.1    | Fuel Assembly and Fuel Insert Specification .....                              | 4-12 |
| 4.4.2    | Storage Rack Specification .....   | 4-13 |
| 4.4.3    | Spent Fuel Pool Specification.....   | 4-13 |
| 4.5      | Methodology .....  | 4-13 |
| 4.6      | Analysis.....  | 4-16 |
| 4.6.1    | Bounding BPRAs Inserts and Fuel Assemblies .....                               | 4-17 |
| 4.6.2    | Moderator Temperature Effect .....   | 4-19 |
| 4.6.3    | Pool Water Temperature Effects.....  | 4-20 |
| 4.6.4    | Manufacturing Tolerances .....   | 4-21 |
| 4.6.5    | Temperature Bias and Uncertainties at Higher Soluble Boron Levels .....        | 4-22 |
| 4.6.6    | Uncertainty in Depletion Calculations and Burnup Records.....                  | 4-23 |
| 4.6.7    | Isotopic Compositions .....  | 4-23 |
| 4.6.8    | Eccentric Fuel Assembly Positioning .....                                      | 4-24 |
| 4.6.9    | Reactivity Effect of Axial Burnup and Enrichment Distribution .....            | 4-24 |
| 4.6.10   | Calculation of Burnup vs. Enrichment Curves .....                              | 4-27 |
| 4.6.11   | Interfaces.....  | 4-30 |
| 4.6.11.1 | Case to Case Interfaces in the Region 2 Area of the Pool .....                 | 4-30 |
| 4.6.11.2 | Case to Case Interfaces in the Region 1 Area of the Pool .....                 | 4-31 |
| 4.6.11.3 | Region 1 to Region 2 Interface .....   | 4-32 |
| 4.6.11.4 | Cells Facing the Pool Wall in Region 2 Racks .....                             | 4-33 |
| 4.6.11.5 | Configuration During Loading and Unloading of Assemblies .....                 | 4-34 |
| 4.6.11.6 | Interface with the Cask Area Rack .....  | 4-35 |

|            |   |      |
|------------|---|------|
| 4.6.12     | Soluble Boron Concentration for Maximum $K_{eff}$ of 0.95 ..... | 4-35 |
| 4.6.13     | Abnormal and Accident Conditions.....                           | 4-36 |
| 4.6.13.1   | Temperature and Water Density Effects.....                      | 4-36 |
| 4.6.13.2   | Dropped Assembly - Horizontal.....                              | 4-36 |
| 4.6.13.3   | Dropped Assembly - Vertical .....                               | 4-37 |
| 4.6.13.4   | Abnormal Location of a Fuel Assembly .....                      | 4-37 |
| 4.6.13.4.1 | Misloaded Fresh Fuel Assembly.....                              | 4-37 |
| 4.6.13.4.2 | Mislocated Fresh Fuel Assembly.....                             | 4-38 |
| 4.6.13.5   | Removed Insert or RCCA.....                                     | 4-38 |
| 4.6.14     | Postulated Damage to Inserts.....                               | 4-38 |
| 4.6.15     | Fuel Rod Baskets .....  | 4-39 |
| 4.7        | References.....   | 4-40 |

## Appendix A Benchmark Calculations

|         |  |      |
|---------|--|------|
| 5.0     | THERMAL-HYDRAULIC CONSIDERATIONS.....                    | 5-1  |
| 5.1     | Introduction.....  | 5-1  |
| 5.2     | Maximum SFP Local Water Temperature.....                 | 5-2  |
| 5.3     | Fuel Rod Cladding Temperature.....                       | 5-5  |
| 5.4     | Results.....   | 5-6  |
| 5.5     | References.....  | 5-6  |
| 6.0     | EXISTING RACK STRUCTURAL/SEISMIC CONSIDERATIONS .....    | 6-1  |
| 6.1     | Introduction.....  | 6-1  |
| 6.2     | Overview of Rack Structural Analysis Methodology .....   | 6-1  |
| 6.2.1   | Background of Analysis Methodology .....                 | 6-2  |
| 6.3     | Description of Racks.....                                | 6-4  |
| 6.3.1   | Fuel and Metamic Insert Weights.....                     | 6-5  |
| 6.4     | Synthetic Time-Histories .....                           | 6-5  |
| 6.5     | WPMR Methodology.....                                    | 6-6  |
| 6.5.1   | Model Details for Spent Fuel Racks .....                 | 6-7  |
| 6.5.1.1 | Assumptions.....   | 6-7  |
| 6.5.1.2 | Element Details .....                                    | 6-8  |
| 6.5.2   | Fluid Coupling Effect .....                              | 6-9  |
| 6.5.2.1 | Multi-Body Fluid Coupling Phenomena.....                 | 6-10 |
| 6.5.3   | Stiffness Element Details.....                           | 6-11 |
| 6.5.4   | Coefficients of Friction .....                           | 6-12 |
| 6.5.5   | Governing Equations of Motion .....                      | 6-13 |
| 6.6     | Structural Evaluation of Spent Fuel Rack Design .....    | 6-14 |
| 6.6.1   | Kinematic and Stress Acceptance Criteria.....            | 6-14 |
| 6.6.2   | Stress Limit Evaluation.....                             | 6-15 |
| 6.6.3   | Dimensionless Stress Factors.....                        | 6-18 |
| 6.6.4   | Loads and Loading Combinations for Spent Fuel Racks..... | 6-19 |
| 6.7     | Parametric Simulations .....                             | 6-20 |
| 6.8     | Time History Simulation Results.....                     | 6-22 |
| 6.8.1   | Rack Displacements.....                                  | 6-22 |
| 6.8.2   | Pedestal Vertical Forces.....                            | 6-23 |
| 6.8.3   | Pedestal Friction Forces.....                            | 6-23 |

|         |  |      |
|---------|--|------|
| 6.8.4   | Rack Impact Loads .....  | 6-23 |
| 6.8.4.1 | Impacts External to the Rack .....                                       | 6-24 |
| 6.8.4.2 | Impacts Internal to the Rack .....                                       | 6-24 |
| 6.9     | Rack Structural Evaluation .....   | 6-25 |
| 6.9.1   | Rack Stress Factors .....  | 6-25 |
| 6.9.2   | Pedestal Thread Shear Stress .....                                       | 6-26 |
| 6.9.3   | Local Stress Due to Impacts .....  | 6-26 |
| 6.9.4   | Weld Stresses .....  | 6-27 |
| 6.10    | Level A Evaluation .....   | 6-29 |
| 6.11    | Hydrodynamic Loads on the Pool Walls .....                               | 6-29 |
| 6.12    | Local Stress Considerations .....  | 6-30 |
| 6.12.1  | Cell Wall Buckling .....   | 6-30 |
| 6.13    | Conclusion .....   | 6-30 |
| 6.14    | References .....   | 6-31 |
| 7.0     | STRUCTURAL INTEGRITY CONSIDERATIONS FOR THE FUEL POOL<br>STRUCTURE ..... | 7-1  |
| 7.1     | Introduction .....   | 7-1  |
| 7.2     | References .....   | 7-3  |
| 8.0     | RADIOLOGICAL EVALUATION .....  | 8-1  |
| 8.1     | Fuel Handling Accident .....   | 8-1  |
| 8.2     | Solid Radwaste .....   | 8-1  |
| 8.3     | Gaseous Release .....  | 8-2  |
| 8.4     | Personnel Exposures .....  | 8-2  |
| 8.5     | Anticipated Exposures During the Addition of Metamic Inserts .....       | 8-3  |
| 8.6     | References .....   | 8-5  |
| 9.0     | INSTALLATION AND OPERATION .....   | 9-1  |
| 9.1     | Metamic Insert Installation and Handling .....                           | 9-1  |
| 9.2     | Operation .....  | 9-2  |
| 9.2.1   | Seismic Loads .....  | 9-3  |
| 9.2.2   | Movement Loads .....   | 9-3  |
| 9.2.2.1 | Insertion/Withdrawal Loads .....   | 9-4  |
| 9.2.2.2 | Horizontal Movement Loads .....  | 9-4  |
| 9.3     | Safety, Health Physics, and ALARA Methods .....                          | 9-5  |
| 9.3.1   | Safety .....   | 9-5  |
| 9.3.2   | Health Physics .....   | 9-5  |
| 9.3.3   | ALARA .....  | 9-5  |
| 9.4     | Radwaste Material Control .....  | 9-6  |
| 10.0    | ENVIRONMENTAL AND COST / BENEFIT ASSESSMENT .....                        | 10-1 |
| 10.1    | Introduction .....   | 10-1 |
| 10.2    | Imperative for Metamic Inserts .....                                     | 10-1 |
| 10.3    | Appraisal of Alternative Options .....                                   | 10-1 |
| 10.3.1  | Alternative Option Cost Summary .....                                    | 10-5 |

|      |                                   |      |
|------|-----------------------------------|------|
| 10.4 | Cost Estimate .....               | 10-5 |
| 10.5 | Resource Commitment.....          | 10-6 |
| 10.6 | Environmental Consideration ..... | 10-6 |
| 10.7 | References.....                   | 10-6 |

## **Figures**

- 1.1.1 Unit 3 Spent Fuel Pool Layout
- 1.1.2 Unit 4 Spent Fuel Pool Layout
  
- 2.5.1 Metamic Insert
  
- 4.1.1 Loading Patterns Near Pool Walls in Region 2 Racks with Case 3 Fuel on Rack Periphery
- 4.4.1 Schematic View of Region 1 Cell
- 4.4.2 Schematic View of Region 2 Cell with Insert
- 4.6.1 Example of Interface Between Case 1 and Case 3
- 4.6.2 Example of Loading Steps for a Single Assembly in Case 3
  
- 5.2.1 CFD Model Isometric View
- 5.4.1 CFD Model with Converged Temperature Contours
  
- 6.4.1 Time History Accelerogram – E/W SSE @ 2% Damping
- 6.4.2 Time History Accelerogram – N/S SSE @ 2% Damping
- 6.4.3 Time History Accelerogram – Vertical SSE @ 2% Damping
- 6.5.1 Schematic of the Dynamic Model of a Single Rack Module Used in DYNARACK
- 6.5.2 Fuel-to-Rack Gap/Impact Elements at Level of Rattling Mass
- 6.5.3 Two Dimensional View of the Spring-Mass Simulation
- 6.5.4 Rack Degrees-of-Freedom with Shear and Bending Springs
- 6.5.5 Rack Periphery Gap/Impact Elements
- 6.12.1 Loading on Rack Wall

## 1.0 INTRODUCTION

The Turkey Point Nuclear Plant (Units 3 and 4) is operated by Florida Power and Light Company (FPL). The plant is located on the shore of Biscayne Bay in Miami-Dade County, Florida, about 25 miles south of Miami, Florida. The plant consists of two Westinghouse-supplied pressurized water reactors (PWR). Unit 3 has been in commercial operation since 1972 and Unit 4 since 1973. Each unit uses a spent fuel pool (SFP) for the storage of irradiated nuclear fuel in order to maintain a subcritical array, remove decay heat and provide radiation shielding. The Spent Fuel Pool is also referred to as the "Spent Fuel Pit" in the plant UFSAR and Technical Specifications.

Each of the Unit 3 and Unit 4 spent fuel pools are currently licensed for 1535 fuel assembly storage locations, arranged in 12 distinct freestanding rack modules and one cask area rack. Both units feature the so-called Distinct Zone Two Region (DZTR) rack design. Region 1 utilizes a flux-trap approach and was designed to accommodate fresh fuel while Region 2 has a smaller center-to-center pitch and was designed for burned fuel. The existing rack modules (except the cask area racks) use Boraflex as the neutron absorber material. In this report, the term "existing racks" refers to Boraflex-poisoned racks and excludes the Boral cask area racks.

The criticality analysis of record for the existing storage racks in each spent fuel pool credits the presence of Boraflex, and it includes partial credit for the presence of soluble boron during normal operation, as permitted by 10CFR 50.68(b)(4). The continuing degradation of Boraflex will reduce available margin to criticality limits such that certain specific spent fuel storage locations may require additional administrative controls to remain operable or be precluded from use. In recognition of the fact that Boraflex may experience further degradation, FPL is initiating a program to eliminate Turkey Point's reliance on Boraflex as a credited neutron absorber. The fuel rack enhancement program proposed by this application intends to rely on Metamic™ inserts for reactivity control. Crediting Metamic™ as the neutron absorber, along with optimized fuel storage patterns and other reactivity reduction techniques, provides a robust means of ensuring that the current inventory of stored irradiated fuel can be accommodated without losing spent fuel storage locations and while maintaining an acceptable neutron multiplication factor. The Boraflex panels will remain in place providing additional

(not credited) neutron absorption. The method for storage cell criticality enhancement, proposed in this license amendment request, is disclosed in several U.S. Patents [1.1.1-1.1.4].

The current maximum allowable enrichment, 4.5 weight percent (w/o) U-235, will be retained as the Technical Specification limit. The fuel rack enhancement program will be implemented in conjunction with the placement of a Cask Area rack into each unit. The Cask Area rack has been designed to store fresh unburned fuel enriched up to 4.5 w/o U-235. The Cask Area rack, therefore, will be utilized to store the most reactive fuel during a full core offload. Generally, the Cask Area rack is not discussed in this report because it is not affected by the fuel rack enhancement program. Calculations have shown that the Cask Area rack has no reactivity coupling with the existing racks in the main pool .

The fuel storage rack arrays for Units 3 and 4 are shown in the plan views provided by Figures 1.1.1 and 1.1.2, respectively. The proposed rack enhancement program does not require any physical modifications to the existing storage rack arrays other than insertion of the Metamic™ panels into certain storage cells.

This report documents the design and analyses performed to demonstrate that the new inserts and existing racks for both Units 3 & 4 meet all governing requirements of the applicable codes and standards, in particular, "OT Position for Review and Acceptance of Spent Fuel Storage and Handling Applications", USNRC (1978) and 1979 Addendum thereto [1.1.5]. The new inserts introduce additional mass in the storage racks and greater coolant flow restriction in individual storage cells. These changes have been addressed by performing appropriate evaluations. Summaries of the results of these evaluations are presented within this report.

Sections 2 and 3 of this report provide a brief abstract of the design and material information for the existing racks and a detailed description of the new Metamic™ inserts. Section 4 provides a summary of the methods and results of criticality evaluations performed for the existing racks considering various fuel storage configurations with and without the new borated inserts. The criticality safety analysis requires that the effective neutron multiplication factor ( $k_{eff}$ ) be less than or equal to 0.95 when the

storage racks are fully loaded with fuel meeting appropriate burnup, cooling time, and storage pattern restrictions and the pool is flooded with borated water at a temperature corresponding to the highest reactivity. In addition, it is demonstrated that  $k_{\text{eff}}$  is less than 1.0 under the assumed accident of the loss of soluble boron in the pool water, i.e. assuming unborated water in the spent fuel pool. The maximum calculated neutron multiplication factors include a margin for uncertainty in reactivity calculations, consider manufacturing tolerances, and are calculated with a 95% probability at a 95% confidence level. The criticality safety analysis sets the requirements on the Metamic™ panel length and the amount of  $B^{10}$  per unit area (i.e., areal density) of the borated insert.

Thermal-hydraulic considerations (Section 5.0) require that local boiling not occur in the racks, and that the pool bulk temperature remain within the 150°F limit prescribed in the UFSAR. This ensures that pool structural strength, operational, and regulatory requirements are satisfied.

Rack module structural analyses require that the primary stresses in the rack module structure remain below the ASME B&PV Code (Subsection NF) [1.1.6] allowable limits. Demonstrations of seismic and structural adequacy are presented in Section 6.0. The structural qualification criteria also require that the array of stored fuel remain subcritical under all postulated accident scenarios.

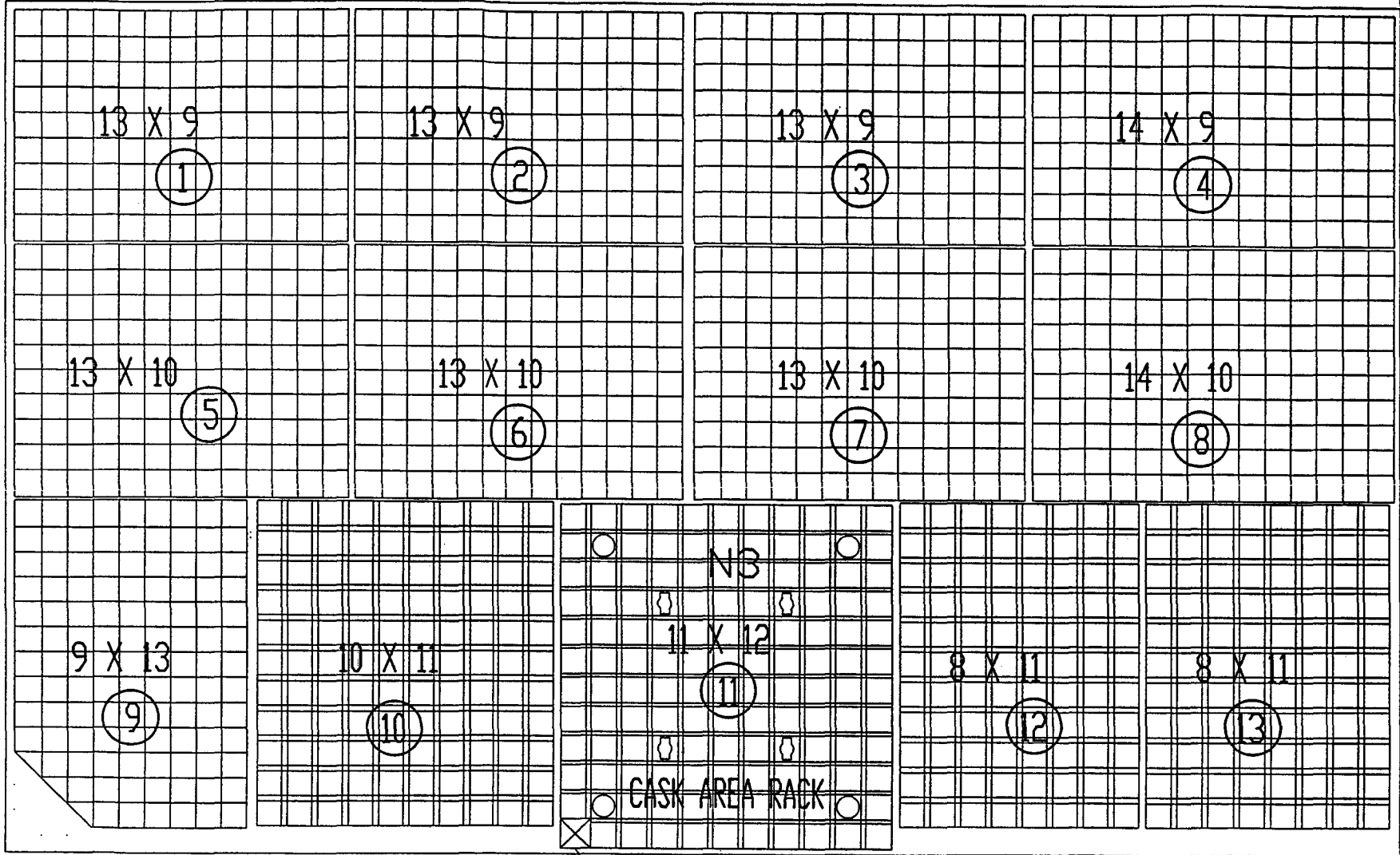
Section 7 discusses the evaluation of the Spent Fuel Pool structure to ensure it can withstand the increased rack loads resulting from the slight increase in the dead load represented by the addition of the Metamic™ inserts. Radiological consequences of the proposed fuel rack enhancement are documented in Section 8. Section 9 discusses the salient considerations in the installation of the new borated inserts. Section 10 discusses a cost/benefit and environmental assessment to establish the acceptability of the fuel rack enhancement program.

All computer programs utilized to perform the analyses documented in this report are benchmarked and verified. Holtec International has utilized these programs in numerous license applications over the past decade.

The analyses presented herein demonstrate that when fuel storage racks at Turkey Point are enhanced with Metamic™ inserts, the resulting modules possess wide margins of safety with respect to all considerations specified in the OT Position Paper [1.1.5], namely, nuclear subcriticality, thermal-hydraulic safety, seismic and structural adequacy, radiological compliance, and mechanical integrity.

## 1.1 References

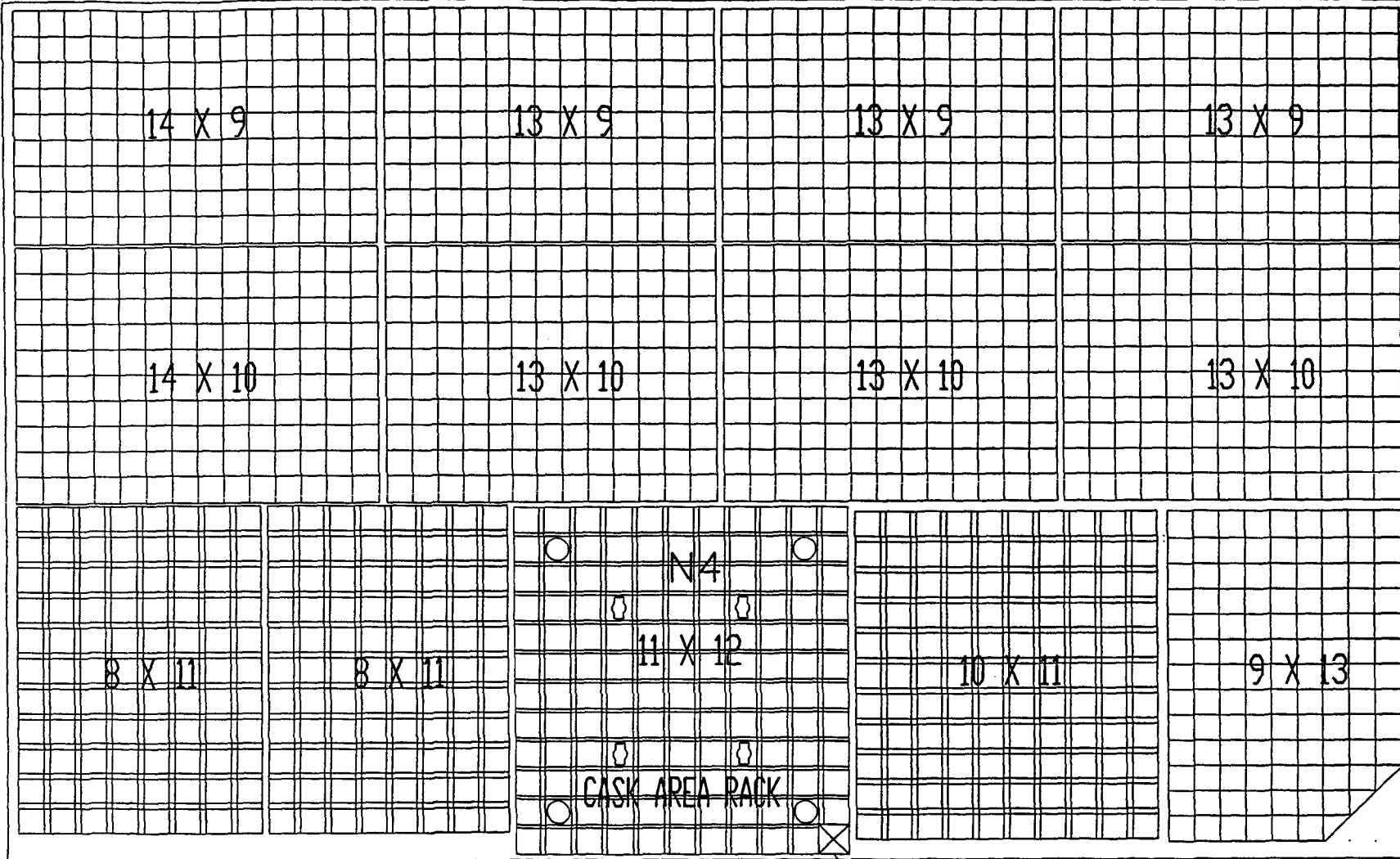
- [1.1.1] Metamic™ U.S. Patent # 5,965,829 entitled " Radiation Absorbing Refractory Composition and Method of Manufacture" Dr. Kevin Anderson, Thomas G. Haynes III, & Edward Oschmann, issued Oct. 12, 1999
- [1.1.2] Metamic™ U.S. Patent # 6,042,779 entitled "Extrusion Fabrication Process for Discontinuous Carbide Particulate Metal and Super Hypereutectic Al/Si Alloys" Thomas G. Haynes III and Edward Oschmann, issued March 28, 2000.
- [1.1.3] Metamic™ U.S. Patent # 6,332,906 entitled " Aluminum - Silicon Alloy Formed by Powder" Thomas G. Haynes III and Dr. Kevin Anderson, issued Dec. 25, 2001.
- [1.1.4] Metamic™ U.S. Patent Application 09/433773 entitled "High Surface Area Metal Matrix Composite Radiation Absorbing Product" Thomas G. Haynes III and Goldie Oliver, filed May 1, 2002.
- [1.1.5] USNRC, "OT Position for Review and Acceptance of Spent Fuel Storage and Handling Applications, April 14, 1978, and Addendum dated January 18, 1979.
- [1.1.6] American Society of Mechanical Engineers (ASME), Boiler & Pressure Vessel Code, Section III, 1989 Edition, Subsection NF, and Appendices.



303.5 (REF.)

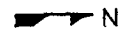
FIGURE 1.1.1; UNIT 3 SPENT FUEL POOL LAYOUT





303.75  
(REF.)

FIGURE 1.1.2; UNIT 4 SPENT FUEL POOL LAYOUT



## 2.0 RACK MODIFICATION DESCRIPTION, PRINCIPAL DESIGN CRITERIA & REFERENCES

### 2.1 Introduction

As noted in Section 1, each Turkey Point (PTN) spent fuel pool contains twelve fuel storage racks that use Boraflex as a neutron absorber and one Region 1-style, Cask Area rack that uses Boral as the neutron absorber. Each Cask Area rack is licensed to store 131 fuel assemblies; the remaining racks are licensed to store 1404 fuel assemblies.

The array of existing racks consists of three Region 1 style racks and nine Region 2 style racks. Each rack is a freestanding module, made primarily of austenitic stainless steel, and containing a honeycomb array of storage cells interconnected through longitudinal welds and upper and lower reinforcement grids. Dimensional data, as well as weight and cell count information for the various size rack modules are presented in Tables 2.1.1 and 2.1.2. As noted in Section 1, the rack module layout for each unit is shown in Figures 1.1.1 and 1.1.2.

The rack enhancement proposed by this license amendment seeks to equip certain storage cells with inserts made of the neutron absorber Metamic™. This rack enhancement is designed to compensate for the ongoing loss in neutron attenuation capability of the originally-installed Boraflex material. Details of the Metamic™ insert design are provided in Section 2.5.

### 2.2 Summary of Principal Design Criteria

The key design criteria for the racks are set forth in the USNRC memorandum entitled "OT Position for Review and Acceptance of Spent Fuel Storage and Handling Applications", dated April 14, 1978 as modified by amendment dated January 18, 1979. The "OT Position Paper" remains applicable for re-evaluation of the racks to consider the addition of Metamic™ panels. The individual sections of this report address the specific design bases derived from the above-mentioned "OT Position Paper".

The design bases for the racks and Metamic™ inserts are summarized in the following:

- a. Rack Module Configuration: The rack modules remain freestanding during a seismic event.
- b. Kinematic Stability: Each freestanding module must be kinematically stable (resist tipping or overturning) under the plant's design basis seismic events.
- c. Structural Compliance: All primary stresses in the rack modules must satisfy the limits in Section III subsection NF of the ASME B&PV Code.

The Metamic™ inserts to be installed in the rack modules are non-structural components. Nevertheless, to ensure that they will continue to perform their intended function under all service conditions, the following requirements are imposed:

Under normal handling or seismic loads, the stress (or strains, as appropriate) in the body of the Metamic™ insert shall be less than 50% of the value at which the insert would suffer a loss of physical integrity (i.e., complete separation into multiple parts, or buckling collapse).

The above structural integrity requirement on the neutron absorber material is derived from Holtec International's fuel rack design practice; it is not a prescribed requirement in the NRC or Code documents applicable to this project. Additionally, it is noted that this acceptance criterion is conservative in some respects, since failure of the insert weld or buckling does not necessarily compromise the design function of the Metamic™ insert.

- d. Thermal-Hydraulic Compliance: The spatial average bulk pool temperature is required to remain below 150°F following a normal partial core offload or full core offload.
- e. Criticality Compliance: The racks must be capable of storing fuel enriched to as much as 4.5 weight percent (w/o) U-235 while maintaining the effective neutron multiplication factor ( $k_{eff}$ ) of the stored array less than or equal to 0.95. This requirement considers the specific storage configurations and fuel parameters discussed in Section 4 and it assumes the pool is flooded with borated water at a temperature corresponding to the highest

reactivity. In addition, calculations have demonstrated that  $k_{\text{eff}}$  is less than 1.0 under the assumed accident of the loss of soluble boron in the pool water, i.e. assuming unborated water in the spent fuel pool, for all proposed fuel storage configurations. The maximum calculated neutron multiplication factors include a margin for uncertainty in reactivity calculations, including manufacturing tolerances, and are calculated with a 95% probability at a 95% confidence level.

- f. Accident Events: In the event of postulated drop events (e.g., an uncontrolled lowering of a fuel assembly), it is necessary to demonstrate that the subcritical configuration of stored fuel is not jeopardized. Credit for the negative reactivity of soluble boron is taken during accident conditions.
  
- g. Retrievability: Under normal operating conditions the insert must be readily retrievable and must not adversely affect retrievability of the host fuel assembly (once the insert has been removed from the cell).

The foregoing design bases are further articulated in Sections 4 through 7 of this licensing report.

### 2.3 Applicable Codes and Standards

The following codes, standards and practices were used as applicable for the design, construction, and assembly of the fuel storage racks. Because Metamic™ inserts do not perform a structural function, only the criticality safety related codes and standards cited hereunder are germane to the evaluations and analyses presented in this report. Additional specific references related to detailed analyses are also provided, as appropriate.

- [2.3.1] ASME B&PV Code Section III, 1998 Edition; ASME Section IX, 1998 Edition.
- [2.3.2] American Society for Nondestructive Testing SNT-TC-1A, June 1980, Recommended Practice for Personnel Qualifications and Certification in Non-destructive Testing.
- [2.3.3] ASTM C750 - Standard Specification for Nuclear-Grade Boron Carbide Powder.
- [2.3.4] ASTM C992 - Standard Specification for Boron-Based Neutron Absorbing Material Systems for Use in Nuclear Spent Fuel Storage Racks.
- [2.3.5] ASME B&PV Code, Section IX - Welding and Brazing Qualifications, 1998.
- [2.3.6] ANSI N45.2.1 - Cleaning of Fluid Systems and Associated Components during Construction Phase of Nuclear Power Plants - 1973 (R.G. 1.37).
- [2.3.7] ANSI N45.2.2 - Packaging, Shipping, Receiving, Storage and Handling of Items for Nuclear Power Plants - 1972 (R.G. 1.38).
- [2.3.8] ASME NQA-1 – Quality Assurance Program Requirements for Nuclear Facilities.
- [2.3.9] ASME NQA-2 – Quality Assurance Requirements for Nuclear Power Plants.
- [2.3.10] "OT Position for Review and Acceptance of Spent Fuel Storage and Handling Applications," dated April 14, 1978, and the modifications to this document of January 18, 1979.
- [2.3.11] ANSI/ANS 8.1 - Nuclear Criticality Safety in Operations with Fissionable Materials Outside Reactors.
- [2.3.12] ANSI/ANS 8.17 - Criticality Safety Criteria for the Handling, Storage, and Transportation of LWR Fuel Outside Reactors.
- [2.3.13] 10CFR21 - Reporting of Defects and Non-compliance.

- [2.3.14] 10CFR50 Appendix B - Quality Assurance Criteria for Nuclear Power Plants and Fuel Reprocessing Plants.
- [2.3.15] 10CFR50.68 "Criticality Accident Requirements".
- [2.3.16] AWS D1.1 - Structural Welding Code - Steel.
- [2.3.17] AWS D1.3 - Structure Welding Code - Sheet Steel.
- [2.3.18] AWS D9.1 - Sheet Metal Welding Code.
- [2.3.19] Holtec International Quality Assurance Manual, Latest Revision.

#### 2.4 Quality Assurance Program

The governing quality assurance requirements for design and fabrication of the spent fuel racks are stated in 10CFR50 Appendix B. Holtec's Nuclear Quality Assurance program complies with this regulation and is designed to provide a system for the design, analysis and licensing of customized components, such as the Metamic inserts, in accordance with the applicable codes, specifications, and regulatory requirements.

In recognition of the central role of the neutron absorber in maintaining subcriticality, Holtec International utilizes appropriately rigorous technical and quality assurance criteria and acceptance protocols to ensure satisfactory neutron absorber performance over the service life of the fuel racks.

Holtec International's Q.A. program ensures that the chosen neutron absorber material will be manufactured under the control and surveillance of a Quality Assurance/Quality Control Program that conforms to the requirements of 10CFR50 Appendix B, "Quality Assurance Criteria for Nuclear Power Plants". Consistent with its role in reactivity control, all neutron absorbing material procured for use in the Holtec racks is categorized as Safety Related (SR). SR manufactured items, as required by Holtec's NRC-approved Quality Assurance program, must be produced to essentially preclude the potential of an error in the procurement of constituent materials and the manufacturing processes. Accordingly, material and manufacturing control processes must be established to eliminate the incidence of errors, and inspection steps are implemented to serve as an independent set of barriers to ensure that all critical

characteristics defined for the material by Holtec's design team are met in the manufactured product [3.6.7, 3.6.11].

Metamic LLC has manufactured Metamic™ panels for previous fuel storage projects, including ANO Unit 1 poison insert assemblies and Clinton Station spent fuel racks. All major steps in the manufacture of Metamic™ are governed by formalized procedures. Raw materials (Al-6061 and B<sub>4</sub>C) used to make Metamic are obtained from qualified suppliers and overcheck analyses are performed to confirm the claims of the materials vendors. Separate mass spectroscopic determination of the fraction of the boron-10 nuclide in the boron is performed for each lot of B<sub>4</sub>C. Each batch mixture of B<sub>4</sub>C and Al-6061 is chemically analyzed to assure a composition that conforms to the design specification for the weight percentage of B<sub>4</sub>C. Permanent records of these analyses with unique identification numbers are maintained in the Holtec QA files. Each completed Metamic™ panel has a unique identification number that permits traceability to the extruded ingot and to the material batch numbers of the constituent powders. Once the powders are thoroughly mixed, there is no known mechanism that might cause re-segregation of the powders. After the isostatic pressing and sintering, the ingots are extruded and cleaned by glass-beading. At this point, visual inspection confirms the removal of foreign particles from the surface of the extrusion piece. The extrusion piece is then rolled to a specified thickness and dimensions are confirmed with a precision jig. Random samples from the rolled panels are measured by neutron attenuation to confirm the proper B<sup>10</sup> areal density and to qualify the homogeneity achieved in the fabrication process. As a qualified process, further neutron attenuation testing of the finished product is not required.

The Quality Assurance system enforced on the manufacturer's shop floor shall provide for all controls necessary to fulfill all quality assurance requirements. The final inspection and acceptance criteria of the manufactured Metamic™ inserts focus on the insert's dimensions, bow, twist, profile, lift block orientation and location, cleanliness, and identifying markings.

## 2.5 Metamic™ Insert Mechanical Design

The design objective for Metamic™ inserts is to provide a neutron absorber having material composition and dimensions suitable for co-residence with fuel in a storage cell, and that can be easily inserted and relocated within the storage racks. Further, neutron absorption properties of the insert must be sufficient to eliminate reliance on the existing Boraflex. As noted elsewhere, a major goal of the rack enhancement project is to recapture use of every storage cell within the Spent Fuel Pool.

Turkey Point Metamic™ inserts are designed for insertion in any rack storage cell subsequent to placing a fuel assembly in that cell. Each insert consists of Metamic™ panels attached to a top landing surface. The insert rests on the fuel assembly top nozzle, and it does not extend to the baseplate of the storage cell. In other words, the insert hangs from the top of the assembly. The landing surface is the underside of the “landing element” which is metallurgically compatible with the neutron absorber material.

An installed Metamic insert blankets two of the four walls of the host storage cell. The insert’s landing element is equipped with interfaces for lifting and handling by an appropriate custom-designed tool. Different tools are used to manipulate Turkey Point fuel assemblies and Metamic™ inserts. The position of the landing element at the top of the fuel assembly will be visually evident and it provides confirmation of the orientation of the Metamic™ inserts within each cell.

The design of the insert ensures that, when seated, the active fuel region is shadowed by Metamic™. The nominal dimensional differences between a fuel assembly (8.426 inches square) and the inside dimension of a Region 2 storage cell (8.80 inches square) provide a sufficient gap (0.374 inches nominal) for the 0.073 inch thick (nom.) insert panels to be easily inserted. The base of each panel is skew cut and beveled to ensure that the panels will readily slide into this gap and not snag on any fuel straps or end fittings.

The Metamic inserts may be manufactured by forming operations or by welding contiguous panels and the landing element as shown in Figure 2.5.1.

Because Metamic™ is not an ASME Code material and does not serve a structural function, provisions of Section IX of the ASME Code [2.3.5] are not applicable to the welding of Metamic™ (if a welding method for assembling the insert is employed). Consistent with the past fuel rack design practice for non-Code materials, the designer (Holtec International) has specified that compliance with strength and failure strain requirements of the welds must be demonstrated by destructive testing of weld coupons. Design details of the required coupons and their testing requirements are also specified by the designer-of-record (Holtec International). In Chapter 9 of this report, margins of safety in the Metamic™ inserts under applicable mechanical and inertial loads are provided using coupon test data collected during weld qualification tests. Any inserts fabricated by forming in lieu of welding will have an equivalent or greater structural strength.

**Table 2.1.1**  
**Geometric and Physical Data for Existing Storage Racks**

| RACK I.D. | QUANTITY OF THIS RACK SIZE | RACK TYPE | CELL-TO-CELL PITCH (in.) | NO. OF CELLS  |               | MODULE ENVELOPE SIZE |           | WEIGHT (lbs) | NO. OF CELLS PER RACK |
|-----------|----------------------------|-----------|--------------------------|---------------|---------------|----------------------|-----------|--------------|-----------------------|
|           |                            |           |                          | N-S Direction | E-W Direction | N-S (in.)            | E-W (in.) |              |                       |
| 1         | 1                          | Region 2  | 9.00                     | 13            | 9             | 117.60               | 81.60     | 13,000       | 117                   |
| 2         | 2                          | Region 2  | 9.00                     | 13            | 9             | 117.60               | 81.60     | 13,000       | 117 †                 |
| 3         | 1                          | Region 2  | 9.00                     | 14            | 9             | 126.60               | 81.60     | 13,900       | 126                   |
| 4         | 1                          | Region 2  | 9.00                     | 13            | 10            | 117.60               | 90.60     | 14,300       | 130                   |
| 5         | 2                          | Region 2  | 9.00                     | 13            | 10            | 117.60               | 90.60     | 14,300       | 130 †                 |
| 6         | 1                          | Region 2  | 9.00                     | 14            | 10            | 126.60               | 90.60     | 15,400       | 140                   |
| 7         | 1                          | Region 2  | 9.00                     | 9             | 13            | 81.60                | 117.60    | 12,200       | 111 ††                |
| 8         | 1                          | Region 1  | 10.60                    | 10            | 11            | 105.99               | 116.59    | 27,100       | 110                   |
| 9         | 1                          | Region 1  | 10.60                    | 8             | 11            | 84.79                | 116.59    | 27,100       | 88                    |
| 10        | 1                          | Region 1  | 10.60                    | 8             | 11            | 84.79                | 116.59    | 27,100       | 88 †                  |

† Differs from the previous entry only by placement of the support pedestals.

†† Six cells eliminated from corner of rack.

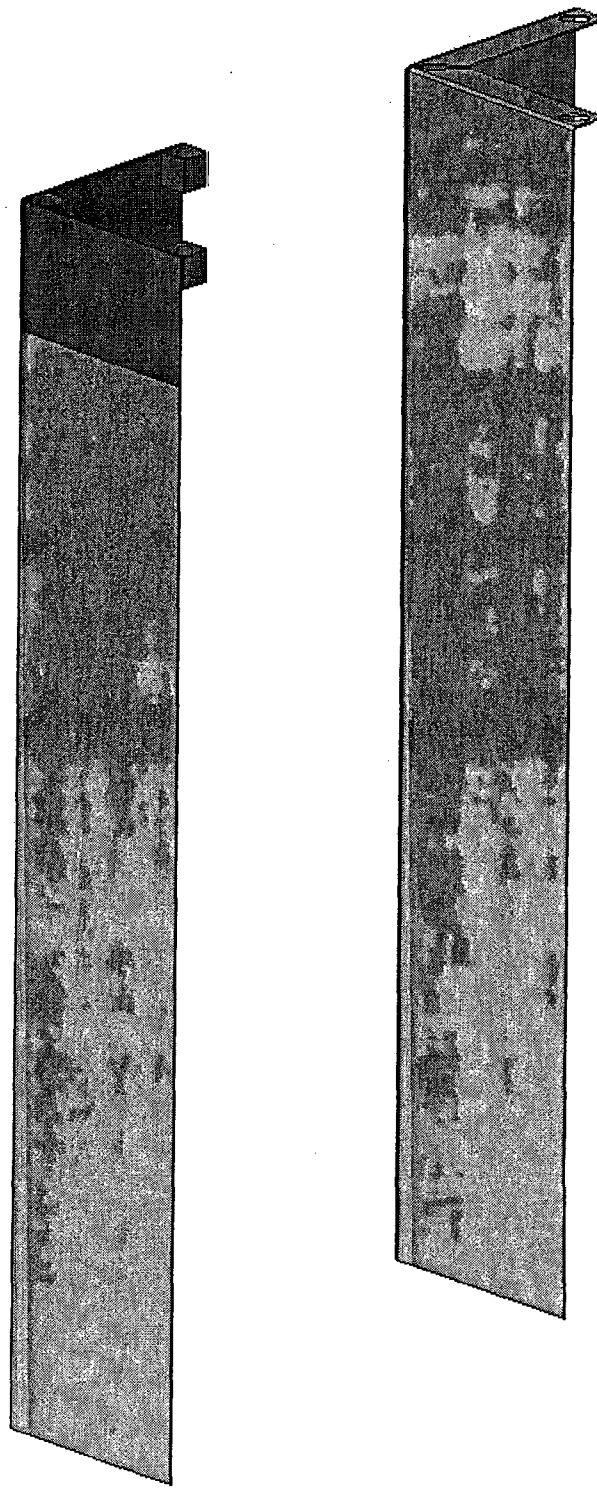
| Table 2.1.2                               |            |            |
|---|------------|------------|
| MODULE DATA FOR EXISTING RACKS †          |            |            |
|   | Region 1   | Region 2   |
| Storage cell inside nominal dimension     | 8.75 in.   | 8.8 in.    |
| Cell wall thickness                       | 0.075 in.  | 0.075 in.  |
| Cell pitch                                | 10.60 in.  | 9.0 in.    |
| Storage cell height (above the baseplate) | 165.61 in. | 165.61 in. |
| Baseplate hole size                       | 4.0 in.    | 4.0 in.    |
| Baseplate thickness                       | 0.5 in.    | 0.5 in.    |
| Support pedestal height                   | 3.25 in.   | 3.25 in.   |
| Number of support pedestals per rack      | 4††        | 4          |
| Poison material                           | Boraflex   | Boraflex   |

† All dimensions indicate nominal values

†† The Region 1 racks in Unit 4 have four additional pedestals near the center of each rack for a total of eight.

| Table 2.5.1<br>METAMIC INSERT PHYSICAL PARAMETERS     |                          |
|---|--------------------------|
| Maximum Width of Metamic™ Insert (inches)             | [REDACTED]               |
| Minimum Length of Metamic™ Insert (inches)†           | [REDACTED]               |
| Thickness of Metamic™ Insert (inches)                 | [REDACTED]               |
| B <sub>10</sub> Loading (grams per square centimeter) | [REDACTED]<br>[REDACTED] |
| Weight of Metamic™ Insert (lbs)                       | 24                       |

† The criticality analysis assumes Metamic coverage of the entire length of active fuel with the exception of the bottom six inches (this requires a minimum insert length of 151.785 inches). The physical minimum insert length of 151.8125 inches meets this requirement.



Welded Insert

Formed Insert

Figure 2.5.1: METAMIC INSERT

### 3.0 MATERIAL CONSIDERATIONS

#### 3.1 Introduction

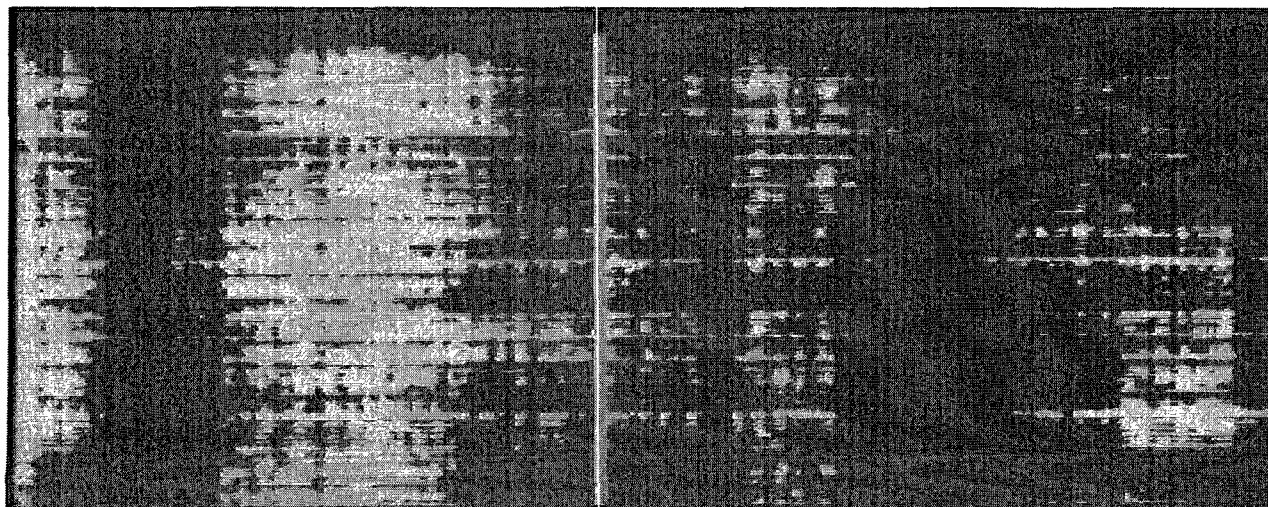
A primary consideration in design of the rack enhancement device (i.e. Metamic™ insert) proposed in this amendment request is that materials introduced into the pool water be of proven durability and compatible with the fuel pool environment. This section summarizes the considerations that provide assurance that the Metamic™ inserts installed in Turkey Point racks will perform their intended function for the design life of the fuel racks.

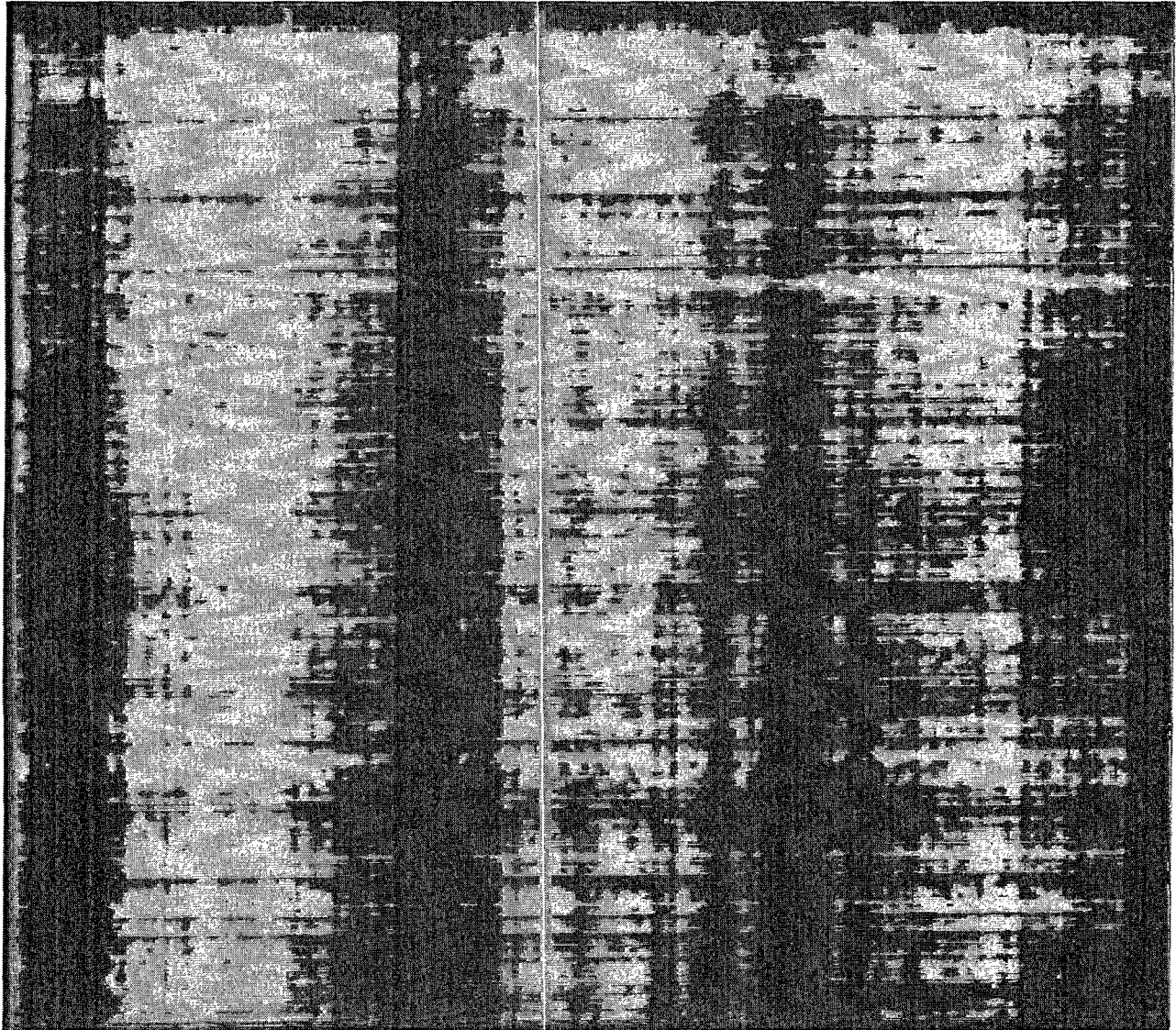
#### 3.2 Materials Used in the Insert

The Metamic™ neutron absorber material is the principal material for manufacturing the insert. Metamic itself is comprised of aluminum alloy 6061 and boron carbide ( $B_4C$ ). Strips of alloy 6061 of aluminum, which is chemically compatible with Metamic™, may be used to manufacture the landing element, if an integral landing element construction technique is not employed. In the integral insert construction, Metamic™ is the sole material of construction.

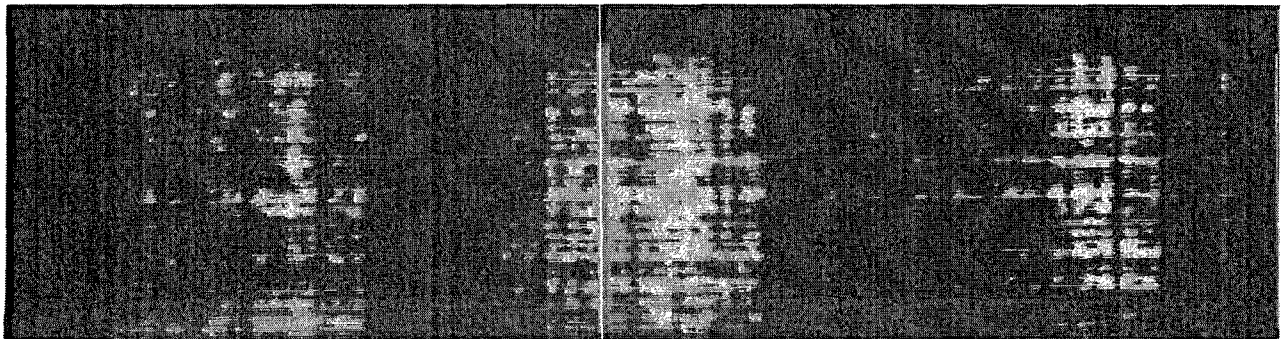
#### 3.3 Neutron Absorbing Material

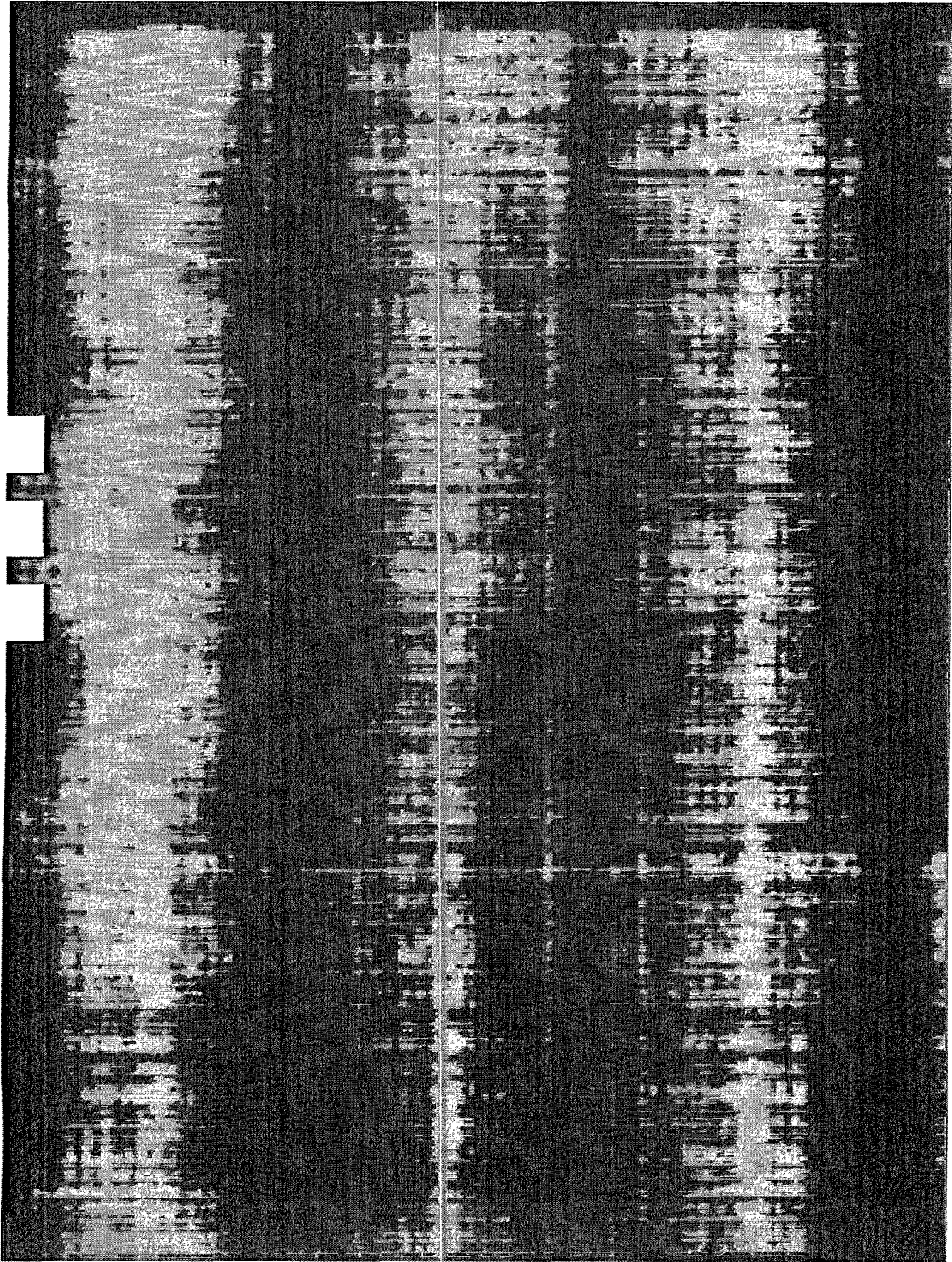
##### 3.3.1 Metamic™ Insert Assembly

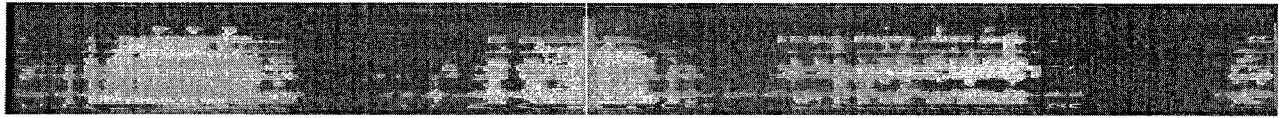




### 3.3.2 Characteristics of Metamic™



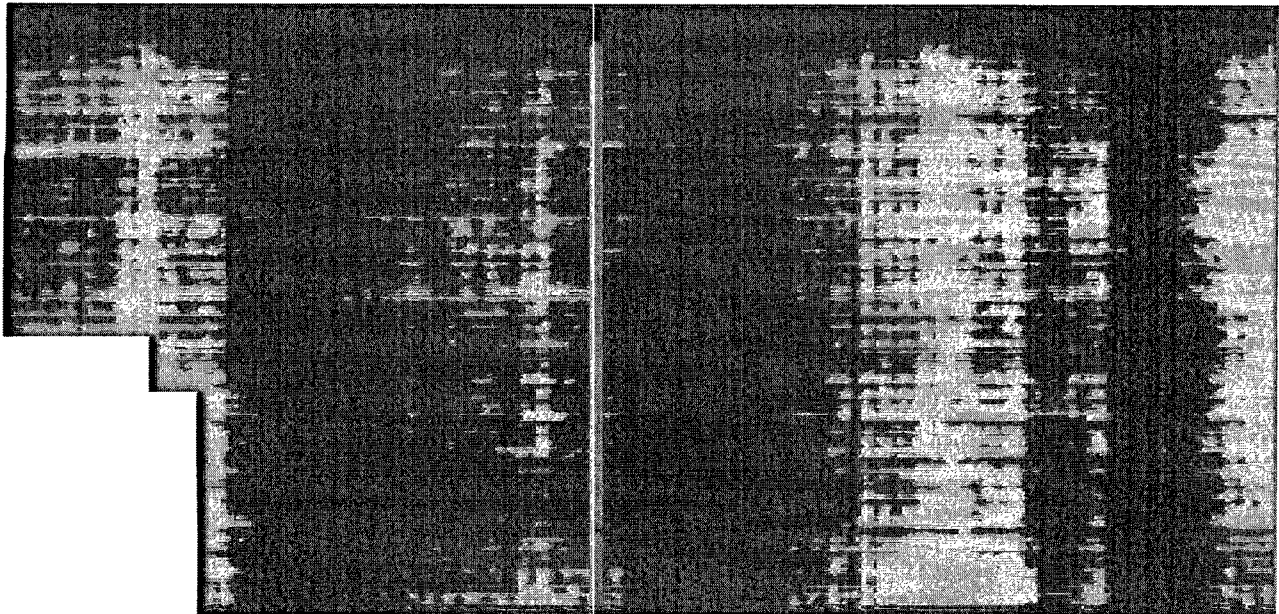




### 3.4 Compatibility with Environment

Typically, Metamic™ inserts installed at Turkey Point will experience an environment of heated, boric acid water. Usual bulk water temperatures will be between 80 °F and 150 °F; soluble boron concentrations will range between 2,000 and 3,000 ppm. Because both constituents of Metamic™ (the Al 6061 alloy and boron carbide) are known to maintain physical and chemical stability in PWR applications, and Metamic™ has no internal porosity (i.e., panels are fabricated at essentially 100% of the theoretical density) there is no known mechanism for Metamic's degradation in Turkey Point's spent fuel pools. Further, over many years, it has been shown that galvanic corrosion of aluminum and aluminum alloys in contact with other metals (i.e. zircaloy or stainless steel), does not occur in water or boric acid solutions [3.6.5, 3.6.6, & 3.6.10].

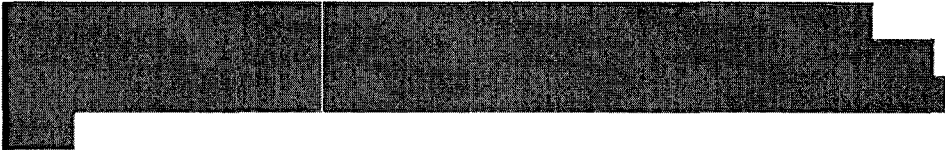
### 3.5 Potential for Abrasion







3.6 References

- [3.6.1] 
- [3.6.2] 
- [3.6.3] 
- [3.6.4] 
- [3.6.5] 
- [3.6.6] 
- [3.6.7] "Safety Evaluation by the Office of Nuclear Reactor Regulation Related to Holtec International Report HI-2022871 Regarding Use of Metamic in Fuel Pool Applications," Facility Operating License Nos. DPR-51 and NPF-6, Entergy Operations, Inc., Docket No. 50-313 and 50-368, USNRC, June 2003.
- [3.6.8] USNRC Docket No. 72-1004, NRC's Safety Evaluation Report on NUHOMS 61BT (2002).
- [3.6.9] "METAMIC 6061 + 40% boron Carbide Metal Matrix Composite Test Program for NAC International, Inc.," California Consolidated Technology, Inc. (2001).
- [3.6.10] "METAMIC" Qualification Program for Nuclear Fuel Storage Applications, Final Test Results", Report NET 152-03, Prepared for Reynolds Metal Company, Inc. by Northeast Technology Corporation.
- [3.6.11] "Use of METAMIC<sup>®</sup> in Fuel Pool Applications," Holtec Information Report No. HI-2022871, Revision 1 (2002).

- [3.6.12] "Sourcebook for Metamic™ Performance Assessment" by Dr. Stanley Turner, Holtec Report No. HI-2043215 (2004).
- [3.6.13] "Qualification of Metamic™ for Use as a Neutron Poison Material", Holtec Report No. HI-2033129 (2004).

## 4.0 CRITICALITY SAFETY ANALYSES

### 4.1. Introduction and Summary

#### Overview

This section documents the criticality safety evaluation for the storage of PWR spent nuclear fuel in Region 1 & 2 style spent fuel storage racks at Turkey Point Units 3 & 4. The Turkey Point spent fuel pools currently (as of 8/05) contain approximately 2020 permanently discharged fuel assemblies. The evaluation in this document is performed to qualify the racks from a criticality perspective under the assumption of a complete loss of the Boraflex™ neutron poison.

This evaluation complements the installation of the cask area racks at Turkey Point<sup>†</sup>. These cask area racks are designed to accommodate fresh fuel enriched to 4.5 weight percent (wt%) U-235. The existing Region 1 & 2 style racks analyzed in this report will therefore be predominantly used for the storage of less reactive irradiated fuel.

The objective of the analysis is to qualify the existing racks, i.e. racks other than the cask area rack for the current inventory of stored fuel and for future discharges of spent fuel, with additional neutron absorber inserts placed into the racks, as required, to offset an assumed loss of the Boraflex. In this evaluation of the current inventory and future discharges of burned fuel, credit is taken for the negative reactivity associated with post-irradiation cooling time. Additionally, credit is taken for the presence of soluble boron in the spent fuel pool and for the presence of full-length rod control cluster assemblies (RCCAs) placed in selected fuel

---

<sup>†</sup> Enclosures to NRC letter dated November 24, 2004, Turkey Point Units 3 and 4 - Issuance of Amendments Regarding Temporary Spent Fuel Pool Cask Racks (TAC Nos. MB6909 and MB6910)

assemblies. To clearly distinguish between the inserts placed into rack cells and the control components inserted into fuel assemblies, in this section, the term “insert” by itself always refers to the Metamic™ neutron absorber inserts placed into the racks, while the full-length control components are always referred to as RCCAs, and other inserts placed into assemblies during depletion are always clearly characterized, e.g. as Pyrex inserts, WABA inserts or hafnium inserts.

The relevant fuel assembly and fuel rack specifications are identical between Turkey Point Unit 3 and Unit 4. All analyses and conclusions presented in this section therefore apply to both units.

### Fuel Storage Configurations Analyzed

In order to achieve the stated objective of qualifying the existing racks, it is necessary to separate fuel assemblies into groups based on burnup and cooling time and establish an appropriate storage configuration for each fuel assembly grouping.

A total of 10 (ten) storage configurations (Cases) were established, which are characterized as follows:

- Case 1: An array of stored fuel in Region 2 racks requiring no inserts
- Case 2: An array of stored fuel in Region 2 racks requiring one insert in every four cells
- Case 3: An array of stored fuel in Region 2 racks requiring two inserts in every four cells
- Case 4: An array of stored fuel in Region 1 racks requiring no inserts
- Case 5: An array of stored fuel in Region 1 racks where certain fuel assemblies contain an RCCA
- Case 6: A checkerboard array of fresh fuel and water-filled cells in Region 1 racks
- Case 7: A checkerboard array of high and low reactive fuel in Region 2 racks requiring no inserts

- Case 8: A checkerboard array of high and low reactive fuel in Region 2 racks requiring one insert in every four cells
- Case 9: An array of three fuel assemblies and one water-filled cell in every four cells of Region 2 racks
- Case 10: An array of stored fuel in Region 2 racks containing RCCAs instead of inserts

Burnup vs. Enrichment Curves

For Cases 1 through 4 and 7 through 9, curves specifying the minimum required burnup as a function of the initial enrichment (loading curves) are developed, for freshly discharged fuel and for discharged fuel with post-irradiation cooling times of up to 20 years. Case 5 does not require a separate loading curve, since the assemblies loaded in this array without RCCAs use the Case 4 loading curve, and the fuel assemblies containing RCCAs can be fresh assemblies of the highest enrichment, i.e. 4.5 wt% U-235. Case 6 considers the storage of 4.5 wt% fresh fuel; as this condition bounds all irradiated fuel at Turkey Point, no fuel loading curves are required. The purpose of Case 10 is to demonstrate that an array of Case 2 or Case 3 fuel containing RCCAs (but no storage cell neutron absorber inserts) is less reactive than an equivalent array of Case 2 or Case 3 fuel assemblies (without RCCAs) placed in storage locations containing inserts. As a result, Case 10 does not require a separate loading curve.

The loading curves are established as polynomial functions in the form of

$$Bu = A * En + B * En^2 + C * Ct + D * Ct^2 + E * Ct * En + F * Ct^2 * En + G$$

With:

|               |  |
|---------------|--|
| Bu            | Minimum required assembly average burnup (GWD/MTU) |
| En            | Initial U-235 Enrichment (wt%)                     |
| Ct            | Cooling Time (years)                               |
| A,B,C,D,E,F,G | Coefficients                                       |

Separate functional relationships are developed for fuel assemblies containing axial blankets and for fuel assemblies without axial blankets. Note that for blanketed assemblies, the enrichment to be used in the loading curve equation is the enrichment of the axial section between the blanket material, i.e. the enrichment of the axial blankets is excluded when determining assembly enrichment for application of loading curves.

Only values of 0, 2.5, 5, 10, 15 and 20 years are allowed to be used in burnup requirement equations (i.e. loading curves), since only these specific cooling times were explicitly analyzed. The actual cooling times of fuel assemblies are to be rounded down to one of these values.

Coefficients for all loading curves, for non-blanketed and blanketed assemblies, are listed in Tables 4.1.1 and 4.1.2. Additionally, required burnup values for selected initial enrichments are determined from these coefficients and are listed in Tables 4.1.3 and 4.1.4.

Results of Case 5 analyses demonstrate that in Region 1, a fresh assembly containing an RCCA may be placed in any location instead of a Case 4-qualified assembly, without requiring a specific pattern.

Results for Case 10 confirm that the presence of an RCCA in an assembly bounds (i.e., is less reactive than) the condition where that assembly is placed (without the RCCA) in a cell containing an insert. For Case 2 and 3 storage arrays, it is therefore acceptable to omit the insert from a cell, if the assembly in that cell contains an RCCA.

Additionally, analyses demonstrate that any assembly in the Case 8 checkerboard array may contain the Metamic™ insert.

### Special Fuel Loading Rules

Fuel rod baskets may be placed in any Region 2 storage cell designated for fuel assemblies.

To the extent possible, neutron absorber inserts placed in storage racks shall be positioned with the same spatial orientation. Any inserts installed in the storage racks with an orientation different from the predominant orientation of installed inserts are not to be credited for reactivity control unless specific calculations considering the as-installed geometric arrangement are performed and demonstrate acceptable results. Along with the as-installed geometry, this case by case evaluation will utilize the actual fuel assembly burnups and cooling times to demonstrate compliance with regulatory limits.

Empty, i.e. water-filled cells required in the Case 6 and Case 9 configurations are not to contain trash or other non-fuel hardware, unless condition-specific calculations are performed to show that these items do not increase reactivity.

Each 2x2 array in the Region 2 area of the pool that does not contain cells facing the pool wall or facing Region 1 racks, including overlapping 2x2 configurations, must match one of the fuel storage arrangements analyzed in Cases 1 through 3 or 7 through 9.

For any 2x2 array of stored fuel in the Region 2 area of the pool that does contain cells facing the pool wall, the cells facing the pool wall may contain Case 3 fuel without inserts or RCCAs.

Additionally, each of these 2x2 arrays must meet the following criteria:

- Contain at least one insert if fuel placed in the 2<sup>nd</sup> and 3<sup>rd</sup> row of cells matches Case 2 or Case 3 criteria, or
- Contain at least one empty cell if fuel placed in the 2<sup>nd</sup> and 3<sup>rd</sup> row of cells matches Case 9 criteria.

All permissible arrangements along the pool walls with Case 3 fuel on the periphery are also shown in Figure 4.1.1.

Along the interface between Region 1 and Region 2 racks the following restrictions apply to the placement of assemblies in the Region 2 racks:

- Case 3 assemblies may not be placed in the outer row of Region 2 racks facing Region 1 racks; and
- For fuel arranged as required by Cases 2, 8 and 9, the inserts or empty cells required by these cases, as applicable, must be located in the outer row of Region 2 cells facing the Region 1 rack.

Each 2x2 array in the Region 1 area of the pool, including overlapping 2x2 arrays, must match one of the fuel storage arrangements analyzed in Cases 4 through 6.

In this context, the term “match” means that the configuration has at least the required number of inserts (or RCCAs) and that the fuel assemblies forming the array have at least the required burnup for one of the cases.

Criticality calculations are based on the insert specifications listed in Table 4.4.6, which is consistent with the design specifications listed in Table 2.5.1.

### Analysis Results

Analyses demonstrate that the effective neutron multiplication factor ( $k_{eff}$ ) of all permissible fuel storage arrangements is less than or equal to 0.95 when the storage racks are assumed to be fully loaded with fuel of the highest permissible reactivity and the pool is assumed to be flooded with borated water at a temperature within the normal operating range corresponding to the highest reactivity. In addition, the analyses demonstrate that  $k_{eff}$  of each fuel storage arrangement remains less than 1.0 when the fuel pool is assumed to be flooded with unborated water. The maximum calculated values of the neutron multiplication factor include appropriate bias effects,

a margin for uncertainty in reactivity calculations, the effect of manufacturing tolerances on reactivity, and are calculated with a 95% probability at a 95% confidence level [4.7.1].

A minimum soluble boron concentration of 560 ppm must be maintained in the spent fuel pool to ensure that  $k_{\text{eff}}$  is less than or equal to 0.95 under all normal conditions.

Reactivity effects of accident conditions have also been evaluated. The most limiting accident condition involves placing a fresh fuel assembly, enriched to 4.5 wt% U-235, into the water-filled cell in a Case 9 storage arrangement. A minimum soluble boron concentration of 1462 ppm must be maintained in the spent fuel pool to ensure that  $k_{\text{eff}}$  is less than or equal to 0.95 under this condition.

Turkey Point Unit 3 and Unit 4 Technical Specifications require that the fuel pool soluble boron concentration be maintained  $\geq 1950$  ppm at all times.

#### 4.2. ACCEPTANCE CRITERIA

The objective of this analysis is to ensure that all calculations of the effective neutron multiplication factor ( $k_{\text{eff}}$ ) performed for each permissible storage arrangement, yield results less than or equal to 0.95 when the storage racks are fully loaded with fuel of the highest permissible reactivity, and assuming the fuel pool is flooded with borated water at a temperature corresponding to the highest reactivity. In addition, this analysis must demonstrate that  $k_{\text{eff}}$  is less than 1.0 following the assumed accident of the loss of soluble boron in the pool water, i.e. assuming unborated water in the spent fuel pool. The maximum calculated values of neutron multiplication must include a margin for uncertainty in reactivity calculations, include the effect of manufacturing tolerances, and be calculated with a 95% probability at a 95% confidence level [4.7.1].

### 4.3. ASSUMPTIONS

To provide added assurance that the actual  $k_{\text{eff}}$  of the racks is below the regulatory limits, a significant number of conservative assumptions are used in the analyses. The major assumptions are listed below:

1) No credit is taken for the remaining Boraflex neutron absorber panels in the racks, although even degraded Boraflex would still provide some neutron absorption.

2) There are three major assumptions regarding burnable poison rod assemblies (BPRAs):

a) All Turkey Point fuel assemblies are assumed to contain a BPRA during depletion; b) of the two BPRA types used at the plant (i.e., Pyrex and WABA), the Pyrex BPRA is used in the analysis since it results in higher reactivities; and c) all BPRAs are assumed to contain the maximum number of poison rods. Each of these three assumptions represent a major conservatism, since in reality: a) only about 1/3 of all fuel assemblies were exposed to a BPRA of either type; b) the Pyrex BPRA was only used in some early fuel cycles of the plant; and c) most BPRAs contain less than the maximum number of poison rods.

Calculations specific to Turkey Point fuel were performed to verify that Pyrex represents the limiting absorber material. Note that for an individual assembly, depletion calculations with and without a BPRA demonstrate a conservatism in reactivity between about 0.0050 and 0.0200 delta-k as a result of these assumptions.

3) Calculations are based on the current reactor thermal power output value of 2300 MWt, although the plant operated at 2200 MWt prior to September 1996.

4) No credit is taken for the potential presence of burnable absorber inserts or hafnium inserts in fuel assemblies when the assemblies are in the spent fuel racks.

- 5) The moderator (i.e. fuel pool) temperature reactivity bias is determined for various conditions, e.g. cells with and without inserts, and for a series of representative burnup, enrichment and cooling time combinations. A bounding value is then chosen for each case, and is subsequently applied to all calculations for the case.
- 6) A conservatively high in-core moderator temperature is used in the depletion calculations.
- 7) Manufacturing tolerance effects on neutron multiplication are determined for various conditions, e.g. cells with and without inserts (if the case contains inserts), and for a series of representative burnup, enrichment and cooling time combinations. A bounding value of the combined effect is then chosen for each case, and is subsequently applied to all calculations for the case.
- 8) The increase in reactivity due to the presence of non-uniform axial burnup profiles is considered in the analysis, while any possible reduction in reactivity due to an axial burnup profile is conservatively neglected.
- 9) Bounding loading curves are presented in the form of polynomial functions. For some burnup, enrichment and cooling time combinations, these functions embed additional safety margins of up to about 0.0100 delta-k.
- 10) The configurations analyzed qualify both long-term storage patterns and the temporary patterns encountered during the loading, unloading and repositioning of fuel assemblies.
- 11) Uncertainties in the depletion calculations and in burnup records are considered.
- 12) The effective multiplication factor of an infinite radial array of fuel assemblies or assembly patterns was used in the analyses, except for the assessment of peripheral and interface effects. Specifically, all gaps between adjacent Region 2 rack modules were conservatively ignored, i.e.

cells in neighboring Region 2 rack modules were assumed to be separated by a single cell wall only. The actual configuration in the Turkey Point spent fuel pool has a cell wall on each side of the Region 2 rack-to-rack gap.

Additionally, a number of other modeling assumptions were applied. These assumptions are not necessarily conservative, but they have only a negligible effect on results.

- 1) Neutron absorption in minor structural members is neglected, i.e., spacer grids are replaced by water.
- 2) For freshly unloaded fuel (i.e. irradiated fuel with 0 years cooling time), a cooling time of less than 0.1 hours is used in the analysis. This value bounds (i.e. is lower than) any realistic cooling time of irradiated fuel placed in the spent fuel pool and it results in fuel with a conservatively high reactivity. Also, the Xe-135 concentration in the fuel is conservatively set to zero.
- 3) Most fuel rods have a nominal pellet OD of 0.3659 inches, and this value is used in the analyses. However, there are some assemblies with a slightly smaller pellet OD of 0.3649 inches, and there are 4 rods with a slightly larger pellet OD of 0.3671 inches. The smaller pellet OD is conservatively bounded by the value used in the analysis, since the larger Pellet OD results in a higher reactivity. The effect of the rods with the larger pellet OD is negligible since there are only 4 rods of this diameter.
- 4) The bounding assembly design (see Section 4.6.1 and Table 4.4.1 for information on differences in the fuel used at Turkey Point) was determined based on nominal assembly dimensions. This approach is acceptable since the analyzed manufacturing tolerances, i.e. tolerances on those parameters relevant to criticality analyses, are identical between the two assembly types.

- 5) In the MCNP models, 30 cm of axial water reflector is used above and below the active region of the fuel, i.e. all structures of the assembly, racks and poison inserts above and below the active region are replaced by water.
- 6) In this calculation, it is assumed that all rack cell inserts are installed with the same spatial orientation. This is a significant assumption, and it is necessary that the actual configurations in the pool be consistent with this assumption or that any different as-installed configuration of inserts be specifically evaluated. It is not feasible to analyze all permutations of insert orientations in advance. Therefore, any inserts installed in the storage racks having an orientation different from the predominant orientation of inserts are not to be credited for reactivity control until specific calculations considering the as-installed geometric arrangement are performed and demonstrate acceptable results. It is envisioned that the 10CFR 50.59 process would be used to evaluate this condition, should it occur. Any condition-specific evaluation may utilize actual fuel assembly burnups, as well as the as-installed geometry to demonstrate compliance with regulatory limits.
- 7) Empty cells required in Case 6 and Case 9 arrays were modeled as containing only water, at fully dense conditions for the evaluated temperature. This is a significant assumption, and it is necessary that the actual configurations in the pool be consistent with this assumption or that any non-fuel hardware configuration in empty cells be specifically evaluated. It is envisioned that the 10CFR 50.59 process would be used to evaluate this condition, should it be necessary.
- 8) Fuel assemblies and the Metamic<sup>†</sup> inserts are modeled so that the bottom 6 inches of active fuel is not covered by the insert. This uncovered length will be slightly larger than the actual uncovered length, based on insert and fuel assembly dimensions with uncertainties.

---

<sup>†</sup> See Section 3.3.1

#### 4.4. DESIGN AND INPUT DATA

##### 4.4.1 Fuel Assembly and Fuel Insert Specifications

The design specifications of fuel assemblies, which were used for this analysis, are given in Table 4.4.1. Table 4.4.2 shows specifications of the burnable absorber insert (WABA and Pyrex), and Table 4.4.3 contains the specifications of control inserts (RCCA and hafnium) used in the evaluations.

The tables also contain tolerances for the fuel and the RCCA control insert (except for the RCCA poison density). Using a nominal value for the RCCA poison density is acceptable because calculations crediting the RCCA show a significant safety margin to the regulatory limit (see Cases 5 and 10 in Section 4.6). Prior to initiating work on this criticality analysis, the supplier of nuclear fuel for Turkey Point was asked to identify and independently verify nominal values, as well as maximum and minimum values of a variety of fuel parameters, relevant to analyses, for each reload batch. Similar information was obtained for RCCAs. Parameter values that bound all reload batches of a given fuel type were subsequently used as verified input to this criticality analysis. As a result, most criticality analysis input parameters contain a small amount of recoverable margin that could be used in the future to accommodate unforeseen deviations.

For the burnable poison inserts and the hafnium insert, nominal specifications are used because these absorber materials are only used in the depletion calculations to establish a bounding approach for representing poison inserts. Any effect from the tolerances of these specifications would be small. As noted earlier, conservative results are assured by the assumption that, during the first cycle depletion, each assembly contains a burnable poison insert with the maximum number of poison rods.

The operating parameters used in the depletion analysis are given in Table 4.4.4.

The Region 2 racks were analyzed to allow storage of one or more fuel rod baskets. These baskets consist of regular arrays of stainless steel tubes. Individual fuel rods are placed in these tubes. The specifications of these fuel rod baskets used in this analysis are given in Table 4.4.8.

#### 4.4.2 Storage Rack Specification

The storage cell characteristics that are used in criticality evaluations are summarized in Table 4.4.5 for the Region 1 and Region 2 racks, and in Table 4.4.6 for the Metamic rack cell inserts. Note that the insert length used in analyses is approximately 6 inches shorter than the active fuel length, i.e. the lower 6 inches of the active length are not covered by the insert. This insures that the insert can be placed in a storage cell without interfering with the lower grid strap of an assembly. Figures 4.4.1 and 4.4.2 show sketches of the cells for the Region 1 and Region 2 racks, respectively, indicating all relevant nominal dimensions.

#### 4.4.3 Spent Fuel Pool Specification

Characteristics of the spent fuel pool used in the criticality analyses are listed in Table 4.4.7.

### 4.5. METHODOLOGY

The principal analytical tool used in criticality analyses of Turkey Point spent fuel storage racks is the three-dimensional Monte Carlo code MCNP4a [4.7.2]. MCNP4a is a continuous energy spectrum Monte Carlo code developed at the Los Alamos National Laboratory. MCNP4a was selected because it has been used previously and verified for criticality analyses and because it has all of the necessary features for the Turkey Point analysis. MCNP4a calculations used continuous energy cross-section data based on ENDF/B-V and ENDF/B-VI. Exceptions are two lumped fission products and one individual fission product calculated by the CASMO depletion

code (see below), that do not have corresponding cross sections in MCNP. For these isotopes, the CASMO cross sections are used in MCNP. This approach has been validated by showing that the cross sections result in the same reactivity effect in both CASMO and MCNP4a.

Benchmark calculations, presented in Appendix A, indicate a bias of 0.0009 with an uncertainty of  $\pm 0.0011$  for MCNP4a, evaluated with a 95% probability at the 95% confidence level [4.7.1]. The benchmark calculations utilize the same computer platform and cross-section libraries as are used for the design basis calculations.

The convergence of a Monte Carlo criticality problem is sensitive to the following parameters: (1) number of particle histories per generation, (2) the number of generations skipped before averaging, (3) the total number of generations and (4) the initial source distribution. The MCNP4a criticality output contains a great deal of useful information that may be used to determine the acceptability of the problem convergence. This information has been used in parametric studies to develop appropriate values for the aforementioned parameters applied in storage rack criticality calculations. Based on these studies, the calculations use a minimum of 5,000 histories per generation, a minimum of 40 generations were skipped before averaging, and a minimum of 100 generations were accumulated. These parameters represent an acceptable compromise between calculational precision and computational time for design basis calculations. Further, the output was reviewed to ensure that each calculation achieved acceptable convergence. The initial source was specified as uniform over the fueled regions (assemblies) for calculations with axially constant burnup. For calculations with a burnup profile, a higher number of initial neutrons were started near the lower burned upper and lower sections of the fuel.

Fuel depletion analyses during core operation were performed with CASMO-4 (using the 70-group cross-section library), a two-dimensional multigroup transport theory code based on capture probabilities [4.7.3-4.7.5]. CASMO-4 is used to determine the isotopic composition of the spent fuel. In addition, the CASMO-4 calculations are restarted in the storage rack geometry yielding the

two-dimensional infinite multiplication factor ( $k_{inf}$ ) for the storage rack to determine the reactivity effect of fuel and rack tolerances, and to perform various studies. For all calculations in the spent fuel pool racks, the Xe-135 concentration in the fuel is conservatively set to zero. In all calculations, cross sections from the CASMO N-Library are used, which is predominantly based on ENDF/B-V, except for some Eu and Gd isotopes, which are based on ENDF/B-VI [4.7.8]. The later version Eu and Gd cross sections are used because they provide a conservative (reduced) production of Gd-155 during decay, resulting in higher reactivity for fuel evaluated with cooling time.

Cooling time for the fuel was modeled in the CASMO-4 code through execution of a zero power time step for the period of interest. As provided in Reference 4.7.6, subsequent decay over time on longer-life nuclides such as Pu-241 may be accounted for to reduce the minimum burnup required to meet the reactivity requirements. All decay chains are considered in this analysis, consistent with the licensed approach for other FPL units.

The evaluation performed to develop Tables 4.1.1 and 4.1.2 of this report consists of MCNP4a calculations performed at many combinations of enrichment, burnup and post-irradiation cooling time for each of the proposed fuel storage patterns.

The methodology used to calculate the data points consists of a series of steps. First, three-dimensional MCNP4a calculations are utilized to develop estimates of the appropriate enrichment, cooling time and burnup combinations that will maintain  $k_{eff}$  less than 1.0 without soluble boron. As discussed elsewhere in this report, calculations considered fuel with conservative axial burnup distributions. Results of this first step produced a series of acceptable enrichment/burnup/cooling time combinations.

Next, equivalent burnup values for all relevant enrichment and cooling time combinations were developed using CASMO-4 calculations in conjunction with the acceptable values developed by the first step. The sum of all these efforts produced burnup versus enrichment polynomial curves for all

loading arrangements and cooling times. These data points were then approximated by the multi-variable equations whose coefficients are contained in Tables 4.1.1 and 4.1.2.

To verify the equations conservatively bound the  $k_{\text{eff}} = 1.0$  condition, MCNP4a was used to perform a series of confirmatory calculations in three dimensions. These confirmatory calculations selected allowable combinations of initial enrichment, burnup and cooling time and evaluated them in the appropriate storage configuration. All confirmatory calculations demonstrated that  $k_{\text{eff}}$  is less than 1.0 without credit for soluble boron.

Finally, soluble boron requirements for each developed curve of required burnup vs. enrichment are set using an interpolation process, with a target  $k_{\text{eff}}$  of 0.94. MCNP4a results from cases modeling each storage arrangement, parametric in soluble boron concentration, are used as input.

#### 4.6. ANALYSIS

This section describes the calculations that were used to determine acceptable storage criteria for both the Region 1 and Region 2 style racks and it summarizes the results of these calculations. In addition, this section discusses the possible abnormal and accident conditions.

Unless otherwise stated, all calculations assumed nominal characteristics for the fuel and the fuel storage cells. The effect of the manufacturing tolerances is accounted for with a reactivity adjustment as discussed below.

As discussed in Section 4.5, MCNP4a was the primary code used in Turkey Point criticality calculations. CASMO-4 was used to determine the reactivity effect of tolerances and to perform depletion calculations. MCNP4a was used for reference cases and to perform calculations that are not possible with CASMO-4 (e.g. eccentric fuel positioning, axial burnup distributions, and fuel misloading).

All calculations are made using an explicit model of the fuel and storage cell geometry. MCNP three-dimensional calculations model a 2-by-2 array of cells surrounded by periodic boundary conditions. In CASMO, only a single cell is modeled. Since CASMO-4 is a two-dimensional code, the fuel assembly hardware above and below the active fuel length is not represented. The three-dimensional MCNP4a models that included axial leakage assumed 30 cm of water above and below the active fuel length. Additional models with more than four cells and different boundary conditions were generated for MCNP to investigate the effect of interfaces between racks and to analyze accident conditions. These models are discussed in the appropriate sections below.

#### 4.6.1 Bounding BPRA Inserts and Fuel Assemblies

There are two different burnable poison insert designs (see Table 4.4.2) and two slightly different assembly types (see Table 4.4.1). The presence of these BPRA inserts in the fuel assembly during depletion has a significant effect on reactivity; this BPRA effect is much larger than the reactivity effect of the differences in fuel design, which affect only guide tube and instrument tube dimensions. Therefore, the bounding BPRA insert is determined first, and then the bounding assembly type is identified, using the bounding BPRA inserts.

To determine the bounding BPRA insert, three sets of CASMO fuel lattice calculations are performed: one set without any BPRA insert, one set modeling a fuel assembly containing a WABA insert, and one set considering a fuel assembly with a Pyrex insert. Note that for these evaluations the insert is only assumed to be present during the initial part of the fuel depletion (equivalent to the first cycle). The calculations are performed for enrichments of 1.8 wt%, 3.3 wt% and 4.5 wt%, cooling times of 0 and 20 years, and burnups up to 60 GWD/MTU (depending on the enrichment). These parameters bound all realistic conditions, and are used in all CASMO evaluations that determine bounding conditions, biases or uncertainty effects. The

fuel assembly depletion with Pyrex inserts produces the highest reactivity in fuel storage racks and is therefore used in all subsequent calculations. Note that, as discussed earlier, the presence of Pyrex inserts in all assemblies during depletion is a significant conservative assumption. In reality, only a limited number of assemblies are exposed to any burnable inserts. Further, only a fraction of the assemblies exposed to a burnable absorber would have been exposed to a Pyrex insert, since this absorber design was only used in the earliest cycles of plant operation. As noted earlier, the BPRA insert is only assumed present during part of the assembly depletion, i.e. Pyrex absorbers were inserted in fuel for the first 16,000 MWD/MTU, because this depletion point is representative of first-cycle fuel burnup when Pyrex was in use and because its presence increases the reactivity of the assembly when later placed in the fuel pool. No credit is taken for the potential presence of burnable poison inserts when determining neutron multiplication in the spent fuel pool.

The increased reactivity of Turkey Point fuel assemblies that undergo fission while containing burnable poison material is the result of two factors, the effect of the poison itself, and the effect of the reduced water fraction in the assembly. Assemblies containing integral absorbers (IFBAs) are therefore bounded by the BPRA inserts, since assemblies with IFBAs have the poison effect but not the reduced water effect. This is supported by independent studies documented in [4.7.9], where various types of integral burnable absorbers were evaluated, including IFBAs using  $ZrB_2$  similar to the IFBAs used at Turkey Point.

The two assembly types only differ in the guide and instrument tube dimensions (see Table 4.4.1). A comparison of the reactivity of the two fuel types shows that the assembly types are practically identical from a reactivity perspective, with differences less than  $\pm 0.0001$  (see Table 4.6.1). For all subsequent calculations, the OFA/DRFA fuel dimensions are used.

In addition to the burnable poison inserts, there are also control components containing hafnium that can be placed in an assembly prior to depletion. These are called reduced length annular Hafnium Vessel Flux Depression (HFVD) absorbers. The hafnium absorber material is

positioned near the mid-plane of the fuel assembly's axial length, and is typically only inserted in an assembly on the core periphery during its third cycle of operation. However, it is possible that an assembly contained a burnable poison insert during its first cycle of operation and a hafnium insert in its third cycle, and therefore this is the configuration that was evaluated in the Turkey Point analysis. To accurately model the effect of the hafnium present in only part of the active fuel length, a three-dimensional MCNP model is required. Two CASMO assembly depletion calculations are used to determine the isotopic composition of the fuel. For the part of the active length containing the hafnium insert, a calculation is performed with a Pyrex insert present in the first cycle and the hafnium insert present in the third cycle. For the remainder of the active length, the standard CASMO calculation is used, with only the Pyrex insert present during the first cycle of operation. Also, these MCNP calculations use a different axial profile, which includes the effect of the hafnium, and which is slightly flatter than the standard profile due to the higher burnup of these assemblies. These calculations demonstrate that the effect of the hafnium inserts on assembly reactivity is statistically equivalent to, or lower than, the effect of the standard cases assuming the Pyrex inserts only. Assemblies exposed to hafnium inserts are therefore bounded by the calculations performed assuming only Pyrex inserts, and no further calculations are performed for hafnium inserts.

#### 4.6.2 Moderator Temperature Effect

For the depletion calculations, conservative moderator temperatures in the core are used. Two different temperature values are used, depending on whether the fuel section contains a hafnium insert or not. For the depletion calculations without the hafnium insert, the core outlet temperature of 611.3 °F is conservatively used as the moderator temperature. However, this same assumption would be excessively conservative for fuel sections with the hafnium insert, since the hafnium is only present in a short axial section positioned at or below the mid-plane elevation of the active fuel region, where the moderator temperature is no more than 590 °F.

The depletion calculations for fuel sections with hafnium inserts therefore use a moderator temperature of 590 °F.

#### 4.6.3 Pool Water Temperature Effects

Pool water temperature effects on reactivity have been calculated with CASMO-4 for various temperatures between 39.2 °F (4 °C) and 248 °F (120 °C), including cases with 10% and 20% void to simulate boiling. Typical results are presented in Table 4.6.2; these results show that the spent fuel pool temperature coefficient of reactivity is generally positive for assemblies without inserts (directly applicable to Cases 1, 4, 6, 7 and 9). In these cases, a higher temperature usually results in a higher reactivity, and a maximum pool temperature of 185 °F was conservatively used as the bounding condition. This value is higher than the design basis SFP maximum bulk water temperature limit of 150 °F discussed in Section 5. However, for assemblies with inserts (used in Cases 2, 3 and 8), and for at least one case without inserts, the temperature coefficient is negative, i.e. a lower temperature results in a higher reactivity. In MCNP, the Doppler treatment is only available for 80.33 °F (300K). Therefore, a temperature bias reactivity effect ( $\Delta k$ ) must be determined in CASMO-4, and then included in the final  $k_{\text{eff}}$  calculation. For cases without any inserts (Cases 1, 4, 6, 7 and 9), this bias is the reactivity difference between 80.33 °F (300K) and 185 °F. For cases that contain cells with and without inserts (Cases 2, 3 and 8) the positive reactivity effect of temperature increases on the cells without inserts would be partially offset by the negative temperature coefficient of the cells with inserts. However, since it is difficult to quantify the extent of this competition of temperature effects, conservatively the larger magnitude reactivity effect is used. Overall, the maximum reactivity effect of changes in pool water temperature is larger for increases in temperature, and therefore, this is used as a bias in all final  $k_{\text{eff}}$  calculations. Conservatively, the temperature bias effect is determined from 68 °F (20 °C) (this value is selected to be lower than 80.33 °F / 300K) to 185 °F, and the maximum number from each of these generalized storage arrangements, i.e. Region 1, Region 2, and Region 2 with inserts, is used in the respective final  $k_{\text{eff}}$  calculations. Cases with RCCAs (i.e.

Cases 5 and 10) were not explicitly considered in these analyses because they are similar to the cases with inserts and are therefore bounded by the temperature bias effect for the cells without inserts.

Temperatures exceeding 185 °F are considered accident conditions, and are discussed in Section 4.6.13.1.

#### 4.6.4 Manufacturing Tolerances

In calculating the final value of  $k_{\text{eff}}$ , the effect of manufacturing tolerances on reactivity must be included. CASMO-4 was used to quantify these effects. As allowed in [4.7.6], the methodology employed to quantify the tolerance effects combines both the worst-case bounding value and the sensitivity study approaches. The required evaluations include determining the reactivity effect of tolerances in the rack dimensions (see Table 4.4.5), tolerances of the fuel dimensions (see Table 4.4.1), tolerances of the RCCA specifications (see Table 4.4.3), and tolerances of the inserts (see Table 4.4.6). In addition to the tolerances specified in these tables, an enrichment tolerance of 0.05 wt% is analyzed. Note that for items such as fuel cladding, the dimensions, i.e. inner diameter, outer diameter and thickness, are linked and can therefore not be varied independently of each other. As a result, when evaluating the tolerance effects for this item, only two variations are performed: for the outer diameter, with a constant thickness, and for the inner diameter, with a corresponding change in thickness. Note also that no width tolerance for the insert is analyzed, since all MCNP calculations are performed with the minimum insert width. As for the bounding assembly, tolerance effect calculations are performed for a range of enrichments, cooling times and burnups. Tolerance effects on reactivity are established separately for Region 1 and Region 2 racks. The reference condition for each region is the condition with nominal dimensions and properties. Additionally, the presence of RCCAs is considered in assemblies stored in Region 1 racks, and the presence of inserts is considered in Region 2 racks.

To determine the  $\Delta k$  associated with a specific manufacturing tolerance, the  $k_{inf}$  calculated for the reference condition is compared to the  $k_{inf}$  from a calculation with the tolerance included. Note that for the individual parameters associated with a tolerance, no statistical approach is utilized. Instead, the full tolerance value is utilized to determine the maximum reactivity effect. All of the  $\Delta k$  values from the various tolerance effect calculations for Region 1, Region 2, or Region 2 with inserts are statistically combined (square root of the sum of the squares) to determine the final reactivity allowance for manufacturing tolerances. Only the  $\Delta k$  values in the positive direction (increasing reactivity) were used in the statistical combination. In order to develop a worst case combination of reactivity tolerance effects, the largest value of the combined reactivity effect for a fuel storage region (Region 1, Region 2, or Region 2 w/inserts) is used over the whole range of enrichment, burnup and cooling time combinations for that region. The tolerance values resulting in the highest combined reactivity effects are listed in Table 4.6.3. This table only shows statistically combined fuel tolerances, except for fuel density and enrichment, which are listed individually.

#### 4.6.5 Temperature Bias and Uncertainties at Higher Soluble Boron Levels

For calculations with soluble boron in the pool under normal conditions, a separate set of reactivity effects due to uncertainties and biases are calculated for a soluble boron concentration of 800 ppm. This boron value exceeds the soluble boron concentration required to maintain  $k_{eff} \leq 0.95$  under non-accident conditions. For the  $k_{eff}$  calculations performed with soluble boron, the larger of the uncertainty and bias effects on reactivity from either the pure water condition or 800 ppm are used.

For accident conditions, additional temperature bias effects on reactivity were determined at 1000 ppm and 1500 ppm, and for Region 2 only. Uncertainty effects were not evaluated at these soluble boron levels, since the calculations performed at 0 ppm and 800 ppm indicate that the

effect of the soluble boron concentration on uncertainties is negligible. Uncertainties applied at these higher soluble boron levels are therefore determined by linear extrapolation from the pure water and 800 ppm values. Region 1 and storage arrangements involving inserts were not evaluated at these soluble boron levels, because the bounding accident condition is for Case 9, which is in Region 2 and contains no inserts.

#### 4.6.6 Uncertainty in Depletion Calculations and Burnup Records

CASMO-4 was used to perform the depletion calculations. Since critical experiment data with spent fuel is not available for determining the uncertainty in burnup-dependent reactivity calculations, an allowance for uncertainty in reactivity was assigned based upon other considerations. Assuming the uncertainty in depletion calculations is less than 5% of the total reactivity decrement, a burnup dependent uncertainty may be assigned. This approach is consistent with the methodology described in [4.7.6]. The uncertainty is statistically combined with the other reactivity allowances when determining the maximum  $k_{\text{eff}}$  for comparison with the limit of 0.95 for normal and accident conditions.

The uncertainty of the recorded burnup value is 5%. The reactivity effect of this uncertainty is determined and is statistically combined with the other reactivity allowances when determining the maximum  $k_{\text{eff}}$  for comparison with the 0.95 limit applied to normal and accident conditions.

Both uncertainties are included in the evaluations to determine the soluble boron concentration under normal, abnormal and accident conditions.

#### 4.6.7 Isotopic Compositions

To perform the criticality evaluation for spent fuel in MCNP, the isotopic composition of the fuel is calculated with the depletion code CASMO and then this isotopic composition is specified as

input data in the MCNP run. Three isotopes or grouped isotopes in CASMO do not have a corresponding cross section in the standard MCNP cross section library. These are Pm-148M, and the lumped fission products LFP1 and LFP2. However, the CASMO cross sections for these isotopes have been transferred into a MCNP cross section format, and these cross sections are used in all MCNP4a calculations.

The CASMO calculations that produce isotopic compositions for use in MCNP were performed generically, with one set of depletion steps for each enrichment, at burnup increments of 2.5 GWD/MTU or less. The isotopic composition for any given burnup is then determined by linear interpolation.

#### 4.6.8 Eccentric Fuel Assembly Positioning

The fuel assembly is assumed to be normally located in the center of the storage rack cell. Nevertheless, some MCNP4a calculations were performed with fuel assemblies positioned in the corner of storage rack cells (yielding a four-assembly cluster at closest approach). These calculations indicate that eccentric fuel positioning results in an increase in reactivity for Region 1, and in a significant decrease in reactivity for Region 2. Therefore, for Region 1 calculations, the maximum calculated reactivity difference (0.0098  $\Delta k$ ) between the centered and eccentric positioning of fuel is included in the uncertainties applied to derive the final  $k_{\text{eff}}$ .

#### 4.6.9 Reactivity Effect of Axial Burnup and Enrichment Distribution

Initially, fuel loaded into the core will burn with a slightly skewed cosine-shaped power distribution. With continued depletion of fissile material, the axial power distribution will tend to flatten, as fuel rods become more highly burned at mid-plane elevations, compared to their upper and lower ends. This effect of changing power shape, along with spectrum effects enhancing plutonium production, will cause highly burned fuel to have more fissile material

present at the upper and lower ends of fuel rods than at the rod's mid-plane elevation. Absent other effects, this distribution of fissile material would tend to shift peak power production in burned fuel rods to their upper and lower end regions. Observed trends of axial power shapes in highly burned fuel do show increasing contributions to power production by the fuel rod end regions. However, neutron leakage is also greater near rod ends so the importance of this fissile material distribution to sustaining the fission reaction is lessened, i.e. leakage partially compensates for the greater relative quantity of fissile material near rod ends in highly burned fuel. Feedback effects inherent in the shifting regions of peak power production ensure that axial burnup distributions are largely self-regulating, thus producing a relatively flat burnup distribution for highly burned assemblies with the exception of each end where leakage is significant. Consequently, it would be expected that over most of the burnup history, distributed burnup fuel assemblies would exhibit a slightly lower reactivity than that calculated for the average burnup since the lower burnup fuel at each end occurs in lower importance regions.

Generic analytic results of the axial burnup effect for assemblies without axial blankets have been provided by Turner [4.7.7] based upon calculated and measured axial burnup distributions. These analyses confirm the minor and generally negative reactivity effect of the axially distributed burnup, becoming positive at burnups greater than about 30 GWD/MTU. The trends observed [4.7.7] suggest the possibility of a small positive reactivity effect above 30 GWD/MTU increasing to slightly over 1%  $\Delta k$  at 40 GWD/MTU. Since the required burnup for some enrichments and cases is greater than 30 GWD/MTU, the reactivity effect of the axially distributed burnup must be considered.

The plant also possesses fuel assemblies with natural or low enriched uranium (between 0.72 and 0.77 wt%  $^{235}\text{U}$ , modeled as 0.74 wt%  $^{235}\text{U}$ ) axial blankets on the ends, which affect the axial burnup distribution. Conservatively, the profiles resulting in the lowest relative burnup at the upper and lower end of the fuel for twice burned fuel are chosen to be used in the calculations, since the lower burnup results in a higher reactivity.

For lower burnups, the use of the axial burnup profiles could result in a reactivity less than that calculated for an axially constant burnup. Therefore, two calculations are performed for each assembly average burnup: one with an axial burnup distribution (and axial enrichment distribution for blanketed assemblies), and one for an axially constant burnup and enrichment. Conservatively, the higher reactivity from these two calculations is used as the representative value for the corresponding burnup.

Three different axial burnup/enrichment profiles are therefore used in the analyses. The first two are the axial burnup distributions for blanketed and non-blanketed fuel. The blanketed fuel has natural uranium at the upper and lower end, whereas non-blanketed fuel has a constant enrichment over the entire axial length. The third distribution is the axially constant burnup and enrichment profile, which conservatively ensures that only an increase in reactivity due to the axial burnup profiles is considered, but not a reduction. In the spent fuel pool, neighboring assemblies can have different axial burnup and enrichment distributions. To avoid evaluating the numerous permutations of adjacent distributions when developing loading curves, reactivity effects of assemblies with different distributions located next to each other are analyzed separately. The relevant difference between the distributions is the axial location that dominates reactivity. For an axially constant burnup, this is the mid-plane elevation of the assembly; for the non-blanketed profile, the dominant axial region is near the top end of the active length; and for the blanketed profile, the dominant region is also near the top of the active length, but at a slightly greater distance from the end of the fuel rod, due to the presence of the axial blanket. The sections that dominate reactivity are therefore not axially aligned between the different distributions. As a result, it is expected that assemblies with different axial distributions but having comparable reactivity (in an infinite arrangement of the same distribution) would show a lower reactivity when placed next to each other in a mixed configuration. To verify this effect, a representative number of configurations with single and mixed distributions were analyzed for Case 1 and Case 3. The reference cases use the same axial distribution for all assemblies. The mixed cases use a checkerboard arrangement of two of the axial distributions. There are therefore two reference cases for each mixed case. Since the two reference cases do not have

exactly the same reactivity, the result of the mixed case is compared to the average reactivity of the two reference cases. In all analyzed cases, the mixed condition produces the expected reduction in reactivity. As an example, here are the results for blanketed and non-blanketed profiles in a Case 3 configuration: The reference cases show calculated neutron multiplication factors of 0.9584 for blanketed fuel and 0.9629 for non-blanketed fuel. The checkerboard configuration of the same two fuel types results in a calculated neutron multiplication factor of only 0.9543, which is even below the lower value of the two reference cases. This and other comparisons show that mixed cases are bounded by cases for a single axial distribution. Therefore, all subsequent calculations will only be performed using a single axial distribution in each calculation. Note that it is still necessary to evaluate blanketed and non-blanketed fuel for each case, since they will have different burnup requirements. Also, it is necessary to evaluate a constant burnup so that no reduction in reactivity is applied as a result of the axial profile.

Calculations for Case 5 and for the misloading accident require modeling of fresh and spent fuel, while calculations for Case 6 use fresh fuel only. In the fresh fuel models, any axial enrichment distribution is conservatively neglected, i.e. fresh assemblies are always modeled as non-blanketed assemblies, regardless of the enrichment.

#### 4.6.10 Calculation of Burnup versus Enrichment Curves

This analysis considers the following parameters and parameter combinations:

- Two fuel storage rack styles, with a total of ten different fuel and insert loading configurations,
- Assemblies with and without axial blankets,
- Fuel enrichments between 1.8 and 4.0 wt%  $^{235}\text{U}$  for non-blanketed fuel,
- Fuel enrichments between 2.5 and 4.5 wt%  $^{235}\text{U}$  for blanketed fuel, and
- Cooling times between 0 and 20 years.

All calculations to establish and validate the burnup versus enrichment curves are performed as full three-dimensional criticality calculations considering the axial burnup distribution of each assembly in the model.

The coefficients of the burnup vs. enrichment curves for all conditions listed above are shown in Table 4.1.1 for non-blanketed assemblies, and in Table 4.1.2 for assemblies containing axial blankets. The required minimum burnup for selected values of initial enrichment are shown in Tables 4.1.3 and 4.1.4.

Fuel specifications for all cases have been chosen to maximize the calculated reactivity. The results of one representative calculation of  $k_{\text{eff}}$  for each case is shown in Table 4.6.4 along with a tabulation of all biases and uncertainties applied to the calculated value prior to comparison with the 1.0  $k_{\text{eff}}$  limit. This table shows that the total addition for each case, i.e. the sum of all the applicable biases and uncertainties varied between 0.0166 delta-k and 0.0360 delta-k. Table 4.6.5 lists the results for the condition producing the highest k-effective in Case 3; this table also shows all individual fuel tolerance reactivity effect values.

The following equation was used to perform the  $k_{\text{eff}}$  calculation:

$$k_{\text{eff}} = k(\text{calc}) + \delta k(\text{bias}) + \delta k(\text{temp}) + \delta k(\text{uncert})$$

where

$$k(\text{calc}) = \text{nominal conditions } k_{\text{eff}}$$

$$\delta k(\text{bias}) = \text{method bias determined from benchmark critical comparisons}$$

$$\delta k(\text{temp}) = \text{temperature bias}$$

$$\delta k(\text{uncert}) = \text{statistical summation of tolerance and uncertainty components}$$

$$= [\text{tolerance}_{(1)}^2 + \text{tolerance}_{(2)}^2 + \text{uncertainty}_{(1)}^2 + \dots ]^{1/2}$$

It should be noted that no correction for axial distribution in burnup is needed since the effect is included explicitly in  $k(\text{calc})$ ; that is, a full 3-D analysis was utilized in all cases. The tolerance and uncertainty components utilized in Table 4.6.5 may be combined statistically using square root of the sum of the squares since they are independent variables.

Additional results from selected calculations for each case are listed in Table 4.6.6; these results identify the fuel specifications for each side of the checkerboard array and present the maximum  $k_{\text{eff}}$  (after application of biases and uncertainties) for the array as a whole when analyzed at these conditions. Note that Case 5 is also treated as a checkerboard pattern, but with the same burnup vs. enrichment curves for both assemblies in the pattern. The highest maximum  $k_{\text{eff}}$  of any case with any analyzed combination of fuel parameters is below the regulatory limit of 1.000 applicable when considering no soluble boron to be present in the fuel pool water. It should be reiterated that these calculations contain significant amounts of embedded safety margin as a result of the underlying conservative assumptions, such as:

- Considering an unrealistically high maximum normal temperature in the pool,
- Depleting fuel at the upper bound in-core moderator temperature,
- Applying a temperature bias and uncertainties calculated as the maximum over the entire burnup / enrichment / cooling time range, and
- No interpolation of cooling times allowed between loading curves.

The selection of fuel specifications for confirmatory calculations, and the embedded conservatisms will ensure that the actual reactivity of the stored fuel array, under the assumed accident condition of the loss of all soluble boron in the pool, will always be below 1.0. All burnup vs. enrichment curves are therefore acceptable and result in reactivity values below the regulatory limit.

#### 4.6.11 Interfaces

The following subsections discuss the analyses and conclusions for the various interface configurations.

##### 4.6.11.1 Case-to-Case Interfaces in the Region 2 Area of the Pool

Interfaces between different fuel storage arrangements within a rack module and across a rack-to-rack gap between Region 2 rack modules are permissible if the following rules are met:

- Each 2x2 configuration in the Region 2 area of the pool that does not contain cells facing the pool wall or Region 1 racks, including overlapping 2x2 configurations, must match one of the analyzed arrangements presented in Cases 1 through 3 or 7 through 9.
- In this context, the term “match” means that the configuration has at least the required number of inserts, RCCAs or empty cells and that the assemblies have at least the required burnup for one of the cases.

The requirement to check overlapping 2x2 configurations considers each cell as part of up to four 2x2 configurations: one each where the cell is the top left, top right, bottom left and bottom right cell of the configuration. All four of these arrangements must match one of the acceptable cases, but not necessarily all of them will match the same case. The application of this requirement will automatically establish rows or columns of boundary cells at the interface, if required. These boundary cells conservatively fulfill the requirements of cells on each side of the interface. As an example, Figure 4.6.1 shows an acceptable interface between Case 1 and Case 3 fuel. Fulfilling the rules stated above creates a boundary between the two cases matching the Case 2 pattern.

Following these rules, every 2x2 configuration matches an analyzed condition, and therefore no interface-specific analyses are required. Gaps between Region 2 rack modules are conservatively neglected, i.e. cells located across a rack-to-rack gap are considered the same as cells directly facing each other within a rack.

The configurations wherein Region 2 cells face the pool wall or Region 1 rack modules require additional analyses and are discussed in Sections 4.6.11.4 and 4.6.11.3, respectively.

#### 4.6.11.2 Case-to-Case Interfaces in the Region 1 Area of the Pool

In Region 1 racks, the same approach is used as in Region 2 racks, i.e. Case-to-Case interfaces within a rack module and across a rack-to-rack gap between Region 1 rack modules are permissible if the following rules are met:

- Each 2x2 configuration in the Region 1 area of the pool, including overlapping 2x2 configurations, must match one of the analyzed arrangements presented in Cases 4 through 6.
- In this context, the term “match” means that the configuration has at least the required number of empty cells or RCCAs and that the assemblies have at least the required burnup for one of the cases.

No special consideration need be given to cells facing the pool wall or other racks. Additionally, Case 4 and Case 5 cells can be used in any combination without following a specific pattern, since Case 5 cells (containing assemblies with RCCAs) are bounded by Case 4 cells (assemblies without RCCAs).

#### 4.6.11.3 Region 1 to Region 2 Interface

Region 1 and Region 2 rack modules are separated by a gap of at least 1 inch. To model the interface with appropriate boundary conditions, a model was generated with 20 Region 2 cells on one side of the gap, and 17 Region 1 cells on the opposite side. Calculations were performed with Cases 1, 2, 3 and 9 fuel in Region 2, and Case 4 fuel in Region 1. For Case 2, the row of fuel in Region 2 cells along the interface contained the required inserts for that case. For Case 9, the required empty cells were interspersed with fuel in the row along the interface. For each interface combination, a representative calculation is performed with both a uniform axial burnup and the limiting non-uniform axial burnup distribution. The results of the interface calculations are then compared with the reference calculations, i.e. the corresponding infinite array Region 1 and Region 2 calculations. The Region 1 calculations typically have a lower calculated  $k_{\text{eff}}$  than the Region 2 calculations, due to application of a different temperature bias. To enable a better comparison, specific Region 1 reference calculations were performed for some of the cases; these calculations produce a calculated  $k_{\text{eff}}$  similar to that for the corresponding Region 2 calculations. The calculated  $k_{\text{eff}}$  of the interface case is then compared to the average of the calculated  $k_{\text{eff}}$  of the two applicable reference cases. For Cases 1, 2 and 9, the interface shows a lower or statistically equivalent reactivity compared to the reference cases. However, for Case 3, the difference exceeds three standard deviations, and is therefore significant. As a result, Case 3 assemblies are not permitted in the row on the interface with Region 1 racks. Cases 7 and 8 were not explicitly analyzed in Region 2 as part of the interface calculations; however, they are permissible since these cases are equivalent to Cases 1 and 2, respectively. Cases 5 and 6 were not explicitly analyzed in Region 1; however, they are permissible Region 1 storage arrangements because they are bounded by Case 4. The restrictions for the Region 1 to Region 2 fuel storage interface are therefore summarized as follows:

- Case 3 assemblies are not to be placed in the outer row of Region 2 racks facing Region 1 racks.

- For Cases 2, 8 and 9 on an interface to a Region 1 rack module, the inserts or empty cells required by these cases, as applicable, must be located in the outer row of the Region 2 rack facing Region 1.

#### 4.6.11.4 Cells facing the Pool Wall in Region 2 Racks

The outer row of Region 2 racks facing a pool wall is designated for storage of more reactive fuel assemblies, regardless of the arrangement of fuel in the remainder of the rack. These more reactive assemblies correspond to the assemblies permitted by Case 3, without any inserts. To qualify this condition for all Region 2 fuel storage arrangements, a single rack MCNP4a model having an 11 x 13 array of cells is used. This stored array of fuel is assumed to face a pool wall on all four sides, and to contain Case 3 cells without inserts in all peripheral locations. This model contains a larger number of peripheral cells than any actual rack in the Turkey Point fuel pool, and will overestimate the reactivity effect of the rack to wall interface. In case any interface with the fuel pool wall would increase the reactivity, this model would show the increase more clearly. Further, this model assures that all possible orientations of inserts are considered in the analysis. For fuel arranged in accordance with Cases 2 and 9, the required inserts or empty cells are placed in the second row from the interface, i.e. directly adjacent to the row with the Case 3 assemblies. For Case 1, variations of the rack to wall distance are analyzed. The results of this study show no statistically significant effect on the reactivity. Therefore, all other cases are analyzed using a fixed distance of about 2 inches.

For each case, the reactivity of the infinite condition is compared to the reactivity of the single rack surrounded by pool walls. In all cases, the rack to wall interface produces a reactivity lower than the reactivity of the infinite rack configuration.

The conclusions applicable to Turkey Point fuel storage are summarized as follows:

- For any 2x2 arrangement in the Region 2 area of the pool that contains cells facing the pool wall, the cells facing the pool wall may contain Case 3 fuel assemblies without inserts. Fuel stored in these cells need not contain an RCCA. Additionally, the 2<sup>nd</sup> row from the pool wall of each 2x2 array containing cells facing the fuel pool wall must comply with the following criteria:
  - Contain at least one insert if fuel placed in the 2<sup>nd</sup> and 3<sup>rd</sup> row of cells matches Case 2 or Case 3 criteria, or
  - Contain at least one empty cell if fuel placed in the 2<sup>nd</sup> and 3<sup>rd</sup> row of cells matches Case 9 criteria.

#### 4.6.11.5 Configurations during Loading and Unloading of Assemblies

The insert is placed into a cell after the fuel assembly has been placed into the cell. Therefore, during the loading and unloading of fuel, a condition could exist wherein a storage location requiring an insert to comply with the final fuel storage loading pattern does not contain that insert during some intermediate steps. However, under such conditions, the same requirements as for the case-to-case interfaces can be applied (see Section 4.6.11.1), which ensures that all configurations conform to an analyzed condition. As an example, Figure 4.6.2 shows the possible loading sequence for an assembly into a cell ultimately requiring an insert in a Case 3 configuration. Performed in reverse order, the steps of Figure 4.6.2 show an unloading sequence for an assembly in a cell containing an insert. All steps of the loading and unloading sequence conform to an analyzed configuration.

#### 4.6.11.6 Interface with the Cask Area Rack

The interface of the racks analyzed in this report and the cask area rack was examined previously in conjunction with the criticality analysis of the cask area rack<sup>†</sup>. These earlier analyses of the interface considered both the condition where the existing racks contain Boraflex and the condition where the existing racks contain no Boraflex. These analyses demonstrated that there is no significant interaction between the cask area rack and either Region 1 or Region 2 of the pool. The distinguishing factor between this interface and others in the SFP is that the cask area rack has Boral panels on the exterior of the rack. Since there is no significant interaction, no interface restrictions are imposed. As a result, the previous interface analysis is applicable to, and consistent with, the conditions analyzed in this section.

#### 4.6.12 Soluble Boron Concentration for Maximum $k_{eff}$ of 0.95

Calculations have been performed to determine the minimum soluble boron concentration in the spent fuel pool necessary to ensure that  $k$ -effective of the fuel pool does not exceed 0.95. For each fuel storage arrangement, calculations are performed at various soluble boron concentrations up to 700 ppm, and the soluble boron concentration necessary to satisfy the regulatory requirement is then determined by linear interpolation. A target of 0.94 is used for the maximum  $k_{eff}$  value, which is lower, i.e. more conservative, than the regulatory limit. The highest minimum soluble boron concentration calculated is 549 ppm, for Cases 2 and 8. The details of this calculation for Case 2 are shown in Table 4.6.7. For added conservatism, a minimum value of 560 ppm is specified for compliance purposes.

---

<sup>†</sup> Appendix 1 to FPL letter L-2002-214, Turkey Point Units 3 and 4 Proposed License Amendments: Addition of Cask Area Spent Fuel Storage Racks, dated November 26, 2002 (Section 4.5.4).

#### 4.6.13 Abnormal and Accident Conditions

The effects on reactivity of credible abnormal and accident conditions are examined in this section. None of the abnormal or accident conditions that have been identified as credible cause the neutron multiplication factor of Turkey Point Unit 3 and Unit 4 fuel pool storage racks to exceed the limiting value of  $k_{\text{eff}} = 0.95$ , considering the presence of soluble boron. The double contingency principle of ANSI N16.1-1975 (and the USNRC letter of April 1978) specifies that it shall require at least two unlikely, independent and concurrent events to produce a criticality accident. This principle precludes the necessity of considering the simultaneous occurrence of multiple accident conditions.

##### 4.6.13.1 Temperature and Water Density Effects

The reactivity effect of fuel pool water temperatures exceeding 185 °F has been calculated. Temperatures of up to 248 °F (120 C) are evaluated, as are local boiling conditions with void percentages up to 20%. The maximum reactivity increase compared to 68 °F is 0.0483 delta-k for Region 1 and 0.0390 delta-k for Region 2. It has been determined that a soluble boron concentration of 775 ppm is required to ensure a maximum  $k_{\text{eff}}$  of 0.95 is not exceeded under these conditions.

##### 4.6.13.2 Dropped Assembly - Horizontal

In the event a fuel assembly is dropped on top of a storage rack module, the dropped assembly will come to rest horizontally on top of the rack with a minimum separation distance of at least 12 inches from the active region of stored fuel. This distance is sufficient to preclude neutron coupling (i.e., it provides an effectively infinite separation). The maximum expected

deformation resulting from seismic or accident conditions will not reduce this minimum spacing to less than 12 inches. Consequently, the horizontal fuel assembly drop accident will not significantly increase reactivity in the fuel storage racks.

#### 4.6.13.3 Dropped Assembly - Vertical

It is also possible to vertically drop an assembly into a location occupied by another assembly. Such a vertical impact would at most cause a small compression of the stored assembly, reducing the water-to-fuel ratio and thereby potentially increasing local reactivity. However, this reactivity increase would be small compared to the increase in reactivity caused by misloading a fresh fuel assembly as discussed in the following section (Section 4.6.13.4.1). The vertical drop event is therefore bounded by this fresh fuel misload accident and no separate calculation is performed.

#### 4.6.13.4 Abnormal Location of a Fuel Assembly

##### 4.6.13.4.1 Misloaded Fresh Fuel Assembly

The misplacement of a fresh unburned fuel assembly could, in the absence of soluble poison, result in exceeding the regulatory limit ( $k_{\text{eff}}$  of 0.95). This could possibly occur if a fresh fuel assembly of the highest permissible enrichment (4.5 wt% U-235) were to be inadvertently misloaded into a Region 2 or Region 1 storage cell intended to be empty (e.g. as in a Case 9 or Case 6 array). The reactivity consequence of these situations was investigated. The bounding case is the misloading of fresh fuel into a Case 9 cell intended to be empty. The evaluation of this case is presented in Table 4.6.8. To assure that the regulatory limit is not exceeded under this condition, a soluble boron concentration of at least 1462 ppm in the spent fuel pool is required. As noted earlier, Turkey Point Technical Specifications require a fuel pool soluble boron concentration of at least 1950 ppm be maintained at all times.

#### 4.6.13.4.2 Mislocated Fresh Fuel Assembly

The mislocation of a fresh unburned fuel assembly, i.e. the accidental placement of an assembly outside of a storage rack adjacent to other fuel assemblies, has also been considered. However, in such a condition, the assembly can face no more than 2 rack walls, and it has water on the other two sides. This condition is therefore bounded by the misloading accident discussed previously, since the misloading accident has a fresh assembly surrounded by four other assemblies.

#### 4.6.13.5 Removed Insert or RCCA

The accidental removal of an insert from a cell or of an RCCA from an assembly is bounded by the misloading accident presented in Section 4.6.13.4.1, since the reactivity effect of removing an insert or RCCA is less than the reactivity effect of inserting a fresh assembly into a cell intended to be empty.

#### 4.6.14 Postulated Damage to Inserts

Prior to selecting the Metamic neutron absorber material and specifying its dimensions for use in criticality and other analyses, FPL performed an insertion test on full-length simulated poison material in the Turkey Point spent fuel storage racks. Full length aluminum chevrons of 0.080" thickness, i.e. approximately the same nominal thickness as considered in this evaluation, were successfully inserted and removed from a sampling of storage cells, including a few empty cells, but with the majority containing spent fuel. At the conclusion of the test campaign the simulated poison inserts were examined for wear or damage. With the exception of minor surface scratching caused by contact with fuel assembly spacer grids, no damage or wear was observed.

Irrespective of these observed results, MCNP4a calculations have been performed to evaluate the reactivity effects of a variety of minor damage conditions to the neutron absorber inserts planned for installation at Turkey Point. To bound any potential damage, analyzed conditions have been chosen that are far more severe than those observed in the test campaign. Results of these calculations show that the reactivity effects of such damage to neutron absorber inserts are insignificant.

#### 4.6.15 Fuel Rod Baskets

Storage of a fuel rod basket in one or more Region 2 cells, instead of a fuel assembly, has been evaluated. The basket is an 8x8 array of stainless steel tubes with the three tubes closest to each corner of the array omitted, i.e. the total number of tubes is  $8 \times 8 - 4 \times 3 = 52$ . The dimensions used in the analysis are listed in Table 4.4.8. Using CASMO, a comparison is performed between the reactivity of a fuel rod basket in a Region 2 rack cell and a fuel assembly with the lowest reactivity for any of the cases in Region 2 racks. For the fuel rod basket, it is conservatively assumed that all tubes are filled with fuel rods, and that all fuel rods consist of fresh fuel of 4.5 wt% enrichment. The fuel with the lowest reactivity requirement for Region 2 racks corresponds to the higher burnup fuel in a Case 7 checkerboard configuration (no inserts). The comparison shows that the rod basket has a significantly lower reactivity than the fuel assembly. Due to this significantly lower reactivity it is not considered necessary to separately evaluate uncertainty effects for the fuel rod basket, which could differ slightly from the uncertainties derived for the fuel assembly. In summary, these calculations demonstrate that a fuel rod basket may be placed in any cell designated for a fuel assembly in Region 2 racks, and that no neutron absorber insert is required in the cell with the fuel rod basket.

#### 4.7. REFERENCES

- [4.7.1] M.G. Natrella, Experimental Statistics, National Bureau of Standards, Handbook 91, August 1963.
- [4.7.2] J.F. Briesmeister, Editor, "MCNP - A General Monte Carlo N-Particle Transport Code, Version 4A," LA-12625, Los Alamos National Laboratory (1993).
- [4.7.3] M. Edenius, K. Ekberg, B.H. Forssén, and D. Knott, "CASMO-4 A Fuel Assembly Burnup Program User's Manual," Studsvik/SOA-95/1, Studsvik of America, Inc. and Studsvik Core Analysis AB (proprietary).
- [4.7.4] D. Knott, "CASMO-4 Benchmark Against Critical Experiments", SOA-94/13, Studsvik of America, Inc., (proprietary).
- [4.7.5] D. Knott, "CASMO-4 Benchmark Against MCNP," SOA-94/12, Studsvik of America, Inc., (proprietary).
- [4.7.6] L.I. Kopp, "Guidance on the Regulatory Requirements for Criticality Analysis of Fuel Storage at Light-Water Reactor Power Plants," NRC Memorandum from L. Kopp to T. Collins, August 19, 1998.
- [4.7.7] S.E. Turner, "Uncertainty Analysis - Burnup Distributions", presented at the DOE/SANDIA Technical Meeting on Fuel Burnup Credit, Special Session, ANS/ENS Conference, Washington, D.C., November 2, 1988.
- [4.7.8] "CASMO-4 Neutron Library E4LIB-N Dated 020307", Studsvik Report SPP-03/411 Rev. 0.
- [4.7.9] "Study of the Effect of Integral Burnable Absorbers for PWR Burnup Credit", NUREG/CR-6760, USNRC, March 2002.

Table 4.1.1

Coefficients of Loading Curves for Non-Blanketed Assemblies

| Case       | Coefficients <sup>†</sup> |           |           |             |           |            |          |
|------------|---------------------------|-----------|-----------|-------------|-----------|------------|----------|
|            | A                         | B         | C         | D           | E         | F          | G        |
| 1          | 17.5099                   | -0.130912 | -0.143634 | 0.00199657  | -0.235656 | 0.00625103 | -9.1041  |
| 2          | 12.6130                   | 0.436168  | -0.128105 | 0.00275389  | -0.151579 | 0.00377707 | -7.0392  |
| 3          | 11.8419                   | 0.287918  | 0.113820  | -0.00527641 | -0.175033 | 0.00507248 | -9.9305  |
| 4          | 18.1371                   | -0.944126 | 0.253120  | -0.00553408 | -0.151450 | 0.00334051 | -29.3574 |
| 7, Low Bu  | 17.1055                   | -0.116940 | 0.024104  | -0.00410005 | -0.262366 | 0.00761230 | -10.7361 |
| 7, High Bu | 17.9109                   | -0.143928 | -0.308137 | 0.00796481  | -0.209912 | 0.00492410 | -7.4704  |
| 8, Low Bu  | 12.6055                   | 0.361578  | -0.075193 | 0.00118870  | -0.152297 | 0.00386780 | -8.6212  |
| 8, High Bu | 12.6086                   | 0.517311  | -0.185177 | 0.00442008  | -0.150482 | 0.00367344 | -5.3438  |
| 9          | 11.9800                   | 0.158287  | 0.237665  | -0.00688305 | -0.192273 | 0.00492032 | -14.2029 |

<sup>†</sup> See Section 4.1 for the polynomial function.

Table 4.1.2

Coefficients of Loading Curves for Fuel Assemblies containing Axial Blankets

| Case       | Coefficients <sup>†</sup> |           |           |             |           |            |          |
|------------|---------------------------|-----------|-----------|-------------|-----------|------------|----------|
|            | A                         | B         | C         | D           | E         | F          | G        |
| 1          | 13.7900                   | -0.086680 | -0.355570 | 0.00574698  | -0.145745 | 0.00426994 | -2.0705  |
| 2          | 15.3172                   | -0.444842 | -0.114363 | 0.00273060  | -0.162664 | 0.00344467 | -9.1868  |
| 3          | 14.4600                   | -0.372732 | 0.132275  | -0.00617104 | -0.187813 | 0.00526411 | -12.8293 |
| 4          | 18.8602                   | -1.090486 | 0.266387  | -0.00474496 | -0.158563 | 0.00314739 | -30.1637 |
| 7, Low Bu  | 13.4516                   | -0.078364 | -0.266734 | 0.00288411  | -0.147006 | 0.00446530 | -3.3460  |
| 7, High Bu | 14.1212                   | -0.094016 | -0.448138 | 0.00877894  | -0.143511 | 0.00402944 | -0.7808  |
| 8, Low Bu  | 15.4624                   | -0.501267 | -0.065530 | 0.00160009  | -0.161078 | 0.00340497 | -11.2483 |
| 8, High Bu | 15.1701                   | -0.387768 | -0.163521 | 0.00394514  | -0.164014 | 0.00345174 | -7.1273  |
| 9          | 16.2639                   | -0.712257 | 0.175883  | -0.00399237 | -0.166686 | 0.00370969 | -19.5118 |

<sup>†</sup> See Section 4.1 for the polynomial function.

Table 4.1.3

Required Burnup for Selected Values of U-235 Initial Enrichment and Post-Irradiation  
Cooling Time for Non-Blanketed Fuel Assemblies

| Case | Cooling Time | Enrichment |       |       |       |       |
|------|--------------|------------|-------|-------|-------|-------|
|      |              | 1.8        | 2.5   | 3     | 3.5   | 4     |
| 1    | 0            | 21.99      | 33.85 | 42.25 | 50.58 | 58.84 |
|      | 2.5          | 20.65      | 32.13 | 40.25 | 48.31 | 56.29 |
|      | 5            | 19.48      | 30.63 | 38.51 | 46.33 | 54.08 |
|      | 10           | 17.64      | 28.29 | 35.82 | 43.28 | 50.68 |
|      | 15           | 16.45      | 26.83 | 34.16 | 41.42 | 48.62 |
|      | 20           | 15.93      | 26.25 | 33.54 | 40.76 | 47.92 |
| 2    | 0            | 17.08      | 27.22 | 34.73 | 42.45 | 50.39 |
|      | 2.5          | 16.13      | 26.03 | 33.36 | 40.90 | 48.67 |
|      | 5            | 15.31      | 24.99 | 32.16 | 39.56 | 47.17 |
|      | 10           | 14.02      | 23.37 | 30.31 | 37.46 | 44.83 |
|      | 15           | 13.21      | 22.36 | 29.15 | 36.16 | 43.39 |
|      | 20           | 12.88      | 21.96 | 28.70 | 35.67 | 42.85 |
| 3    | 0            | 12.32      | 21.47 | 28.19 | 35.04 | 42.04 |
|      | 2.5          | 11.84      | 20.71 | 27.22 | 33.87 | 40.67 |
|      | 5            | 11.41      | 20.04 | 26.38 | 32.86 | 39.49 |
|      | 10           | 10.69      | 18.98 | 25.07 | 31.30 | 37.68 |
|      | 15           | 10.17      | 18.28 | 24.25 | 30.37 | 36.63 |
|      | 20           | 9.83       | 17.96 | 23.94 | 30.06 | 36.32 |
| 4    | 0            | 0.23       | 10.08 | 16.56 | 22.56 | 28.08 |
|      | 2.5          | 0.18       | 9.79  | 16.08 | 21.90 | 27.25 |
|      | 5            | 0.14       | 9.53  | 15.66 | 21.33 | 26.52 |
|      | 10           | 0.08       | 9.11  | 14.99 | 20.40 | 25.34 |
|      | 15           | 0.05       | 8.84  | 14.55 | 19.79 | 24.56 |
|      | 20           | 0.03       | 8.70  | 14.33 | 19.48 | 24.16 |

Table 4.1.3 (continued)  
 Required Burnup for Selected Values of U-235 Initial Enrichment and Post-Irradiation  
 Cooling Time for Non-Blanketed Fuel Assemblies

| Case                 | Cooling Time | Enrichment |       |       |       |       |
|----------------------|--------------|------------|-------|-------|-------|-------|
|                      |              | 1.8        | 2.5   | 3     | 3.5   | 4     |
| 7,<br>Low<br>Burnup  | 0            | 19.67      | 31.30 | 39.53 | 47.70 | 55.81 |
|                      | 2.5          | 18.61      | 29.81 | 37.74 | 45.61 | 53.42 |
|                      | 5            | 17.67      | 28.51 | 36.18 | 43.79 | 51.35 |
|                      | 10           | 16.15      | 26.47 | 33.77 | 41.01 | 48.20 |
|                      | 15           | 15.11      | 25.18 | 32.30 | 39.36 | 46.36 |
|                      | 20           | 14.55      | 24.63 | 31.76 | 38.83 | 45.85 |
| 7,<br>High<br>Burnup | 0            | 24.30      | 36.41 | 44.97 | 53.45 | 61.87 |
|                      | 2.5          | 22.69      | 34.45 | 42.76 | 51.01 | 59.17 |
|                      | 5            | 21.29      | 32.75 | 40.85 | 48.87 | 56.82 |
|                      | 10           | 19.13      | 30.11 | 37.86 | 45.55 | 53.16 |
|                      | 15           | 17.80      | 28.48 | 36.01 | 43.48 | 50.88 |
|                      | 20           | 17.31      | 27.86 | 35.30 | 42.68 | 49.98 |
| 8,<br>Low<br>Burnup  | 0            | 15.24      | 25.15 | 32.45 | 39.93 | 47.59 |
|                      | 2.5          | 14.42      | 24.08 | 31.20 | 38.50 | 45.98 |
|                      | 5            | 13.70      | 23.14 | 30.11 | 37.25 | 44.58 |
|                      | 10           | 12.56      | 21.68 | 28.41 | 35.32 | 42.41 |
|                      | 15           | 11.83      | 20.76 | 27.35 | 34.12 | 41.07 |
|                      | 20           | 11.51      | 20.38 | 26.92 | 33.65 | 40.56 |
| 8,<br>High<br>Burnup | 0            | 19.03      | 29.41 | 37.14 | 45.12 | 53.37 |
|                      | 2.5          | 17.96      | 28.09 | 35.64 | 43.45 | 51.52 |
|                      | 5            | 17.02      | 26.94 | 34.34 | 42.00 | 49.91 |
|                      | 10           | 15.57      | 25.16 | 32.32 | 39.73 | 47.41 |
|                      | 15           | 14.67      | 24.05 | 31.06 | 38.33 | 45.86 |
|                      | 20           | 14.32      | 23.62 | 30.58 | 37.80 | 45.27 |
| 9                    | 0            | 7.87       | 16.74 | 23.16 | 29.67 | 36.25 |
|                      | 2.5          | 7.62       | 16.16 | 22.36 | 28.64 | 35.00 |
|                      | 5            | 7.38       | 15.66 | 21.66 | 27.75 | 33.91 |
|                      | 10           | 6.99       | 14.85 | 20.56 | 26.35 | 32.22 |
|                      | 15           | 6.69       | 14.31 | 19.85 | 25.46 | 31.16 |
|                      | 20           | 6.49       | 14.04 | 19.53 | 25.10 | 30.74 |

Table 4.1.4

Required Burnup for Selected Values of U-235 Initial Enrichment and Post-Irradiation  
Cooling Time for Blanketed Fuel Assemblies

| Case | Cooling Time | Enrichment |       |       |       |       |
|------|--------------|------------|-------|-------|-------|-------|
|      |              | 2.5        | 3     | 3.3   | 4     | 4.5   |
| 1    | 0            | 31.86      | 38.52 | 42.49 | 51.70 | 58.23 |
|      | 2.5          | 30.17      | 36.65 | 40.53 | 49.50 | 55.86 |
|      | 5            | 28.67      | 35.02 | 38.81 | 47.58 | 53.80 |
|      | 10           | 26.31      | 32.45 | 36.11 | 44.60 | 50.61 |
|      | 15           | 24.76      | 30.80 | 34.41 | 42.76 | 48.67 |
|      | 20           | 24.03      | 30.09 | 33.70 | 42.06 | 47.99 |
| 2    | 0            | 26.33      | 32.76 | 36.52 | 44.96 | 50.73 |
|      | 2.5          | 25.09      | 31.34 | 34.98 | 43.16 | 48.73 |
|      | 5            | 24.00      | 30.08 | 33.61 | 41.55 | 46.96 |
|      | 10           | 22.25      | 28.04 | 31.41 | 38.97 | 44.09 |
|      | 15           | 21.06      | 26.67 | 29.92 | 37.20 | 42.14 |
|      | 20           | 20.44      | 25.94 | 29.13 | 36.27 | 41.10 |
| 3    | 0            | 20.99      | 27.20 | 30.83 | 39.05 | 44.69 |
|      | 2.5          | 20.19      | 26.18 | 29.68 | 37.59 | 43.02 |
|      | 5            | 19.48      | 25.28 | 28.67 | 36.32 | 41.57 |
|      | 10           | 18.32      | 23.85 | 27.07 | 34.35 | 39.32 |
|      | 15           | 17.50      | 22.89 | 26.04 | 33.11 | 37.94 |
|      | 20           | 17.04      | 22.42 | 25.56 | 32.62 | 37.44 |
| 4    | 0            | 10.17      | 16.60 | 20.20 | 27.83 | 32.62 |
|      | 2.5          | 9.87       | 16.11 | 19.59 | 26.96 | 31.57 |
|      | 5            | 9.60       | 15.67 | 19.06 | 26.19 | 30.62 |
|      | 10           | 9.18       | 14.98 | 18.20 | 24.94 | 29.10 |
|      | 15           | 8.92       | 14.52 | 17.62 | 24.08 | 28.04 |
|      | 20           | 8.82       | 14.30 | 17.32 | 23.61 | 27.45 |

Table 4.1.4 (continued)

Required Burnup for Selected Values of U-235 Initial Enrichment and Post-Irradiation  
Cooling Time for Blanketed Fuel Assemblies

| Case                 | Cooling Time | Enrichment |       |       |       |       |
|----------------------|--------------|------------|-------|-------|-------|-------|
|                      |              | 2.5        | 3     | 3.3   | 4     | 4.5   |
| 7,<br>Low<br>Burnup  | 0            | 29.79      | 36.30 | 40.19 | 49.21 | 55.60 |
|                      | 2.5          | 28.30      | 34.64 | 38.42 | 47.20 | 53.42 |
|                      | 5            | 26.97      | 33.17 | 36.87 | 45.45 | 51.53 |
|                      | 10           | 24.86      | 30.85 | 34.43 | 42.73 | 48.61 |
|                      | 15           | 23.44      | 29.35 | 32.88 | 41.05 | 46.85 |
|                      | 20           | 22.73      | 28.66 | 32.20 | 40.41 | 46.23 |
| 7,<br>High<br>Burnup | 0            | 33.93      | 40.74 | 44.80 | 54.20 | 60.86 |
|                      | 2.5          | 32.04      | 38.67 | 42.63 | 51.80 | 58.29 |
|                      | 5            | 30.37      | 36.86 | 40.74 | 49.71 | 56.06 |
|                      | 10           | 27.75      | 34.04 | 37.79 | 46.47 | 52.61 |
|                      | 15           | 26.07      | 32.25 | 35.94 | 44.47 | 50.51 |
|                      | 20           | 25.34      | 31.51 | 35.19 | 43.71 | 49.75 |
| 8,<br>Low<br>Burnup  | 0            | 24.27      | 30.63 | 34.32 | 42.58 | 48.18 |
|                      | 2.5          | 23.17      | 29.33 | 32.91 | 40.90 | 46.31 |
|                      | 5            | 22.19      | 28.18 | 31.65 | 39.41 | 44.65 |
|                      | 10           | 20.60      | 26.32 | 29.63 | 37.00 | 41.97 |
|                      | 15           | 19.53      | 25.05 | 28.25 | 35.36 | 40.13 |
|                      | 20           | 18.96      | 24.38 | 27.51 | 34.47 | 39.14 |
| 8,<br>High<br>Burnup | 0            | 28.37      | 34.89 | 38.71 | 47.35 | 53.29 |
|                      | 2.5          | 27.02      | 33.34 | 37.05 | 45.41 | 51.15 |
|                      | 5            | 25.82      | 31.97 | 35.57 | 43.69 | 49.26 |
|                      | 10           | 23.90      | 29.77 | 33.20 | 40.93 | 46.22 |
|                      | 15           | 22.60      | 28.28 | 31.59 | 39.05 | 44.14 |
|                      | 20           | 21.93      | 27.50 | 30.75 | 38.06 | 43.05 |
| 9                    | 0            | 16.70      | 22.87 | 26.40 | 34.15 | 39.25 |
|                      | 2.5          | 16.13      | 22.10 | 25.52 | 32.99 | 37.90 |
|                      | 5            | 15.62      | 21.43 | 24.74 | 31.96 | 36.70 |
|                      | 10           | 14.82      | 20.34 | 23.49 | 30.32 | 34.78 |
|                      | 15           | 14.27      | 19.61 | 22.65 | 29.23 | 33.50 |
|                      | 20           | 13.99      | 19.24 | 22.22 | 28.67 | 32.85 |

Table 4.4.1  
Turkey Point Fuel Assembly Specifications

| Parameter                                      | Value                            |                    |
|--|----------------------------------|--------------------|
|  | OFA / DRFA                       | LOPAR              |
| Assembly type                                  | OFA / DRFA                       | LOPAR              |
| Rod Array Size                                 | 15x15                            |                    |
| Rod Pitch, Inches                              | 0.563 ± [REDACTED]               |                    |
| Active Fuel Length, Inches                     | 144                              |                    |
| Stack Density (g/cm <sup>3</sup> )             | 10.45 ± [REDACTED]               |                    |
| Maximum Nominal Enrichment, wt%                | 4.5                              |                    |
| Total Number of Fuel Rods                      | 204                              |                    |
| Fuel Cladding Outer Diameter, Inches           | 0.422 ± [REDACTED]               |                    |
| Fuel Cladding Inner Diameter, Inches           | 0.3734 ± [REDACTED]              |                    |
| Fuel Cladding Thickness, Inches                | 0.0225 [REDACTED]                |                    |
| Pellet Diameter, Inches                        | 0.3659 ± [REDACTED] <sup>†</sup> |                    |
| Number of Guide/Instrument Tubes               | 20 / 1                           |                    |
| Guide / Instrument Tube Outer Diameter, Inches | 0.533 ± [REDACTED]               | 0.546 ± [REDACTED] |
| Guide / Instrument Tube Inner Diameter, Inches | 0.499 ± [REDACTED]               | 0.512 ± [REDACTED] |
| Guide / Instrument Tube Thickness, Inches      | 0.0147 [REDACTED]                |                    |

<sup>†</sup> See Section 4.3

Table 4.4.2  
Burnable Absorber Specifications

| Parameter   | Value   |
|---|---|
| <i>Wet Annular Burnable Absorber (WABA)</i>       |   |
| Absorber Material                                 | Al <sub>2</sub> O <sub>3</sub> – B <sub>4</sub> C |
| B <sub>4</sub> C Theoretical Density (Fraction)   | 0.7   |
| B-10 in B, Atom Percent                           | 19.9  |
| B-10 Loading, g/cm                                | 0.0060  |
| Poison ID, Inches                                 | 0.2780  |
| Poison OD, Inches                                 | 0.3180  |
| Inner Clad Thickness, Inches                      | 0.0210  |
| Inner Clad OD, Inches                             | 0.2670  |
| Outer Clad Thickness, Inches                      | 0.0260  |
| Outer Clad OD, Inches                             | 0.3810  |
| Clad Material                                     | Zircaloy  |
| Assembly Burnup when Absorber is removed, GWD/MTU | 22  |
| <i>Pyrex Burnable Absorber</i>                    |   |
| Boric Oxide Content, wt%                          | 12.5  |
| B-10 in B, Atom Percent                           | 19.9  |
| Poison ID, Inches                                 | 0.2430  |
| Poison OD, Inches                                 | 0.3960  |
| Inner Clad ID, Inches                             | 0.2235  |
| Inner Clad OD, Inches                             | 0.2365  |
| Outer Clad ID, Inches                             | 0.4005  |
| Outer Clad OD, Inches                             | 0.4390  |
| Clad Material                                     | SS-304  |
| Assembly Burnup when Absorber is removed, GWD/MTU | 16  |

Table 4.4.3  
Control Component Specifications

| Parameter  | Value                                       |
|--|---|
| <i>RCCAs</i>   |   |
| Material   | Silver-Indium-Cadmium (AgInCd)              |
| Silver content, wt%                                      | 80 ± [REDACTED]                             |
| Indium content, wt%                                      | 15 ± [REDACTED]                             |
| Cadmium content, wt%                                     | 5 ± [REDACTED]                              |
| Poison OD, Inches  | 0.3975 ± [REDACTED] and 0.3900 ± [REDACTED] |
| Clad ID, Inches  | 0.4005 ± [REDACTED]                         |
| Clad OD, Inches  | 0.439 ± [REDACTED]                          |
| Clad Material  | SS  |
| Poison Density, g/cm <sup>3</sup>                        | 10.17                                       |
| <i>Hafnium Inserts</i>                                   |   |
| Material   | Hf  |
| Poison OD, Inches  | 0.3700                                      |
| Clad Thickness, Inches                                   | 0.0310                                      |
| Clad OD, Inches  | 0.4400                                      |
| Clad Material  | Zircaloy                                    |
| Poison Density, g/cm <sup>3</sup>                        | 13.225                                      |
| Length, Inches   | 36  |
| Assembly Burnup when Hafnium Insert is inserted, GWD/MTU | 40  |

Table 4.4.4  
Core Operating Parameters for Depletion Analyses

| Parameter                          | Value              |
|------------------------------------|--------------------|
| Soluble Boron Concentration, ppm   | 780                |
| Reactor Specific Power, MW/MtU     | 31.7               |
| Cycle Average Fuel Temperature, °F | 1280               |
| Moderator Temperature, °F          | 611.3 <sup>†</sup> |
| In-Core Assembly Pitch, Inches     | 8.465              |

---

<sup>†</sup> For fuel sections with Hafnium Insert see Section 4.6.2.

Table 4.4.5  
Fuel Rack Dimensions

| Parameter                       | Value              |  |
|---------------------------------|--------------------|--|
|                                 | Region 1           | Region 2                                 |
| Cell ID, Inches                 | 8.75 ± [REDACTED]  | 8.80 ± [REDACTED] and 8.882 <sup>†</sup> |
| Wall Thickness, Inches          | 0.075 ± [REDACTED] | 0.075 ± [REDACTED]                       |
| Cell Pitch, Inches              | 10.60 ± [REDACTED] | 9.0 + [REDACTED]                         |
| Poison Cavity Thickness, Inches | 0.090 ± [REDACTED] | 0.064 ± [REDACTED]                       |
| Sheathing Thickness, Inches     | 0.02 ± [REDACTED]  | 0.02 ± [REDACTED]                        |
| Sheathing Width, Inches         | 7.5 ± [REDACTED]   | 7.5 ± [REDACTED]                         |

<sup>†</sup> See Figure 4.4.2

Table 4.4.6  
 Insert Specification

| Parameter           | Value  |
|---------------------|--|
| Material            | Al – B <sub>4</sub> C  |
| B-10 Loading        | 0.0160 g/cm <sup>2</sup> nom.,<br> |
| Thickness, Inches   | 0.08  <sup>††</sup> .             |
| Panel Width, Inches | 8.5                               |

---

<sup>††</sup> The criticality calculations were performed for a slightly thicker panel than listed in Table 2.5.1. This is acceptable since the B-10 loading used in the analysis bounds the design conditions, and since the reactivity effect of thickness variations is negligible for a given B-10 loading.

Table 4.4.7

Spent Fuel Pool Specifications Used in the Analyses

| Parameter                                   | Value |
|---|-------|
| Thickness of SS Liner on Pool Walls, Inches | 0.25  |
| Maximum Normal Pool Water Temperature, °F   | 185   |

Table 4.4.8

Fuel Rod Basket Specification

| Parameter              | Value   |
|------------------------|---|
| Tube Array             | 8x8 – 4x3 (see text)  |
| Number of Tubes        | 52  |
| Tube OD, Inches        | 0.625  |
| Tube Thickness, Inches | 0.035  |
| Tube Pitch, Inches     | 0.937   |
| Tube Material          | Stainless Steel   |

Table 4.6.1

Comparison of  $k_{inf}$  for Turkey Point Fuel Assembly Types at Representative Conditions

| Assembly Type   | OFA/DRFA | LOPAR   |
|---|----------|---------|
| 3.3 wt% U-235, 0.1 GWD/MTU Burnup                           |          |         |
| Reactivity  | 1.36131  | 1.36127 |
| 3.3 wt% U-235*, 0 years cooling time and 40 GWD/MTU Burnup  |          |         |
| Reactivity  | 1.00179  | 1.00183 |
| 3.3 wt% U-235*, 20 years cooling time and 40 GWD/MTU Burnup |          |         |
| Reactivity  | 0.91983  | 0.91988 |

\*Initial Enrichment

Table 4.6.2

Effect of Changes in Pool Water Temperature on  $k_{inf}$   
for Fuel of 4.5 wt% U-235, 0 Years Cooling Time at 0 ppm Soluble Boron.

| Burnup<br>(GWD/MTU) | 39 °F (4 °C)                        |                    | 68 °F<br>(20 °C) | 80.3 °F (300 K) |                    | 185 °F    |                    |
|---------------------|-------------------------------------|--------------------|------------------|-----------------|--------------------|-----------|--------------------|
|                     | $k_{inf}$                           | delta- $k^\dagger$ | $k_{inf}$        | $k_{inf}$       | delta- $k^\dagger$ | $k_{inf}$ | delta- $k^\dagger$ |
|                     | <i>Region 1</i>                     |                    |                  |                 |                    |           |                    |
| 20                  | 1.03248                             | -0.00400           | 1.03648          | 1.03813         | 0.00165            | 1.05133   | 0.01485            |
| 30                  | 0.96808                             | -0.00399           | 0.97207          | 0.97372         | 0.00165            | 0.98698   | 0.01491            |
| 40                  | 0.90532                             | -0.00402           | 0.90934          | 0.91101         | 0.00167            | 0.92459   | 0.01525            |
|                     | <i>Region 2</i>                     |                    |                  |                 |                    |           |                    |
| 30                  | 1.17241                             | -0.00020           | 1.17261          | 1.17262         | 0.00001            | 1.17134   | -0.00127           |
| 40                  | 1.09663                             | -0.00050           | 1.09713          | 1.09727         | 0.00014            | 1.09717   | 0.00004            |
| 50                  | 1.02421                             | -0.00085           | 1.02506          | 1.02536         | 0.00030            | 1.02668   | 0.00162            |
| 60                  | 0.95815                             | -0.00121           | 0.95936          | 0.95981         | 0.00045            | 0.96262   | 0.00326            |
|                     | <i>Region 2, Cells with Inserts</i> |                    |                  |                 |                    |           |                    |
| 30                  | 0.97393                             | 0.00163            | 0.97230          | 0.97146         | -0.00084           | 0.96199   | -0.01031           |
| 40                  | 0.90863                             | 0.00134            | 0.90729          | 0.90658         | -0.00071           | 0.89837   | -0.00892           |
| 50                  | 0.84650                             | 0.00101            | 0.84549          | 0.84494         | -0.00055           | 0.83816   | -0.00733           |
| 60                  | 0.79030                             | 0.00068            | 0.78962          | 0.78922         | -0.00040           | 0.78389   | -0.00573           |

<sup>†</sup> Relative to 20 °C

Table 4.6.3

Values of Tolerances and Uncertainties Yielding the Maximum Combined Reactivity Effect for  
Each Region

| <b>Tolerance</b>   | <b>Region 1</b><br>(@ 1.8 w/o U-235,<br>0.1 GWD/MtU, 0<br>year cooling) | <b>Region 2</b><br>(@ 1.8 w/o U-235, 4<br>GWD/MtU, 20 year<br>cooling) | <b>Region 2 with Insert</b><br>(@ 1.8 w/o U-235, 4<br>GWD/MtU, 20 year<br>cooling) |
|--|---|--|--|
| <i>Rack Tolerances</i>   |   |  |  |
| <b>Cell ID</b>   | 0.0001  | 0.0019   | 0.0012   |
| <b>Wall Thickness</b>  | 0.0046  | 0.0049   | 0.0002   |
| <b>Cell Pitch</b>  | 0.0124  | n/a  | n/a  |
| <b>Sheathing Thickness</b>   | 0.0014  | n/a <sup>†</sup>   | n/a <sup>†</sup>   |
| <b>Boraflex Gap Thickness</b>  | 0.0002  | negligible   | negligible   |
| <i>Fuel Tolerances</i>   |   |  |  |
| <b>Density</b>   | 0.0030  | 0.0017   | 0.0030   |
| <b>Enrichment</b>  | 0.0085  | 0.0080   | 0.0071   |
| <b>Other</b><br>(Statistically Combined)                                       | 0.0019  | 0.0013   | 0.0014   |
| <i>Insert &amp; RCCA Tolerances</i>  |   |  |  |
| <b>All Insert/RCCA</b><br><b>Tolerances (Statistically</b><br><b>Combined)</b> | 0.0043<br>(RCCA)  | n/a  | 0.0029<br>(Insert)   |
| <b>All Tolerances</b><br>(Statistically Combined)                              | 0.0162<br>0.0169 with<br>RCCA   | 0.0098   | 0.0085   |

<sup>†</sup> included in wall thickness tolerance

Table 4.6.4

Representative Calculation for each Case

| Case                       | 1      | 2      | 3      | 4      | 5              |
|----------------------------|--------|--------|--------|--------|----------------|
| Region                     | 2      | 2      | 2      | 1      | 1              |
| Enrichment                 | 4.5    | 4.5    | 4.5    | 4.5    | 4.5            |
| Burnup                     | 58.23  | 50.73  | 44.69  | 32.62  | 32.62<br>and 0 |
| Cooling Time               | 0      | 0      | 0      | 0      | 0              |
| Calculated k-eff           | 0.9777 | 0.9798 | 0.9772 | 0.9573 | 0.9428         |
| Bias                       | 0.0009 | 0.0009 | 0.0009 | 0.0009 | 0.0009         |
| Temperature Correction     | 0.0058 | 0.0058 | 0.0058 | 0.0155 | 0.0155         |
| Uncertainties              |        |        |        |        |                |
| Bias                       | 0.0011 | 0.0011 | 0.0011 | 0.0011 | 0.0011         |
| Calculational <sup>†</sup> | 0.0010 | 0.0010 | 0.0010 | 0.0010 | 0.0010         |
| Eccentricity               | 0.0000 | 0.0000 | 0.0000 | 0.0098 | 0.0098         |
| Tolerances                 | 0.0098 | 0.0098 | 0.0098 | 0.0162 | 0.0169         |
| Total Uncertainties        | 0.0099 | 0.0099 | 0.0099 | 0.0190 | 0.0196         |
| Total Addition             | 0.0166 | 0.0166 | 0.0166 | 0.0354 | 0.0360         |
| Maximum k-eff              | 0.9943 | 0.9964 | 0.9938 | 0.9927 | 0.9788         |

<sup>†</sup> Two times the standard deviation of the calculated  $k_{\text{eff}}$

Table 4.6.4 (continued)

Representative Calculation for each Case

| Case                       | 6      | 7                     | 8                     | 9      | 10     |
|----------------------------|--------|-----------------------|-----------------------|--------|--------|
| Region                     | 1      | 2                     | 2                     | 2      | 2      |
| Enrichment                 | 4.5    | 4.5                   | 4.5                   | 4.5    | 4.5    |
| Burnup                     | 0      | 55.60<br>and<br>60.86 | 48.18<br>and<br>53.29 | 39.25  | 50.73  |
| Cooling Time               | 0      | 0                     | 0                     | 0      | 0      |
| Calculated k-eff           | 0.9163 | 0.9791                | 0.9793                | 0.9752 | 0.9700 |
| Bias                       | 0.0009 | 0.0009                | 0.0009                | 0.0009 | 0.0009 |
| Temperature Correction     | 0.0155 | 0.0058                | 0.0058                | 0.0058 | 0.0058 |
| Uncertainties              |        |                       |                       |        |        |
| Bias                       | 0.0011 | 0.0011                | 0.0011                | 0.0011 | 0.0011 |
| Calculational <sup>†</sup> | 0.0012 | 0.0010                | 0.0010                | 0.0010 | 0.0010 |
| Eccentricity               | 0.0098 | 0.0000                | 0.0000                | 0.0000 | 0.0000 |
| Tolerances                 | 0.0162 | 0.0098                | 0.0098                | 0.0098 | 0.0098 |
| Total Uncertainties        | 0.0190 | 0.0099                | 0.0099                | 0.0099 | 0.0099 |
| Total Addition             | 0.0354 | 0.0166                | 0.0166                | 0.0166 | 0.0166 |
| Maximum k-eff              | 0.9517 | 0.9957                | 0.9959                | 0.9918 | 0.9866 |

<sup>†</sup> Two times the standard deviation of the calculated  $k_{eff}$

Table 4.6.5

Bounding Results for Case 3 without Soluble Boron

| Description  | Reactivity or Reactivity Effect |                              |
|--|---------------------------------|------------------------------|
| Case 3 MCNP Base Calculation, (2.5 wt% U-235 initial enrichment, 20.99 GWD/MTU, axially constant burnup, 0 years cooling time) |                                 | 0.9811                       |
| Calculational Bias   |                                 | 0.0009                       |
| Temperature Bias   |                                 | 0.0058                       |
| Axial Burnup Distribution  |                                 | included in Base Calculation |
| Uncertainties <sup>†</sup> :   |                                 |                              |
| Calculational (2*Sigma)  | 0.0010                          |                              |
| Bias Uncertainty   | 0.0011                          |                              |
| Rack Cell ID   | 0.00188                         |                              |
| Rack Wall Thickness  | 0.00493                         |                              |
| Fuel Enrichment  | 0.00797                         |                              |
| Fuel Density   | 0.00171                         |                              |
| Fuel Rod Pitch   | 0.00096                         |                              |
| Fuel Clad OD   | 0.00015                         |                              |
| Fuel Clad ID   | 0.00084                         |                              |
| Fuel Pellet OD   | 0.00023                         |                              |
| Guide Tube OD  | 0.00001                         |                              |
| Guide Tube ID  | 0.00013                         |                              |
| Fuel Eccentricity  | negative                        |                              |
| Statistically Combined Uncertainties   |                                 | 0.0099                       |
| Total Additions (Biases and Uncertainties)   |                                 | 0.0166                       |
| Maximum $k_{eff}$  |                                 | 0.9977                       |
| Regulatory Limit   |                                 | 1.0000                       |

<sup>†</sup> Although Case 3 contains inserts, conservatively the uncertainties for non-insert conditions are used since they result in a higher combined uncertainty. Therefore, no insert uncertainties are listed here.

Table 4.6.6

Results of Additional Selected Calculations for each Case

| <i>Case 1</i>                       |               |                |                 |                |
|-------------------------------------|---------------|----------------|-----------------|----------------|
| <b>Enr/Bu/Cool/Type<sup>†</sup></b> | 3.0/42.25/0/N | 4.5/47.99/20/B | 3.3/40.53/2.5/B | 3.0/34.16/15/N |
| <b>max. k<sub>eff</sub></b>         | 0.9972        | 0.9851         | 0.9920          | 0.9960         |
| <i>Case 2</i>                       |               |                |                 |                |
| <b>Enr/Bu/Cool/Type</b>             | 3.0/32.76/0/B | 4.0/42.85/20/N | 3.3/34.98/2.5/B | 3.0/29.15/15/N |
| <b>max. k<sub>eff</sub></b>         | 0.9977        | 0.9822         | 0.9930          | 0.9922         |
| <i>Case 3</i>                       |               |                |                 |                |
| <b>Enr/Bu/Cool/Type</b>             | 2.5/20.99/0/B | 1.8/11.41/5/N  | 3.3/29.68/2.5/B | 3.0/24.25/15/N |
| <b>max. k<sub>eff</sub></b>         | 0.9977        | 0.9827         | 0.9931          | 0.9880         |
| <i>Case 4</i>                       |               |                |                 |                |
| <b>Enr/Bu/Cool/Type</b>             | 2.5/10.08/0/N | 1.8/0.23/0/N   | 3.3/19.59/2.5/B | 3.0/14.55/15/N |
| <b>max. k<sub>eff</sub></b>         | 0.9952        | 0.9769         | 0.9895          | 0.9897         |
| <i>Case 5</i>                       |               |                |                 |                |
| <b>Enr/Bu/Cool/Type<br/>1</b>       | 2.5/10.17/0/B | 4.5/32.62/0/B  | 1.8/0.23/0/N    | 4.0/28.08/0/N  |
| <b>Enr/Bu/Cool/Type<br/>2</b>       | 4.5/0/0/N     | 4.5/0/0/N      | 4.5/0/0/N       | 4.5/0/0/N      |
| <b>max. k<sub>eff</sub></b>         | 0.9799        | 0.9788         | 0.9706          | 0.9771         |

<sup>†</sup> Enr = Enrichment in wt%; Bu = Burnup in GWD/MTU; Cool = Cooling Time in years;  
 Type = B for blanketed fuel, N for non-blanketed fuel;  
 1 & 2 = Two assemblies in Checkerboard Pattern

Table 4.6.6 (continued)

Results of Additional Selected Calculations for each Case

| <i>Case 7</i>                             |               |                |                 |                |
|---|---------------|----------------|-----------------|----------------|
| <b>Enr/Bu/Cool/Type<br/>1<sup>†</sup></b> | 3.0/36.30/0/B | 4.5/46.23/20/B | 3.3/38.42/2.5/B | 3.0/32.30/15/N |
| <b>Enr/Bu/Cool/Type<br/>2</b>             | 3.0/40.74/0/B | 4.5/49.75/20/B | 3.3/42.63/2.5/B | 3.0/36.01/15/N |
| <b>max. k<sub>eff</sub></b>               | 0.9976        | 0.9845         | 0.9916          | 0.9955         |
| <i>Case 8</i>                             |               |                |                 |                |
| <b>Enr/Bu/Cool/Type<br/>1</b>             | 3.0/32.45/0/N | 4.0/40.56/20/N | 3.3/32.91/2.5/B | 3.0/27.35/15/N |
| <b>Enr/Bu/Cool/Type<br/>2</b>             | 3.0/37.14/0/N | 4.0/45.27/20/N | 3.3/37.05/2.5/B | 3.0/31.06/15/N |
| <b>max. k<sub>eff</sub></b>               | 0.9984        | 0.9829         | 0.9933          | 0.9917         |
| <i>Case 9</i>                             |               |                |                 |                |
| <b>Enr/Bu/Cool/Type</b>                   | 2.5/16.7/0/B  | 4.0/30.74/20/N | 3.3/25.52/2.5/B | 3.0/19.85/15/N |
| <b>max. k<sub>eff</sub></b>               | 0.9968        | 0.9836         | 0.9879          | 0.9885         |
| <i>Case 10</i>                            |               |                |                 |                |
| <b>Enr/Bu/Cool/Type</b>                   | 4.0/50.39/0/N | 4.0/42.85/20/N | 3.3/31.41/10/B  | 3.0/30.31/10/N |
| <b>max. k<sub>eff</sub></b>               | 0.9865        | 0.9754         | 0.9850          | 0.9846         |

<sup>†</sup> Enr = Enrichment in wt%; Bu = Burnup in GWD/MTU; Cool = Cooling Time in years;  
 Type = B for blanketed fuel, N for non-blanketed fuel;  
 1 & 2 = Two assemblies in Checkerboard Pattern

Table 4.6.7

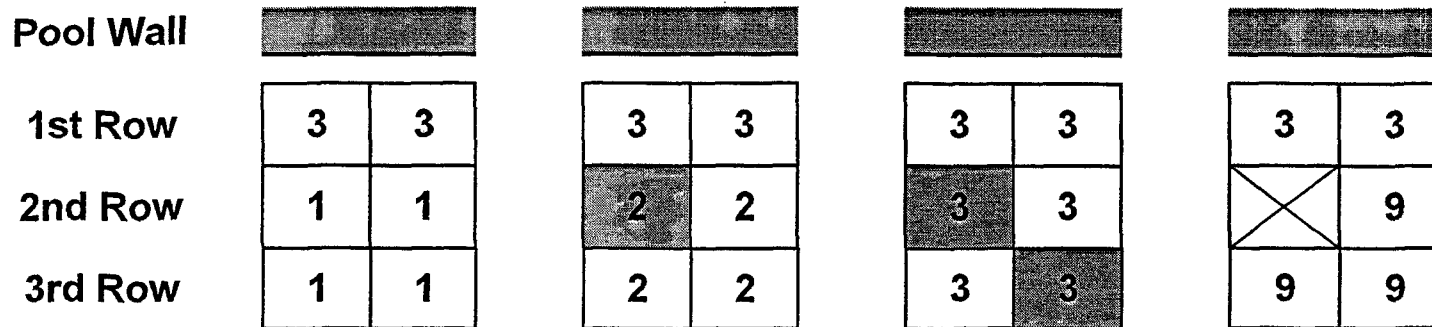
Soluble Boron Concentration Required to Maintain  $k_{eff}$  less than or equal to 0.95 under Normal Conditions.

|   |                  |        |
|---|------------------|--------|
| <b>Case</b>                                 | 2                | 2      |
| <b>Region</b>                               | 2                | 2      |
| <b>Soluble Boron Concentration</b>          | 500              | 700    |
| <b>4.5% Fresh Fuel <math>k_{inf}</math></b> | 1.2820           | 1.2484 |
| <b>Enrichment</b>                           | 4.5              | 4.5    |
| <b>Burnup</b>                               | 50.73            | 50.73  |
| <b>Cooling Time</b>                         | 0                | 0      |
| <b>Calculated <math>k_{eff}</math></b>      | 0.9075           | 0.8815 |
| <b>Bias</b>                                 | 0.0009           | 0.0009 |
| <b>Temperature Correction</b>               | 0.0109           | 0.0109 |
| <b>Uncertainties</b>                        |                  |        |
| <b>Bias</b>                                 | 0.0011           | 0.0011 |
| <b>Calculational</b>                        | 0.0014           | 0.0012 |
| <b>Eccentricity</b>                         | 0                | 0      |
| <b>Depletion</b>                            | 0.0187           | 0.0183 |
| <b>Assembly Burnup</b>                      | 0.0171           | 0.0154 |
| <b>Tolerances</b>                           | 0.0103           | 0.0103 |
| <b>Total Uncertainties</b>                  | 0.0274           | 0.0261 |
| <b>Total Addition</b>                       | 0.0392           | 0.0379 |
| <b>Maximum <math>k_{eff}</math></b>         | 0.9467           | 0.9194 |
|   | Target $k_{eff}$ | 0.94   |
|   | Soluble Boron    | 549    |

Table 4.6.8

Soluble Boron Concentration Required to Maintain  $k_{eff}$  less than or equal to 0.95 under Accident Conditions.

|   |                                   |        |
|---|-----------------------------------|--------|
| <b>Case</b>                                 | 9                                 | 9      |
| <b>Region</b>                               | 2                                 | 2      |
| <b>Soluble Boron Concentration</b>          | 1000                              | 1500   |
| <b>4.5% Fresh Fuel <math>k_{inf}</math></b> | 1.1432                            | 1.0745 |
| <b>Enrichment</b>                           | 4.5                               | 4.5    |
| <b>Burnup</b>                               | 39.25                             | 39.25  |
| <b>Cooling Time</b>                         | 0                                 | 0      |
| <b>Calculated <math>k_{eff}</math></b>      | 0.9636                            | 0.9065 |
| <b>Bias</b>                                 | 0.0009                            | 0.0009 |
| <b>Temperature Correction</b>               | 0.0121                            | 0.0131 |
| <b>Uncertainties</b>                        |                                   |        |
| <b>Bias</b>                                 | 0.0011                            | 0.0011 |
| <b>Calculational</b>                        | 0.0016                            | 0.0014 |
| <b>Eccentricity</b>                         | 0.0000                            | 0.0000 |
| <b>Assembly Burnup</b>                      | 0.0069                            | 0.0066 |
| <b>Depletion</b>                            | 0.0090                            | 0.0084 |
| <b>Tolerances</b>                           | 0.0104                            | 0.0107 |
| <b>Total Uncertainties</b>                  | 0.0155                            | 0.0152 |
| <b>Total Addition</b>                       | 0.0285                            | 0.0292 |
| <b>Maximum <math>k_{eff}</math></b>         | 0.9921                            | 0.9357 |
|   |                                   |        |
|   | Target $k_{max}$                  | 0.94   |
|   | corresponding soluble boron level | 1462   |



- Notes:
- 1) Numbers in above cells are Case numbers of the assemblies in the cells
  - 2) Shaded cells contain an insert
  - 3) Cells with a cross contain only water

Figure 4.1.1 Loading Patterns near Pool Walls in Region 2 Racks with Case 3 Fuel on the Rack Periphery

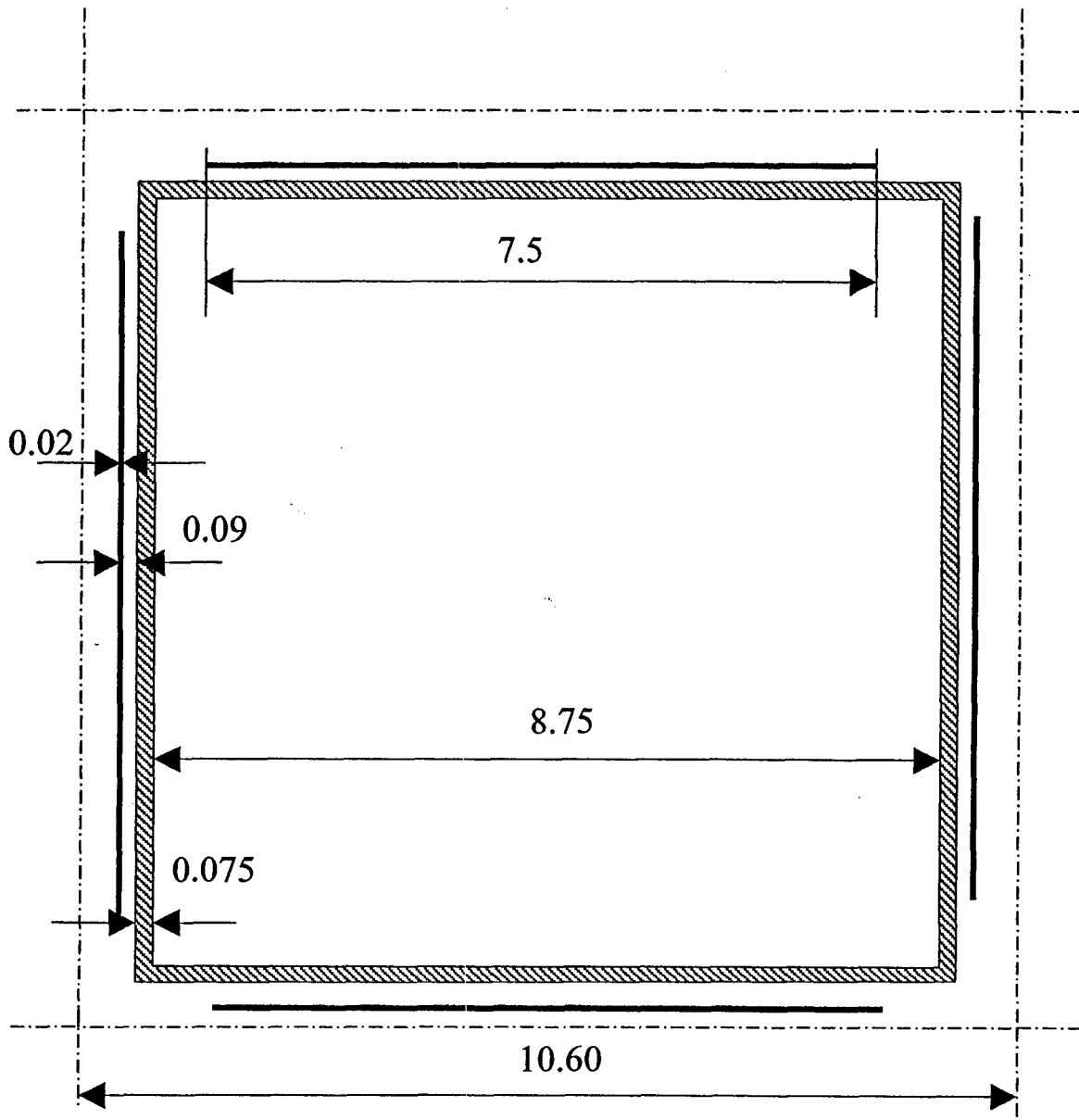


Figure 4.4.1: Schematic View of Region 1 Cell (not to scale)

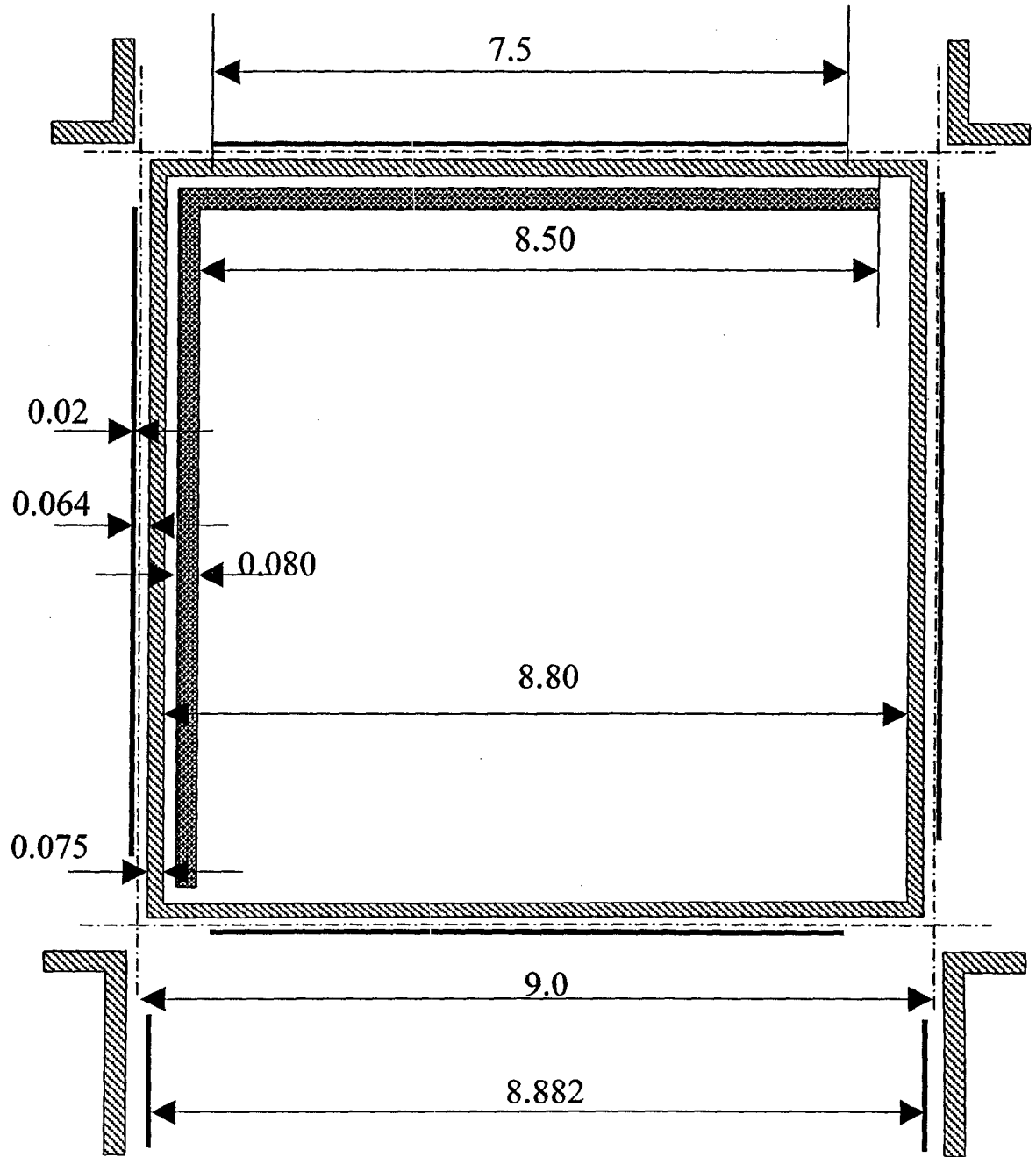


Figure 4.4.2: Schematic View of Region 2 Cell with Insert (not to scale)

|   |   |   |   |   |   |
|---|---|---|---|---|---|
| 1 | 1 | 1 | 2 | 3 | 3 |
| 1 | 1 | 1 | 2 | 3 | 3 |
| 1 | 1 | 1 | 2 | 3 | 3 |
| 1 | 1 | 1 | 2 | 3 | 3 |

- Notes:
- 1) Numbers in above cells are Case numbers of the assemblies in the cells
  - 2) Shaded cells contain an insert

Figure 4.6.1 Example of an Interface between Case 1 and Case 3

**Loading Step 1**

|   |   |   |   |   |   |
|---|---|---|---|---|---|
| 3 | 3 | 3 | 3 | 3 | 3 |
| 3 | 3 | X | 3 | 3 | 3 |
| 3 | 3 | X | 3 | 3 | 3 |
| 3 | 3 | X | 3 | 3 | 3 |

**Loading Step 2**

|   |   |   |   |   |   |
|---|---|---|---|---|---|
| 3 | 3 | 3 | 3 | 3 | 3 |
| 3 | 3 | X | 3 | 3 | 3 |
| 3 | 3 | 3 | 3 | 3 | 3 |
| 3 | 3 | X | 3 | 3 | 3 |

**Loading Step 3**

|   |   |   |   |   |   |
|---|---|---|---|---|---|
| 3 | 3 | 3 | 3 | 3 | 3 |
| 3 | 3 | X | 3 | 3 | 3 |
| 3 | 3 | 3 | 3 | 3 | 3 |
| 3 | 3 | X | 3 | 3 | 3 |

**Loading Step 4**

|   |   |   |   |   |   |
|---|---|---|---|---|---|
| 3 | 3 | 3 | 3 | 3 | 3 |
| 3 | 3 | 3 | 3 | 3 | 3 |
| 3 | 3 | 3 | 3 | 3 | 3 |
| 3 | 3 | 3 | 3 | 3 | 3 |

- Notes:
- 1) Numbers in above cells are Case numbers of the assemblies in the cells
  - 2) Shaded cells contain an insert
  - 3) Cells with a cross contain only water
  - 4) The reverse sequence is an example of Unloading Steps for a single assembly in Case 3.

Figure 4.6.2 Example of Loading Steps for a single assembly in Case 3

**Appendix A**  
**Benchmark Calculations**

(total number of pages: 26 including this page)

Note: because this appendix was taken from a different report, the next page is labeled  
“Appendix 4A, Page 1”.

## APPENDIX 4A: BENCHMARK CALCULATIONS

### 4A.1 INTRODUCTION AND SUMMARY

Benchmark calculations have been made on selected critical experiments, chosen, in so far as possible, to bound the range of variables in the rack designs. Two independent methods of analysis were used, differing in cross section libraries and in the treatment of the cross sections. MCNP4a [4A.1] is a continuous energy Monte Carlo code and KENO5a [4A.2] uses group-dependent cross sections. For the KENO5a analyses reported here, the 238-group library was chosen, processed through the NITAWL-II [4A.2] program to create a working library and to account for resonance self-shielding in uranium-238 (Nordheim integral treatment). The 238 group library was chosen to avoid or minimize the errors<sup>†</sup> (trends) that have been reported (e.g., [4A.3 through 4A.5]) for calculations with collapsed cross section sets.

In rack designs, the three most significant parameters affecting criticality are (1) the fuel enrichment, (2) the <sup>10</sup>B loading in the neutron absorber, and (3) the lattice spacing (or water-gap thickness if a flux-trap design is used). Other parameters, within the normal range of rack and fuel designs, have a smaller effect, but are also included in the analyses.

Table 4A.1 summarizes results of the benchmark calculations for all cases selected and analyzed, as referenced in the table. The effect of the major variables are discussed in subsequent sections below. It is important to note that there is obviously considerable overlap in parameters since it is not possible to vary a single parameter and maintain criticality; some other parameter or parameters must be concurrently varied to maintain criticality.

One possible way of representing the data is through a spectrum index that incorporates all of the variations in parameters. KENO5a computes and prints the "energy of the average lethargy causing fission" (EALF). In MCNP4a, by utilizing the tally option with the identical 238-group energy structure as in KENO5a, the number of fissions in each group may be collected and the EALF determined (post-processing).

---

<sup>†</sup> Small but observable trends (errors) have been reported for calculations with the 27-group and 44-group collapsed libraries. These errors are probably due to the use of a single collapsing spectrum when the spectrum should be different for the various cases analyzed, as evidenced by the spectrum indices.

Figures 4A.1 and 4A.2 show the calculated  $k_{eff}$  for the benchmark critical experiments as a function of the EALF for MCNP4a and KENO5a, respectively (UO<sub>2</sub> fuel only). The scatter in the data (even for comparatively minor variation in critical parameters) represents experimental error<sup>†</sup> in performing the critical experiments within each laboratory, as well as between the various testing laboratories. The B&W critical experiments show a larger experimental error than the PNL criticals. This would be expected since the B&W criticals encompass a greater range of critical parameters than the PNL criticals.

Linear regression analysis of the data in Figures 4A.1 and 4A.2 show that there are no trends, as evidenced by very low values of the correlation coefficient (0.13 for MCNP4a and 0.21 for KENO5a). The total bias (systematic error, or mean of the deviation from a  $k_{eff}$  of exactly 1.000) for the two methods of analysis are shown in the table below.

| Calculational Bias of MCNP4a and KENO5a |               |
|---|---------------|
| MCNP4a                                  | 0.0009±0.0011 |
| KENO5a                                  | 0.0030±0.0012 |

The bias and standard error of the bias were derived directly from the calculated  $k_{eff}$  values in Table 4A.1 using the following equations<sup>††</sup>, with the standard error multiplied by the one-sided K-factor for 95% probability at the 95% confidence level from NBS Handbook 91 [4A.18] (for the number of cases analyzed, the K-factor is ~2.05 or slightly more than 2).

$$\bar{k} = \frac{1}{n} \sum_i^n k_i \quad (4A.1)$$

---

<sup>†</sup> A classical example of experimental error is the corrected enrichment in the PNL experiments, first as an addendum to the initial report and, secondly, by revised values in subsequent reports for the same fuel rods.

<sup>††</sup> These equations may be found in any standard text on statistics, for example, reference [4A.6] (or the MCNP4a manual) and is the same methodology used in MCNP4a and in KENO5a.

$$\sigma_{\bar{k}}^2 = \frac{\sum_{i=1}^n k_i^2 - (\sum_{i=1}^n k_i)^2 / n}{n(n-1)} \quad (4A.2)$$

$$Bias = (1 - \bar{k}) \pm K \sigma_{\bar{k}} \quad (4A.3)$$

where  $k_i$  are the calculated reactivities of  $n$  critical experiments;  $\sigma_{\bar{k}}$  is the unbiased estimator of the standard deviation of the mean (also called the standard error of the bias (mean));  $K$  is the one-sided multiplier for 95% probability at the 95% confidence level (NBS Handbook 91 [4A.18]).

Formula 4.A.3 is based on the methodology of the National Bureau of Standards (now NIST) and is used to calculate the values presented on page 4.A-2. The first portion of the equation,  $(1 - \bar{k})$ , is the actual bias which is added to the MCNP4a and KENO5a results. The second term,  $K\sigma_{\bar{k}}$ , is the uncertainty or standard error associated with the bias. The  $K$  values used were obtained from the National Bureau of Standards Handbook 91 and are for one-sided statistical tolerance limits for 95% probability at the 95% confidence level. The actual  $K$  values for the 56 critical experiments evaluated with MCNP4a and the 53 critical experiments evaluated with KENO5a are 2.04 and 2.05, respectively.

The bias values are used to evaluate the maximum  $k_{eff}$  values for the rack designs. KENO5a has a slightly larger systematic error than MCNP4a, but both result in greater precision than published data [4A.3 through 4A.5] would indicate for collapsed cross section sets in KENO5a (SCALE) calculations.

#### 4A.2 Effect of Enrichment

The benchmark critical experiments include those with enrichments ranging from 2.46 w/o to 5.74 w/o and therefore span the enrichment range for rack designs. Figures 4A.3 and 4A.4 show the calculated  $k_{eff}$  values (Table 4A.1) as a function of the fuel enrichment reported for the critical experiments. Linear regression analyses for these data confirms that there are no trends, as indicated by low values of the correlation coefficients (0.03 for MCNP4a and 0.38 for KENO5a). Thus, there are no corrections to the bias for the various enrichments.

As further confirmation of the absence of any trends with enrichment, a typical configuration was calculated with both MCNP4a and KENO5a for various enrichments. The cross-comparison of calculations with codes of comparable sophistication is suggested in Reg. Guide 3.41. Results of this comparison, shown in Table 4A.2 and Figure 4A.5, confirm no significant difference in the calculated values of  $k_{eff}$  for the two independent codes as evidenced by the 45° slope of the curve. Since it is very unlikely that two independent methods of analysis would be subject to the same error, this comparison is considered confirmation of the absence of an enrichment effect (trend) in the bias.

#### 4A.3 Effect of $^{10}\text{B}$ Loading

Several laboratories have performed critical experiments with a variety of thin absorber panels similar to the Boral panels in the rack designs. Of these critical experiments, those performed by B&W are the most representative of the rack designs. PNL has also made some measurements with absorber plates, but, with one exception (a flux-trap experiment), the reactivity worth of the absorbers in the PNL tests is very low and any significant errors that might exist in the treatment of strong thin absorbers could not be revealed.

Table 4A.3 lists the subset of experiments using thin neutron absorbers (from Table 4A.1) and shows the reactivity worth ( $\Delta k$ ) of the absorber.<sup>†</sup>

No trends with reactivity worth of the absorber are evident, although based on the calculations shown in Table 4A.3, some of the B&W critical experiments seem to have unusually large experimental errors. B&W made an effort to report some of their experimental errors. Other laboratories did not evaluate their experimental errors.

To further confirm the absence of a significant trend with  $^{10}\text{B}$  concentration in the absorber, a cross-comparison was made with MCNP4a and KENO5a (as suggested in Reg. Guide 3.41). Results are shown in Figure 4A.6 and Table 4A.4 for a typical geometry. These data substantiate the absence of any error (trend) in either of the two codes for the conditions analyzed (data points fall on a 45° line, within an expected 95% probability limit).

---

<sup>†</sup> The reactivity worth of the absorber panels was determined by repeating the calculation with the absorber analytically removed and calculating the incremental ( $\Delta k$ ) change in reactivity due to the absorber.

#### 4A.4 Miscellaneous and Minor Parameters

##### 4A.4.1 Reflector Material and Spacings

PNL has performed a number of critical experiments with thick steel and lead reflectors.<sup>†</sup> Analysis of these critical experiments are listed in Table 4A.5 (subset of data in Table 4A.1). There appears to be a small tendency toward overprediction of  $k_{\text{eff}}$  at the lower spacing, although there are an insufficient number of data points in each series to allow a quantitative determination of any trends. The tendency toward overprediction at close spacing means that the rack calculations may be slightly more conservative than otherwise.

##### 4A.4.2 Fuel Pellet Diameter and Lattice Pitch

The critical experiments selected for analysis cover a range of fuel pellet diameters from 0.311 to 0.444 inches, and lattice spacings from 0.476 to 1.00 inches. In the rack designs, the fuel pellet diameters range from 0.303 to 0.3805 inches O.D. (0.496 to 0.580 inch lattice spacing) for PWR fuel and from 0.3224 to 0.494 inches O.D. (0.488 to 0.740 inch lattice spacing) for BWR fuel. Thus, the critical experiments analyzed provide a reasonable representation of power reactor fuel. Based on the data in Table 4A.1, there does not appear to be any observable trend with either fuel pellet diameter or lattice pitch, at least over the range of the critical experiments applicable to rack designs.

##### 4A.4.3 Soluble Boron Concentration Effects

Various soluble boron concentrations were used in the B&W series of critical experiments and in one PNL experiment, with boron concentrations ranging up to 2550 ppm. Results of MCNP4a (and one KENO5a) calculations are shown in Table 4A.6. Analyses of the very high boron concentration experiments (> 1300 ppm) show a tendency to slightly overpredict reactivity for the three experiments exceeding 1300 ppm. In turn, this would suggest that the evaluation of the racks with higher soluble boron concentrations could be slightly conservative.

---

<sup>†</sup> Parallel experiments with a depleted uranium reflector were also performed but not included in the present analysis since they are not pertinent to the Holtec rack design.

The number of critical experiments with  $\text{PuO}_2$  bearing fuel (MOX) is more limited than for  $\text{UO}_2$  fuel. However, a number of MOX critical experiments have been analyzed and the results are shown in Table 4A.7. Results of these analyses are generally above a  $k_{\text{eff}}$  of 1.00, indicating that when Pu is present, both MCNP4a and KENO5a overpredict the reactivity. This may indicate that calculation for MOX fuel will be expected to be conservative, especially with MCNP4a. It may be noted that for the larger lattice spacings, the KENO5a calculated reactivities are below 1.00, suggesting that a small trend may exist with KENO5a. It is also possible that the overprediction in  $k_{\text{eff}}$  for both codes may be due to a small inadequacy in the determination of the Pu-241 decay and Am-241 growth. This possibility is supported by the consistency in calculated  $k_{\text{eff}}$  over a wide range of the spectral index (energy of the average lethargy causing fission).

#### 4A.6

#### References

- [4A.1] J.F. Briesmeister, Ed., "MCNP4a - A General Monte Carlo N-Particle Transport Code, Version 4A; Los Alamos National Laboratory, LA-12625-M (1993).
- [4A.2] SCALE 4.3, "A Modular Code System for Performing Standardized Computer Analyses for Licensing Evaluation", NUREG-0200 (ORNL-NUREG-CSD-2/U2/R5, Revision 5, Oak Ridge National Laboratory, September 1995.
- [4A.3] M.D. DeHart and S.M. Bowman, "Validation of the SCALE Broad Structure 44-G Group ENDF/B-Y Cross-Section Library for Use in Criticality Safety Analyses", NUREG/CR-6102 (ORNL/TM-12460) Oak Ridge National Laboratory, September 1994.
- [4A.4] W.C. Jordan et al., "Validation of KENO.V.a", CSD/TM-238, Martin Marietta Energy Systems, Inc., Oak Ridge National Laboratory, December 1986.
- [4A.5] O.W. Hermann et al., "Validation of the Scale System for PWR Spent Fuel Isotopic Composition Analysis", ORNL-TM-12667, Oak Ridge National Laboratory, undated.
- [4A.6] R.J. Larsen and M.L. Marx, An Introduction to Mathematical Statistics and its Applications, Prentice-Hall, 1986.
- [4A.7] M.N. Baldwin et al., Critical Experiments Supporting Close Proximity Water Storage of Power Reactor Fuel, BAW-1484-7, Babcock and Wilcox Company, July 1979.
- [4A.8] G.S. Hoovier et al., Critical Experiments Supporting Underwater Storage of Tightly Packed Configurations of Spent Fuel Pins, BAW-1645-4, Babcock & Wilcox Company, November 1991.
- [4A.9] L.W. Newman et al., Urania Gadolinia: Nuclear Model Development and Critical Experiment Benchmark, BAW-1810, Babcock and Wilcox Company, April 1984.

- [4A.10] J.C. Manaranche et al., "Dissolution and Storage Experimental Program with 4.75 w/o Enriched Uranium-Oxide Rods," Trans. Am. Nucl. Soc. 33: 362-364 (1979).
- [4A.11] S.R. Bierman and E.D. Clayton, Criticality Experiments with Subcritical Clusters of 2.35 w/o and 4.31 w/o <sup>235</sup>U Enriched UO<sub>2</sub> Rods in Water with Steel Reflecting Walls, PNL-3602, Battelle Pacific Northwest Laboratory, April 1981.
- [4A.12] S.R. Bierman et al., Criticality Experiments with Subcritical Clusters of 2.35 w/o and 4.31 w/o <sup>235</sup>U Enriched UO<sub>2</sub> Rods in Water with Uranium or Lead Reflecting Walls, PNL-3926, Battelle Pacific Northwest Laboratory, December, 1981.
- [4A.13] S.R. Bierman et al., Critical Separation Between Subcritical Clusters of 4.31 w/o <sup>235</sup>U Enriched UO<sub>2</sub> Rods in Water with Fixed Neutron Poisons, PNL-2615, Battelle Pacific Northwest Laboratory, October 1977.
- [4A.14] S.R. Bierman, Criticality Experiments with Neutron Flux Traps Containing Voids, PNL-7167, Battelle Pacific Northwest Laboratory, April 1990.
- [4A.15] B.M. Durst et al., Critical Experiments with 4.31 wt % <sup>235</sup>U Enriched UO<sub>2</sub> Rods in Highly Borated Water Lattices, PNL-4267, Battelle Pacific Northwest Laboratory, August 1982.
- [4A.16] S.R. Bierman, Criticality Experiments with Fast Test Reactor Fuel Pins in Organic Moderator, PNL-5803, Battelle Pacific Northwest Laboratory, December 1981.
- [4A.17] E.G. Taylor et al., Saxton Plutonium Program Critical Experiments for the Saxton Partial Plutonium Core, WCAP-3385-54, Westinghouse Electric Corp., Atomic Power Division, December 1965.
- [4A.18] M.G. Natrella, Experimental Statistics, National Bureau of Standards, Handbook 91, August 1963.

Table 4A.1

Summary of Criticality Benchmark Calculations

| Reference | Identification  | Enrich.                | Calculated $k_{eff}$ |                 | EALF <sup>†</sup> (eV) |        |        |
|-----------|-----------------|------------------------|----------------------|-----------------|------------------------|--------|--------|
|           |                 |                        | MCNP4a               | KENO5a          | MCNP4a                 | KENO5a |        |
| 1         | B&W-1484 (4A.7) | Core I                 | 2.46                 | 0.9964 ± 0.0010 | 0.9898 ± 0.0006        | 0.1759 | 0.1753 |
| 2         | B&W-1484 (4A.7) | Core II                | 2.46                 | 1.0008 ± 0.0011 | 1.0015 ± 0.0005        | 0.2553 | 0.2446 |
| 3         | B&W-1484 (4A.7) | Core III               | 2.46                 | 1.0010 ± 0.0012 | 1.0005 ± 0.0005        | 0.1999 | 0.1939 |
| 4         | B&W-1484 (4A.7) | Core IX                | 2.46                 | 0.9956 ± 0.0012 | 0.9901 ± 0.0006        | 0.1422 | 0.1426 |
| 5         | B&W-1484 (4A.7) | Core X                 | 2.46                 | 0.9980 ± 0.0014 | 0.9922 ± 0.0006        | 0.1513 | 0.1499 |
| 6         | B&W-1484 (4A.7) | Core XI                | 2.46                 | 0.9978 ± 0.0012 | 1.0005 ± 0.0005        | 0.2031 | 0.1947 |
| 7         | B&W-1484 (4A.7) | Core XII               | 2.46                 | 0.9988 ± 0.0011 | 0.9978 ± 0.0006        | 0.1718 | 0.1662 |
| 8         | B&W-1484 (4A.7) | Core XIII              | 2.46                 | 1.0020 ± 0.0010 | 0.9952 ± 0.0006        | 0.1988 | 0.1965 |
| 9         | B&W-1484 (4A.7) | Core XIV               | 2.46                 | 0.9953 ± 0.0011 | 0.9928 ± 0.0006        | 0.2022 | 0.1986 |
| 10        | B&W-1484 (4A.7) | Core XV <sup>**</sup>  | 2.46                 | 0.9910 ± 0.0011 | 0.9909 ± 0.0006        | 0.2092 | 0.2014 |
| 11        | B&W-1484 (4A.7) | Core XVI <sup>**</sup> | 2.46                 | 0.9935 ± 0.0010 | 0.9889 ± 0.0006        | 0.1757 | 0.1713 |
| 12        | B&W-1484 (4A.7) | Core XVII              | 2.46                 | 0.9962 ± 0.0012 | 0.9942 ± 0.0005        | 0.2083 | 0.2021 |
| 13        | B&W-1484 (4A.7) | Core XVIII             | 2.46                 | 1.0036 ± 0.0012 | 0.9931 ± 0.0006        | 0.1705 | 0.1708 |

Table 4A.1

Summary of Criticality Benchmark Calculations

| Reference | Identification   | Enrich.                       | Calculated $k_{eff}$ |                 | EALF <sup>1</sup> (eV) |        |        |
|-----------|------------------|-------------------------------|----------------------|-----------------|------------------------|--------|--------|
|           |                  |                               | MCNP4a               | KENO5a          | MCNP4a                 | KENO5a |        |
| 14        | B&W-1484 (4A.7)  | Core XIX                      | 2.46                 | 0.9961 ± 0.0012 | 0.9971 ± 0.0005        | 0.2103 | 0.2011 |
| 15        | B&W-1484 (4A.7)  | Core XX                       | 2.46                 | 1.0008 ± 0.0011 | 0.9932 ± 0.0006        | 0.1724 | 0.1701 |
| 16        | B&W-1484 (4A.7)  | Core XXI                      | 2.46                 | 0.9994 ± 0.0010 | 0.9918 ± 0.0006        | 0.1544 | 0.1536 |
| 17        | B&W-1645 (4A.8)  | S-type Fuel, w/886 ppm B      | 2.46                 | 0.9970 ± 0.0010 | 0.9924 ± 0.0006        | 1.4475 | 1.4680 |
| 18        | B&W-1645 (4A.8)  | S-type Fuel, w/746 ppm B      | 2.46                 | 0.9990 ± 0.0010 | 0.9913 ± 0.0006        | 1.5463 | 1.5660 |
| 19        | B&W-1645 (4A.8)  | SO-type Fuel, w/1156 ppm B    | 2.46                 | 0.9972 ± 0.0009 | 0.9949 ± 0.0005        | 0.4241 | 0.4331 |
| 20        | B&W-1810 (4A.9)  | Case 1 1337 ppm B             | 2.46                 | 1.0023 ± 0.0010 | NC                     | 0.1531 | NC     |
| 21        | B&W-1810 (4A.9)  | Case 12 1899 ppm B            | 2.46/4.02            | 1.0060 ± 0.0009 | NC                     | 0.4493 | NC     |
| 22        | French (4A.10)   | Water Moderator 0 gap         | 4.75                 | 0.9966 ± 0.0013 | NC                     | 0.2172 | NC     |
| 23        | French (4A.10)   | Water Moderator 2.5 cm gap    | 4.75                 | 0.9952 ± 0.0012 | NC                     | 0.1778 | NC     |
| 24        | French (4A.10)   | Water Moderator 5 cm gap      | 4.75                 | 0.9943 ± 0.0010 | NC                     | 0.1677 | NC     |
| 25        | French (4A.10)   | Water Moderator 10 cm gap     | 4.75                 | 0.9979 ± 0.0010 | NC                     | 0.1736 | NC     |
| 26        | PNL-3602 (4A.11) | Steel Reflector, 0 separation | 2.35                 | NC              | 1.0004 ± 0.0006        | NC     | 0.1018 |

Table 4A.1

Summary of Criticality Benchmark Calculations

| Reference | Identification   | Enrich.                                       | Calculated $k_{eff}$ |                 | EALF <sup>†</sup> (eV) |        |        |
|-----------|------------------|---|----------------------|-----------------|------------------------|--------|--------|
|           |                  |   | MCNP4a               | KENO5a          | MCNP4a                 | KENO5a |        |
| 27        | PNL-3602 (4A.11) | Steel Reflector, 1.321 cm sepn.               | 2.35                 | 0.9980 ± 0.0009 | 0.9992 ± 0.0006        | 0.1000 | 0.0909 |
| 28        | PNL-3602 (4A.11) | Steel Reflector, 2.616 cm sepn                | 2.35                 | 0.9968 ± 0.0009 | 0.9964 ± 0.0006        | 0.0981 | 0.0975 |
| 29        | PNL-3602 (4A.11) | Steel Reflector, 3.912 cm sepn.               | 2.35                 | 0.9974 ± 0.0010 | 0.9980 ± 0.0006        | 0.0976 | 0.0970 |
| 30        | PNL-3602 (4A.11) | Steel Reflector, infinite sepn.               | 2.35                 | 0.9962 ± 0.0008 | 0.9939 ± 0.0006        | 0.0973 | 0.0968 |
| 31        | PNL-3602 (4A.11) | Steel Reflector, 0 cm sepn.                   | 4.306                | NC              | 1.0003 ± 0.0007        | NC     | 0.3282 |
| 32        | PNL-3602 (4A.11) | Steel Reflector, 1.321 cm sepn.               | 4.306                | 0.9997 ± 0.0010 | 1.0012 ± 0.0007        | 0.3016 | 0.3039 |
| 33        | PNL-3602 (4A.11) | Steel Reflector, 2.616 cm sepn.               | 4.306                | 0.9994 ± 0.0012 | 0.9974 ± 0.0007        | 0.2911 | 0.2927 |
| 34        | PNL-3602 (4A.11) | Steel Reflector, 5.405 cm sepn.               | 4.306                | 0.9969 ± 0.0011 | 0.9951 ± 0.0007        | 0.2828 | 0.2860 |
| 35        | PNL-3602 (4A.11) | Steel Reflector, Infinite sepn. <sup>††</sup> | 4.306                | 0.9910 ± 0.0020 | 0.9947 ± 0.0007        | 0.2851 | 0.2864 |
| 36        | PNL-3602 (4A.11) | Steel Reflector, with Boral Sheets            | 4.306                | 0.9941 ± 0.0011 | 0.9970 ± 0.0007        | 0.3135 | 0.3150 |
| 37        | PNL-3926 (4A.12) | Lead Reflector, 0 cm sepn.                    | 4.306                | NC              | 1.0003 ± 0.0007        | NC     | 0.3159 |
| 38        | PNL-3926 (4A.12) | Lead Reflector, 0.55 cm sepn.                 | 4.306                | 1.0025 ± 0.0011 | 0.9997 ± 0.0007        | 0.3030 | 0.3044 |
| 39        | PNL-3926 (4A.12) | Lead Reflector, 1.956 cm sepn.                | 4.306                | 1.0000 ± 0.0012 | 0.9985 ± 0.0007        | 0.2883 | 0.2930 |

Table 4A.1

## Summary of Criticality Benchmark Calculations

| Reference | Identification   | Enrich.                           | Calculated $k_{eff}$ |                 | EALF <sup>†</sup> (eV) |        |        |
|-----------|------------------|-----------------------------------|----------------------|-----------------|------------------------|--------|--------|
|           |                  |                                   | MCNP4a               | KENO5a          | MCNP4a                 | KENO5a |        |
| 40        | PNL-3926 (4A.12) | Lead Reflector, 5.405 cm sepn.    | 4.306                | 0.9971 ± 0.0012 | 0.9946 ± 0.0007        | 0.2831 | 0.2854 |
| 41        | PNL-2615 (4A.13) | Experiment 004/032 - no absorber  | 4.306                | 0.9925 ± 0.0012 | 0.9950 ± 0.0007        | 0.1155 | 0.1159 |
| 42        | PNL-2615 (4A.13) | Experiment 030 - Zr plates        | 4.306                | NC              | 0.9971 ± 0.0007        | NC     | 0.1154 |
| 43        | PNL-2615 (4A.13) | Experiment 013 - Steel plates     | 4.306                | NC              | 0.9965 ± 0.0007        | NC     | 0.1164 |
| 44        | PNL-2615 (4A.13) | Experiment 014 - Steel plates     | 4.306                | NC              | 0.9972 ± 0.0007        | NC     | 0.1164 |
| 45        | PNL-2615 (4A.13) | Exp. 009 1.05% Boron-Steel plates | 4.306                | 0.9982 ± 0.0010 | 0.9981 ± 0.0007        | 0.1172 | 0.1162 |
| 46        | PNL-2615 (4A.13) | Exp. 012 1.62% Boron-Steel plates | 4.306                | 0.9996 ± 0.0012 | 0.9982 ± 0.0007        | 0.1161 | 0.1173 |
| 47        | PNL-2615 (4A.13) | Exp. 031 - Boral plates           | 4.306                | 0.9994 ± 0.0012 | 0.9969 ± 0.0007        | 0.1165 | 0.1171 |
| 48        | PNL-7167 (4A.14) | Experiment 214R - with flux trap  | 4.306                | 0.9991 ± 0.0011 | 0.9956 ± 0.0007        | 0.3722 | 0.3812 |
| 49        | PNL-7167 (4A.14) | Experiment 214V3 - with flux trap | 4.306                | 0.9969 ± 0.0011 | 0.9963 ± 0.0007        | 0.3742 | 0.3826 |
| 50        | PNL-4267 (4A.15) | Case 173 - 0 ppm B                | 4.306                | 0.9974 ± 0.0012 | NC                     | 0.2893 | NC     |
| 51        | PNL-4267 (4A.15) | Case 177 - 2550 ppm B             | 4.306                | 1.0057 ± 0.0010 | NC                     | 0.5509 | NC     |
| 52        | PNL-5803 (4A.16) | MOX Fuel - Type 3.2 Exp. 21       | 20% Pu               | 1.0041 ± 0.0011 | 1.0046 ± 0.0006        | 0.9171 | 0.8868 |

Table 4A.1

Summary of Criticality Benchmark Calculations

| Reference | Identification    | Enrich.                                     | Calculated $k_{eff}$ |                 | EALF <sup>†</sup> (eV) |        |        |
|-----------|-------------------|---|----------------------|-----------------|------------------------|--------|--------|
|           |                   |   | MCNP4a               | KENO5a          | MCNP4a                 | KENO5a |        |
| 53        | PNL-5803 (4A.16)  | MOX Fuel - Type 3.2 Exp. 43                 | 20% Pu               | 1.0058 ± 0.0012 | 1.0036 ± 0.0006        | 0.2968 | 0.2944 |
| 54        | PNL-5803 (4A.16)  | MOX Fuel - Type 3.2 Exp. 13                 | 20% Pu               | 1.0083 ± 0.0011 | 0.9989 ± 0.0006        | 0.1665 | 0.1706 |
| 55        | PNL-5803 (4A.16)  | MOX Fuel - Type 3.2 Exp. 32                 | 20% Pu               | 1.0079 ± 0.0011 | 0.9966 ± 0.0006        | 0.1139 | 0.1165 |
| 56        | WCAP-3385 (4A.17) | Saxton Case 52 PuO <sub>2</sub> 0.52" pitch | 6.6% Pu              | 0.9996 ± 0.0011 | 1.0005 ± 0.0006        | 0.8665 | 0.8417 |
| 57        | WCAP-3385 (4A.17) | Saxton Case 52 U 0.52" pitch                | 5.74                 | 1.0000 ± 0.0010 | 0.9956 ± 0.0007        | 0.4476 | 0.4580 |
| 58        | WCAP-3385 (4A.17) | Saxton Case 56 PuO <sub>2</sub> 0.56" pitch | 6.6% Pu              | 1.0036 ± 0.0011 | 1.0047 ± 0.0006        | 0.5289 | 0.5197 |
| 59        | WCAP-3385 (4A.17) | Saxton Case 56 borated PuO <sub>2</sub>     | 6.6% Pu              | 1.0008 ± 0.0010 | NC                     | 0.6389 | NC     |
| 60        | WCAP-3385 (4A.17) | Saxton Case 56 U 0.56" pitch                | 5.74                 | 0.9994 ± 0.0011 | 0.9967 ± 0.0007        | 0.2923 | 0.2954 |
| 61        | WCAP-3385 (4A.17) | Saxton Case 79 PuO <sub>2</sub> 0.79" pitch | 6.6% Pu              | 1.0063 ± 0.0011 | 1.0133 ± 0.0006        | 0.1520 | 0.1555 |
| 62        | WCAP-3385 (4A.17) | Saxton Case 79 U 0.79" pitch                | 5.74                 | 1.0039 ± 0.0011 | 1.0008 ± 0.0006        | 0.1036 | 0.1047 |

Notes: NC stands for not calculated.

<sup>†</sup> EALF is the energy of the average lethargy causing fission.

<sup>††</sup> These experimental results appear to be statistical outliers (> 3σ) suggesting the possibility of unusually large experimental error. Although they could justifiably be excluded, for conservatism, they were retained in determining the calculational basis.

Table 4A.2

COMPARISON OF MCNP4a AND KENO5a CALCULATED REACTIVITIES†  
FOR VARIOUS ENRICHMENTS

| Enrichment | Calculated $k_{\text{eff}} \pm 1\sigma$ |                     |
|------------|---|---------------------|
|            | MCNP4a                                  | KENO5a              |
| 3.0        | 0.8465 $\pm$ 0.0011                     | 0.8478 $\pm$ 0.0004 |
| 3.5        | 0.8820 $\pm$ 0.0011                     | 0.8841 $\pm$ 0.0004 |
| 3.75       | 0.9019 $\pm$ 0.0011                     | 0.8987 $\pm$ 0.0004 |
| 4.0        | 0.9132 $\pm$ 0.0010                     | 0.9140 $\pm$ 0.0004 |
| 4.2        | 0.9276 $\pm$ 0.0011                     | 0.9237 $\pm$ 0.0004 |
| 4.5        | 0.9400 $\pm$ 0.0011                     | 0.9388 $\pm$ 0.0004 |

---

† Based on the GE 8x8R fuel assembly.

Table 4A.3

**MCNP4a CALCULATED REACTIVITIES FOR  
CRITICAL EXPERIMENTS WITH NEUTRON ABSORBERS**

| Ref.  | Experiment |                     | $\Delta k$<br>Worth of<br>Absorber | MCNP4a<br>Calculated<br>$k_{eff}$ | EALF <sup>†</sup><br>(eV) |
|-------|------------|---------------------|------------------------------------|-----------------------------------|---------------------------|
| 4A.13 | PNL-2615   | Boral Sheet         | 0.0139                             | 0.9994±0.0012                     | 0.1165                    |
| 4A.7  | B&W-1484   | Core XX             | 0.0165                             | 1.0008±0.0011                     | 0.1724                    |
| 4A.13 | PNL-2615   | 1.62% Boron-steel   | 0.0165                             | 0.9996±0.0012                     | 0.1161                    |
| 4A.7  | B&W-1484   | Core XIX            | 0.0202                             | 0.9961±0.0012                     | 0.2103                    |
| 4A.7  | B&W-1484   | Core XXI            | 0.0243                             | 0.9994±0.0010                     | 0.1544                    |
| 4A.7  | B&W-1484   | Core XVII           | 0.0519                             | 0.9962±0.0012                     | 0.2083                    |
| 4A.11 | PNL-3602   | Boral Sheet         | 0.0708                             | 0.9941±0.0011                     | 0.3135                    |
| 4A.7  | B&W-1484   | Core XV             | 0.0786                             | 0.9910±0.0011                     | 0.2092                    |
| 4A.7  | B&W-1484   | Core XVI            | 0.0845                             | 0.9935±0.0010                     | 0.1757                    |
| 4A.7  | B&W-1484   | Core XIV            | 0.1575                             | 0.9953±0.0011                     | 0.2022                    |
| 4A.7  | B&W-1484   | Core XIII           | 0.1738                             | 1.0020±0.0011                     | 0.1988                    |
| 4A.14 | PNL-7167   | Expt 214R flux trap | 0.1931                             | 0.9991±0.0011                     | 0.3722                    |

---

<sup>†</sup>EALF is the energy of the average lethargy causing fission.

Table 4A.4

COMPARISON OF MCNP4a AND KENO5a  
CALCULATED REACTIVITIES<sup>†</sup> FOR VARIOUS <sup>10</sup>B LOADINGS

| <sup>10</sup> B, g/cm <sup>2</sup> | Calculated $k_{\text{eff}} \pm 1\sigma$ |                 |
|------------------------------------|---|-----------------|
|                                    | MCNP4a                                  | KENO5a          |
| 0.005                              | 1.0381 ± 0.0012                         | 1.0340 ± 0.0004 |
| 0.010                              | 0.9960 ± 0.0010                         | 0.9941 ± 0.0004 |
| 0.015                              | 0.9727 ± 0.0009                         | 0.9713 ± 0.0004 |
| 0.020                              | 0.9541 ± 0.0012                         | 0.9560 ± 0.0004 |
| 0.025                              | 0.9433 ± 0.0011                         | 0.9428 ± 0.0004 |
| 0.03                               | 0.9325 ± 0.0011                         | 0.9338 ± 0.0004 |
| 0.035                              | 0.9234 ± 0.0011                         | 0.9251 ± 0.0004 |
| 0.04                               | 0.9173 ± 0.0011                         | 0.9179 ± 0.0004 |

<sup>†</sup> Based on a 4.5% enriched GE 8x8R fuel assembly.

Table 4A.5

CALCULATIONS FOR CRITICAL EXPERIMENTS WITH THICK LEAD AND STEEL REFLECTORS<sup>†</sup>

| Ref.  | Case            | E, wt% | Separation, cm | MCNP4a $k_{eff}$ | KENO5a $k_{eff}$ |
|-------|-----------------|--------|----------------|------------------|------------------|
| 4A.11 | Steel Reflector | 2.35   | 1.321          | 0.9980±0.0009    | 0.9992±0.0006    |
|       |                 | 2.35   | 2.616          | 0.9968±0.0009    | 0.9964±0.0006    |
|       |                 | 2.35   | 3.912          | 0.9974±0.0010    | 0.9980±0.0006    |
|       |                 | 2.35   | ∞              | 0.9962±0.0008    | 0.9939±0.0006    |
| 4A.11 | Steel Reflector | 4.306  | 1.321          | 0.9997±0.0010    | 1.0012±0.0007    |
|       |                 | 4.306  | 2.616          | 0.9994±0.0012    | 0.9974±0.0007    |
|       |                 | 4.306  | 3.405          | 0.9969±0.0011    | 0.9951±0.0007    |
|       |                 | 4.306  | ∞              | 0.9910±0.0020    | 0.9947±0.0007    |
| 4A.12 | Lead Reflector  | 4.306  | 0.55           | 1.0025±0.0011    | 0.9997±0.0007    |
|       |                 | 4.306  | 1.956          | 1.0000±0.0012    | 0.9985±0.0007    |
|       |                 | 4.306  | 5.405          | 0.9971±0.0012    | 0.9946±0.0007    |

<sup>†</sup> Arranged in order of increasing reflector-fuel spacing.

Table 4A.6

CALCULATIONS FOR CRITICAL EXPERIMENTS WITH VARIOUS SOLUBLE BORON CONCENTRATIONS

| Reference | Experiment | Boron Concentration, ppm | Calculated $k_{eff}$ |                     |
|-----------|------------|--------------------------|----------------------|---------------------|
|           |            |                          | MCNP4a               | KENO5a              |
| 4A.15     | PNL-4267   | 0                        | $0.9974 \pm 0.0012$  | -                   |
| 4A.8      | B&W-1645   | 886                      | $0.9970 \pm 0.0010$  | $0.9924 \pm 0.0006$ |
| 4A.9      | B&W-1810   | 1337                     | $1.0023 \pm 0.0010$  | -                   |
| 4A.9      | B&W-1810   | 1899                     | $1.0060 \pm 0.0009$  | -                   |
| 4A.15     | PNL-4267   | 2550                     | $1.0057 \pm 0.0010$  | -                   |

Table 4A.7

CALCULATIONS FOR CRITICAL EXPERIMENTS WITH MOX FUEL

| Reference                | Case <sup>†</sup>            | MCNP4a          |                    | KENO5a          |                    |
|--------------------------|------------------------------|-----------------|--------------------|-----------------|--------------------|
|                          |                              | $k_{eff}$       | EALF <sup>††</sup> | $k_{eff}$       | EALF <sup>††</sup> |
| PNL-5803<br>[4A. 16]     | MOX Fuel - Exp. No. 21       | 1.0041 ± 0.0011 | 0.9171             | 1.0046 ± 0.0006 | 0.8868             |
|                          | MOX Fuel - Exp. No. 43       | 1.0058 ± 0.0012 | 0.2968             | 1.0036 ± 0.0006 | 0.2944             |
|                          | MOX Fuel - Exp. No. 13       | 1.0083 ± 0.0011 | 0.1665             | 0.9989 ± 0.0006 | 0.1706             |
|                          | MOX Fuel - Exp. No. 32       | 1.0079 ± 0.0011 | 0.1139             | 0.9966 ± 0.0006 | 0.1165             |
| WCAP-3385-54<br>[4A. 17] | Saxton @ 0.52" pitch         | 0.9996 ± 0.0011 | 0.8665             | 1.0005 ± 0.0006 | 0.8417             |
|                          | Saxton @ 0.56" pitch         | 1.0036 ± 0.0011 | 0.5289             | 1.0047 ± 0.0006 | 0.5197             |
|                          | Saxton @ 0.56" pitch borated | 1.0008 ± 0.0010 | 0.6389             | NC              | NC                 |
|                          | Saxton @ 0.79" pitch         | 1.0063 ± 0.0011 | 0.1520             | 1.0133 ± 0.0006 | 0.1555             |

Note: NC stands for not calculated

† Arranged in order of increasing lattice spacing.

†† EALF is the energy of the average lethargy causing fission.

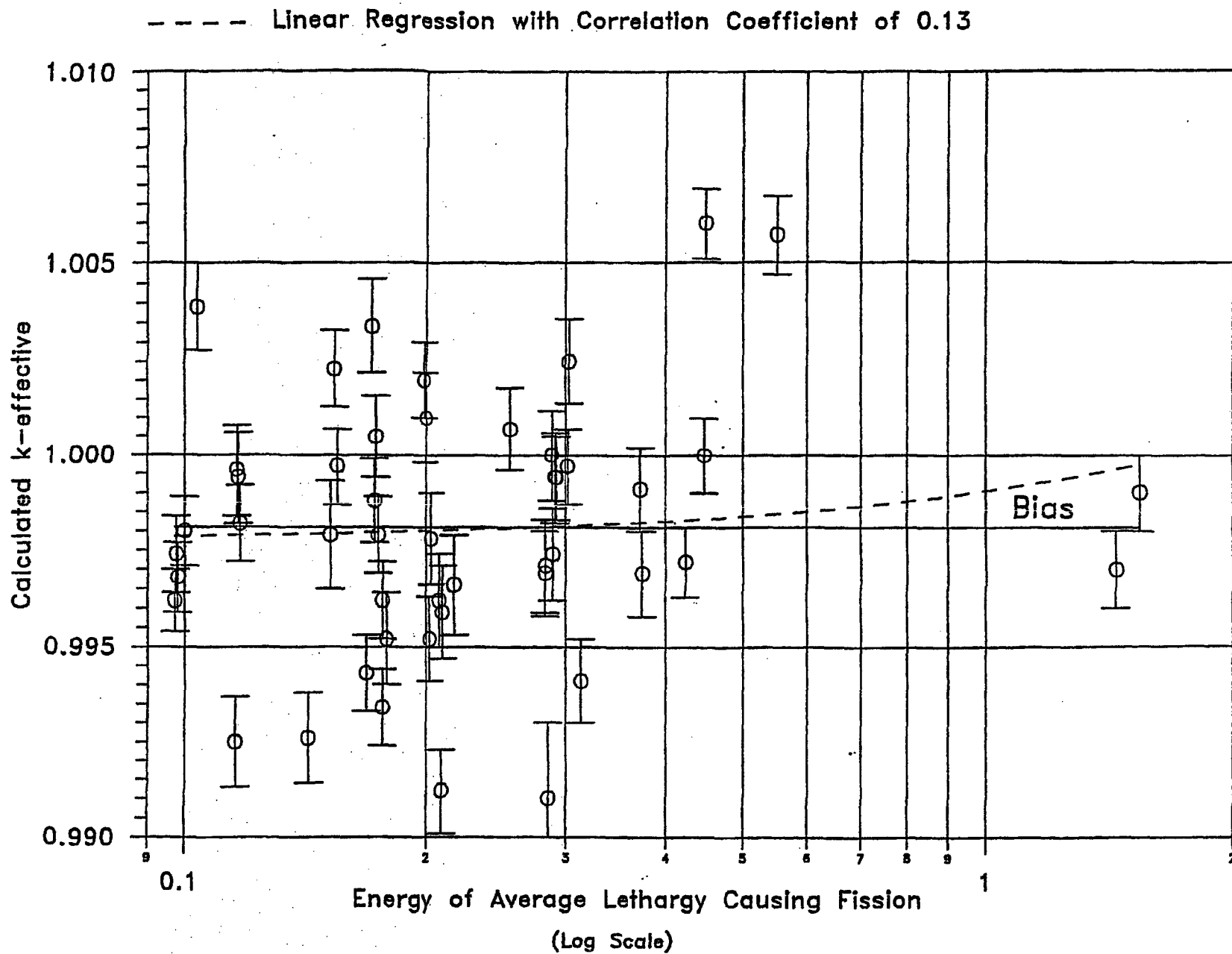


FIGURE 4A.1 MCNP CALCULATED k-eff VALUES for VARIOUS VALUES OF THE SPECTRAL INDEX



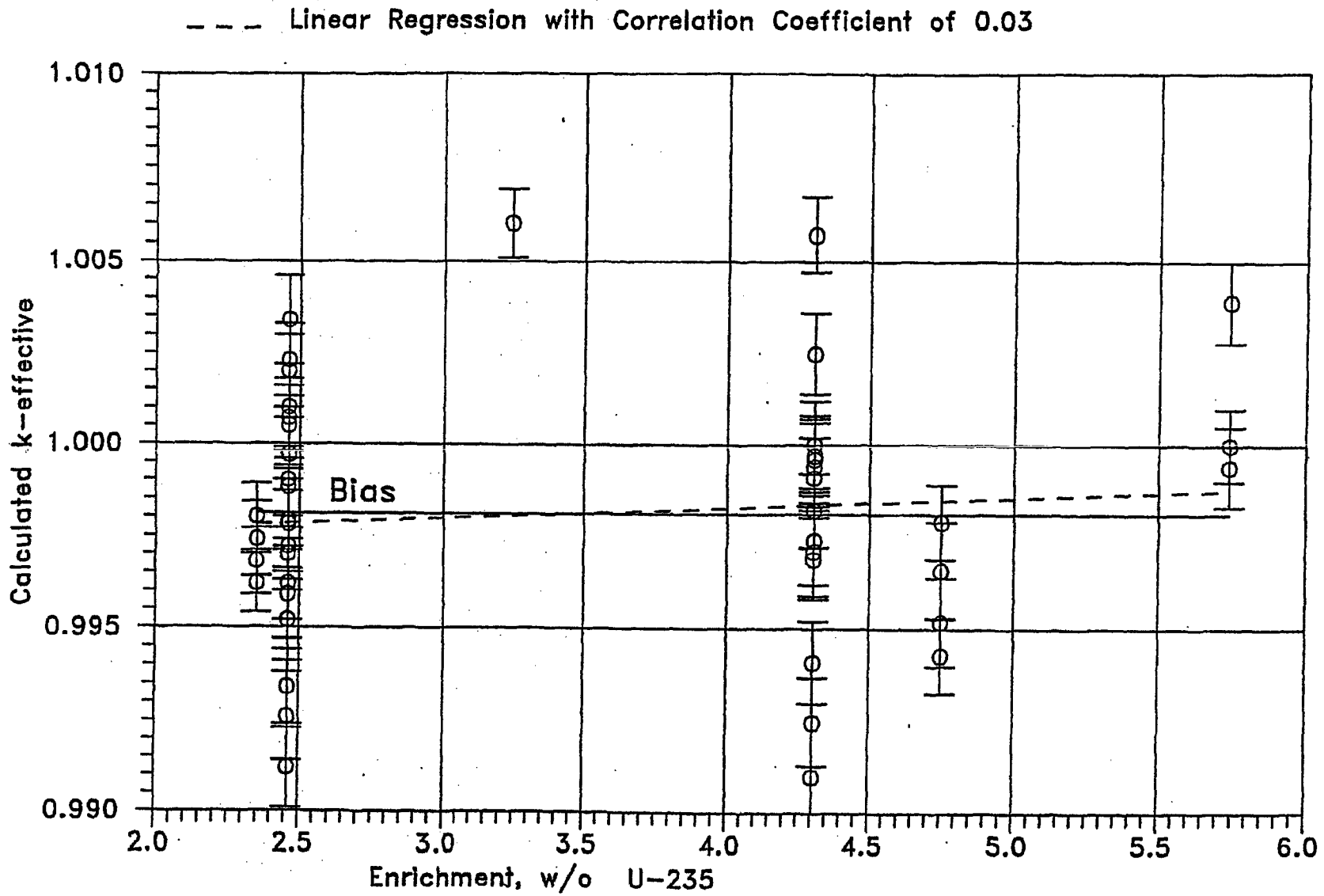


FIGURE 4A.3 MCNP CALCULATED k-eff VALUES  
AT VARIOUS U-235 ENRICHMENTS

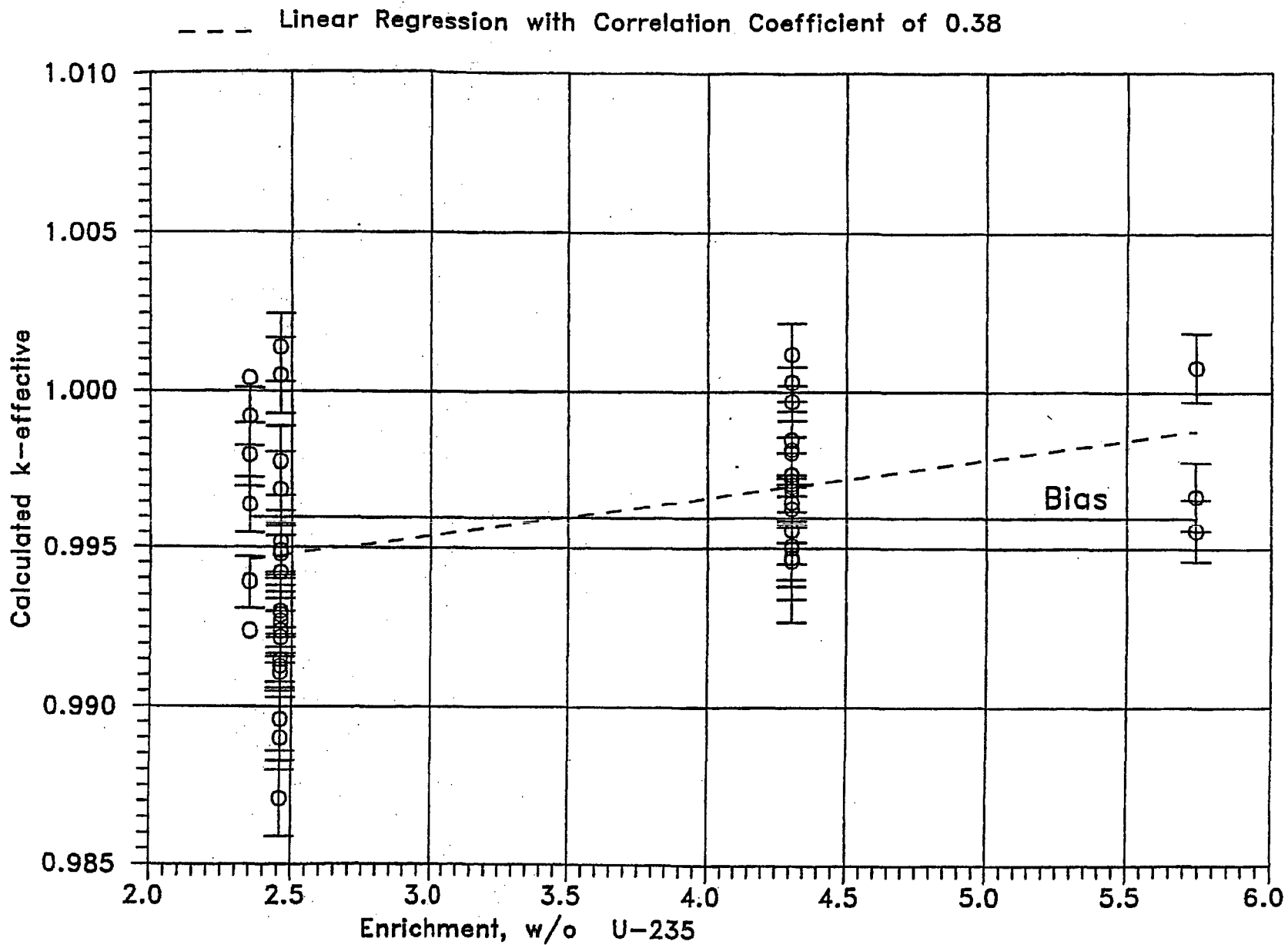


FIGURE 4A.4 KENO CALCULATED k-eff VALUES  
AT VARIOUS U-235 ENRICHMENTS

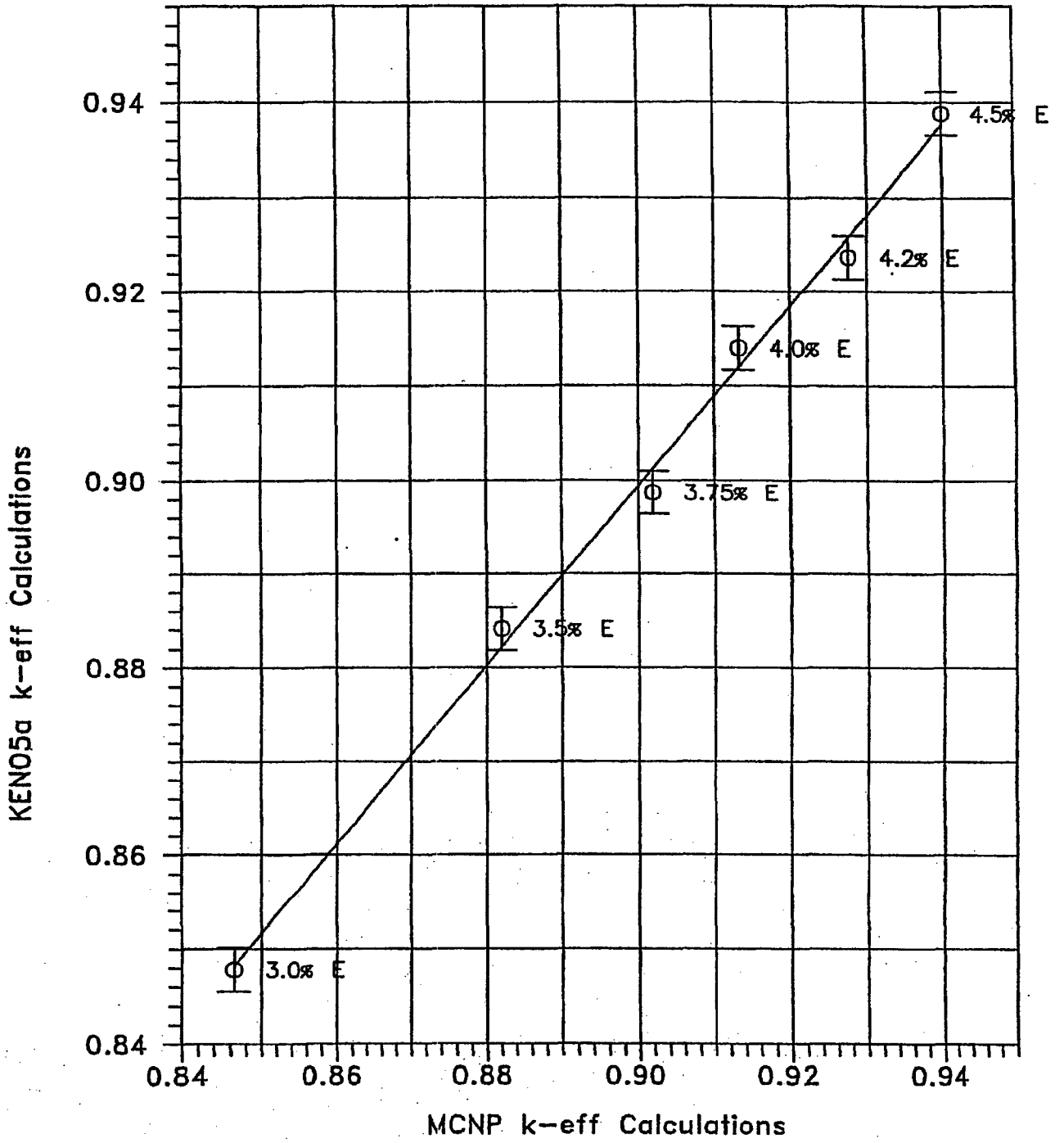


FIGURE 4A.5 COMPARISON OF MCNP AND KENO5A CALCULATIONS FOR VARIOUS FUEL ENRICHMENTS

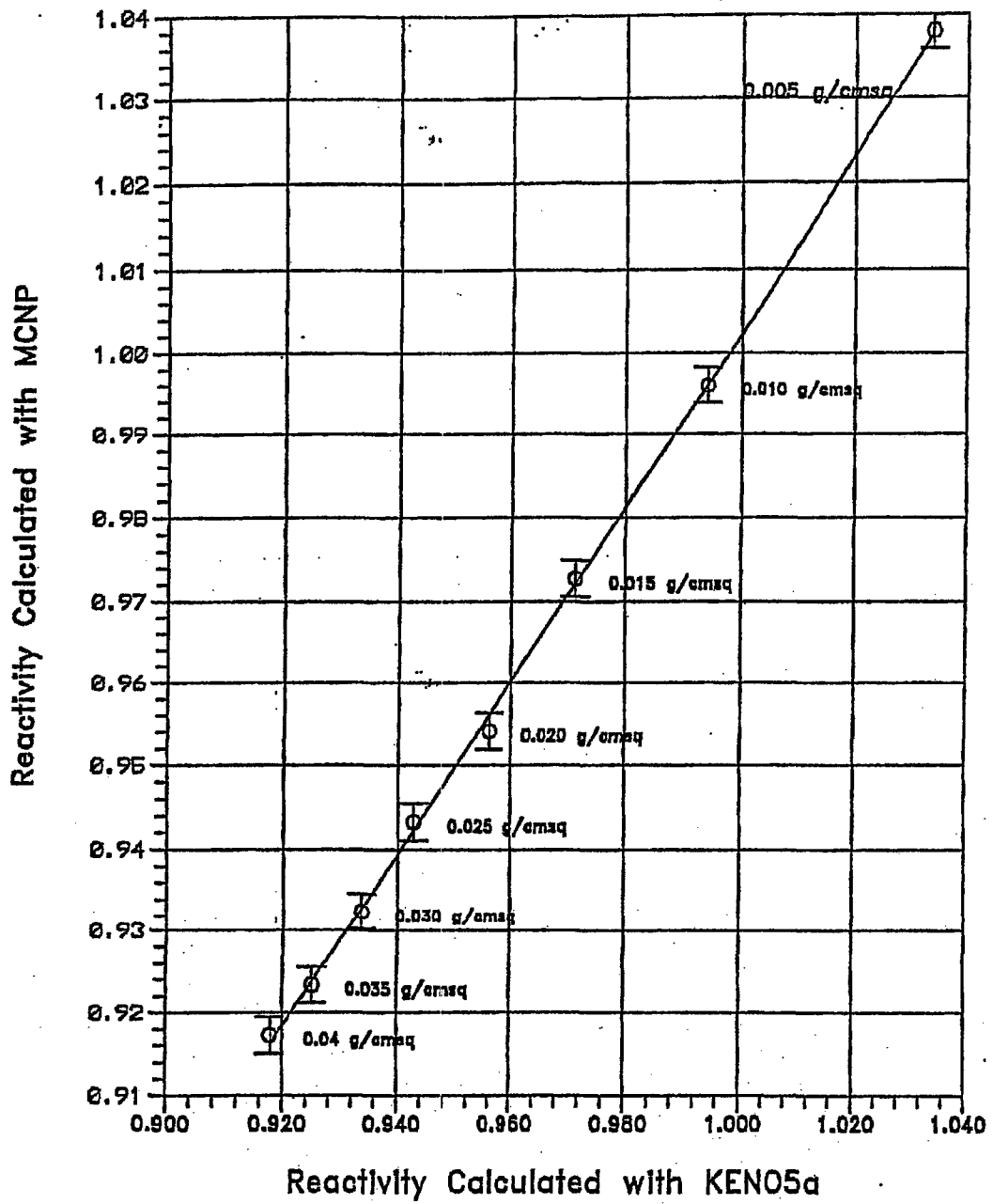


FIGURE 4A.6 : COMPARISON OF MCNP AND KENO5a CALCULATIONS FOR VARIOUS BORON-10 AREAL DENSITIES

## 5.0 THERMAL-HYDRAULIC CONSIDERATIONS

### 5.1 Introduction

This section provides a summary of the analyses performed to demonstrate how the Turkey Point spent fuel pools (SFPs) and their attendant cooling systems meet the intent of USNRC Standard Review Plan (SRP) Section 9.1.3 [5.5.1] and Section III of the USNRC OT Position Paper [5.5.2], following the installation of Metamic inserts into the spent fuel storage racks. Similar methods of thermal-hydraulic analysis have been used in the licensing evaluations for other SFP modification projects.

Thermal-hydraulic analyses for the spent fuel pool may be separated into the following categories:

- i. Evaluation of the maximum SFP bulk temperatures for the various offload scenarios, to demonstrate that temperature limits are not exceeded.
- ii. Evaluation of loss-of-forced cooling scenarios, to establish the time to boil, the minimum time available to perform corrective actions, and the associated makeup water flow rate requirements.
- iii. Determination of the maximum local water temperature under any operating condition with forced-flow cooling available, to establish that localized boiling in the fuel storage racks is not possible at these conditions.
- iv. Evaluation of the potential for departure from nucleate boiling (DNB) under any operating condition, to establish that departure from nucleate boiling is not possible.

An evaluation of the effects of Metamic inserts on the thermal performance of Turkey Point SFPs and their attendant cooling systems has determined that the existing licensing bases<sup>1</sup> for Categories i and ii above contains sufficient conservatism to remain bounding for any possible number of Metamic inserts. Specifically, the thermal capacity and water volumes used in calculations to support the existing licensing bases are sufficiently understated that the amount of

---

<sup>1</sup> Specifically, the bases as described in the Turkey Point Unit 3 and 4 cask area rack license amendment [5.5.3].

water displaced by Metamic inserts is already encompassed. As such, this chapter will only discuss Categories iii and iv, which are not bounded by the existing licensing bases.

The following sections: 1) describe the analysis methodologies and assumptions, 2) provide a synopsis of the input data employed and 3) summarize the calculated results.

## 5.2 Maximum SFP Local Water Temperature

This section summarizes the methodology used to quantify local water temperature within the SFP fuel storage racks. The results of these evaluations are maximum local water temperatures.

In order to determine an upper bound on the maximum local water temperature, a series of conservative assumptions are made. The most important of these assumptions are:

- The walls and floor of the SFP are all modeled as adiabatic surfaces, thereby neglecting conduction heat loss through these items.
- Heat losses by thermal radiation and natural convection from the hot SFP surface to the environment are neglected.
- No downcomer flow is assumed to exist between the rack modules.
- The hydraulic resistance of every fuel storage rack cell is determined based on the most limiting (i.e., highest hydraulic resistance) fuel assembly type.
- The hydraulic resistance of every Region II fuel rack cell is determined assuming that a Metamic insert is installed, that the Metamic insert is positioned to minimize the area available for the fuel assembly, and that all flow outside the Metamic insert (i.e., on the side opposite the fuel assembly) is completely neglected.
- The hydraulic resistance parameters for the rack cells, permeability and inertial resistance, are conservatively adjusted by 5%.
- The bottom plenum heights used in the model are less than the actual heights.
- The hydraulic resistance of each fuel storage cell is determined based on the most restrictive water inlet geometry of cells located over rack support pedestals (i.e., where

all baseplate holes are completely blocked). These cells have a reduced water entrance area, caused by the pedestal blocking the baseplate hole, and a correspondingly increased hydraulic resistance.

- The hydraulic resistance calculated for each fuel storage cell includes effects of a partial exit flow area blockage. This blockage is assumed to be caused by a dropped Metamic insert lying horizontally on top of the racks.
- Fuel assemblies with the highest decay heat generation rates are grouped together in the center of the model. This conservatively maximizes the distance between these hot fuel assemblies and the rack-to-wall downcomers, so the cooled water from the SFP cooling system must travel further along the SFP floor to cool them. Discharge of these assemblies into any rack locations that are closer to a downcomer is bounded by the analyzed configuration.

To demonstrate adequate cooling of hot fuel in the SFP, it is necessary to rigorously quantify the coupled velocity and temperature fields created by the interaction of buoyancy driven and forced water flows. A Computational Fluid Dynamics (CFD) analysis for this demonstration is required. The objective of this study is to demonstrate that the thermal-hydraulic criterion of ensuring local subcooled conditions in the SFP is met for all postulated normal fuel offload/cooling alignment scenarios. The local thermal-hydraulic analysis is performed such that partial cell blockage and slight fuel assembly variations are bounded. An outline of the CFD approach is described in the following.

There are several significant geometric and thermal-hydraulic features of the Turkey Point SFPs that need to be considered for a rigorous CFD analysis. From a fluid flow modeling standpoint, there are two regions to be considered. One region is the SFP bulk region where the classical Navier-Stokes equations [5.5.4] are solved, with turbulence effects included. The other region is the fuel storage racks containing heat generating fuel assemblies, located near the bottom of the SFP. In this region, water flow is directed upwards due to buoyancy forces through relatively small flow channels formed by rods of the fuel assemblies in each rack cell. This situation is modeled as a porous solid region with pressure drop in the flowing fluid governed by Darcy's Law as:

$$\frac{\partial P}{\partial X_i} = - \frac{\mu}{K(i)} V_i - C_i \rho |V_i| \frac{V_i}{2} \quad (5-1)$$

where  $\partial P/\partial X_i$  is the pressure gradient,  $K(i)$ ,  $V_i$  and  $C_i$  are the corresponding permeability, velocity and inertial resistance parameters and  $\mu$  is the fluid viscosity. These terms are added to the classic Navier-Stokes equations. The permeability and inertial resistance parameters for the rack cells loaded with fuel assemblies are determined based on friction factor correlations for the laminar flow conditions that would exist due to the low buoyancy induced velocities and the small size of the flow channels.

The Turkey Point SFP geometries require an adequate portrayal of both large scale and small scale features, spatially distributed heat sources in the racks and water inlet/outlet piping. Relatively cooler bulk water normally flows down between the fuel racks outline and wall liner, a clearance known as the downcomer. Near the bottom of the racks the flow turns from a vertical to horizontal direction into the bottom plenum, supplying cooling water to the rack cells. Heated water issuing out of the top of the racks mixes with the bulk water above the racks.

The distributed heat sources in the racks are modeled by identifying distinct heat generation zones considering recently offloaded fuel, bounding peaking effects, and the presence of background decay heat from previous offloads. Three heat generating zones are identified. The first consists of background fuel from previous offloads. The second and third zones consist of fuel from recently offloaded fuel assemblies. The two recent offload zones are differentiated so one zone has a higher than average decay heat (the hottest batch of 64 assemblies) generation rate and the other zone has less than average decay heat generation (it comprises the remainder of a full core fuel offload). This is a conservative model, since all of the fuel with higher than average decay heat is placed in a contiguous area. A uniformly distributed heat generation rate was applied throughout each distinct zone (i.e., there were no variations in heat generation rate within a single zone).

The CFD analysis was performed on the commercially available FLUENT computational fluid dynamics program, which has been benchmarked under Holtec's QA program [5.5.5]. The FLUENT code enables buoyancy flow and turbulence effects to be included in the CFD analysis.

Buoyancy forces are included by specifying a temperature-dependent density for water and applying an appropriate gravity vector. Turbulence effects are modeled by relating time-varying Reynolds' Stresses to the mean bulk flow quantities with the standard k-ε turbulence model.

Some of the major input values for this analysis are summarized in Table 5.2.1. An isometric view of the assembled CFD model for the Turkey Point units is presented in Figure 5.2.1.

### 5.3 Fuel Rod Cladding Temperature

In this section, the method used to evaluate the potential for DNB is presented. DNB requires the presence of two conditions, a heated surface temperature above the local saturation temperature of the adjacent water and a sufficient heat flux to prevent rewetting of the heated surface as vapor is produced (i.e., vapor blanketing). Incropera and DeWitt [5.5.6] give the critical heat flux at which water begins the transition from nucleate boiling to DNB as about  $10^6$  W/m<sup>2</sup>.

A fuel rod can produce  $F_{total}$  times the average heat generation rate over a small length, where  $F_{total}$  is the maximum localized heat generated divided by the average for the hottest assembly. The total heat distribution in a rod is generally a maximum in the central region, and tapers off at its two extremities. Thus, peak cladding heat flux over an infinitesimal rod section is given by the equation:

$$q_c = \frac{Q \times F_{total}}{A_c} \quad (5-2)$$

where  $Q$  is the rod average heat emission and  $A_c$  is the total cladding external heat transfer area in the active fuel length region. The value of  $q_c$  calculated using Equation 5-2 will be compared to the critical heat flux. If the maximum heat flux is less than the critical heat flux, DNB cannot occur regardless of the surface fuel cladding surface and local water temperatures.

## 5.4 Results

Consistent with our approach of making conservative assessments of temperature, the local water temperature calculations are performed for a SFP with a total decay heat generation rate equal to the decay heat load coincident with the maximum SFP bulk temperature. Thus, the local water temperature evaluation is a calculation of the temperature increment over the theoretical spatially uniform value due to local hot spots (resulting from the presence of highly heat emissive fuel assemblies). As described in Subsection 5.3, the peak fuel cladding heat flux is also determined.

The numeric results of the maximum local water temperature and the fuel cladding heat flux evaluations are presented in Table 5.4.1. Figure 5.4.1 presents converged temperature contours in a vertical slice through the hot fuel region of the SFP.

The maximum local water temperature is lower than the 241°F local boiling temperature at the top of the active fuel length. These results demonstrate that boiling will not occur in the racks while forced-flow cooling is available. Further, the cladding heat flux is insufficient to result in departure from nucleate boiling under any condition (i.e., forced-flow cooling or bulk boiling).

## 5.5 References

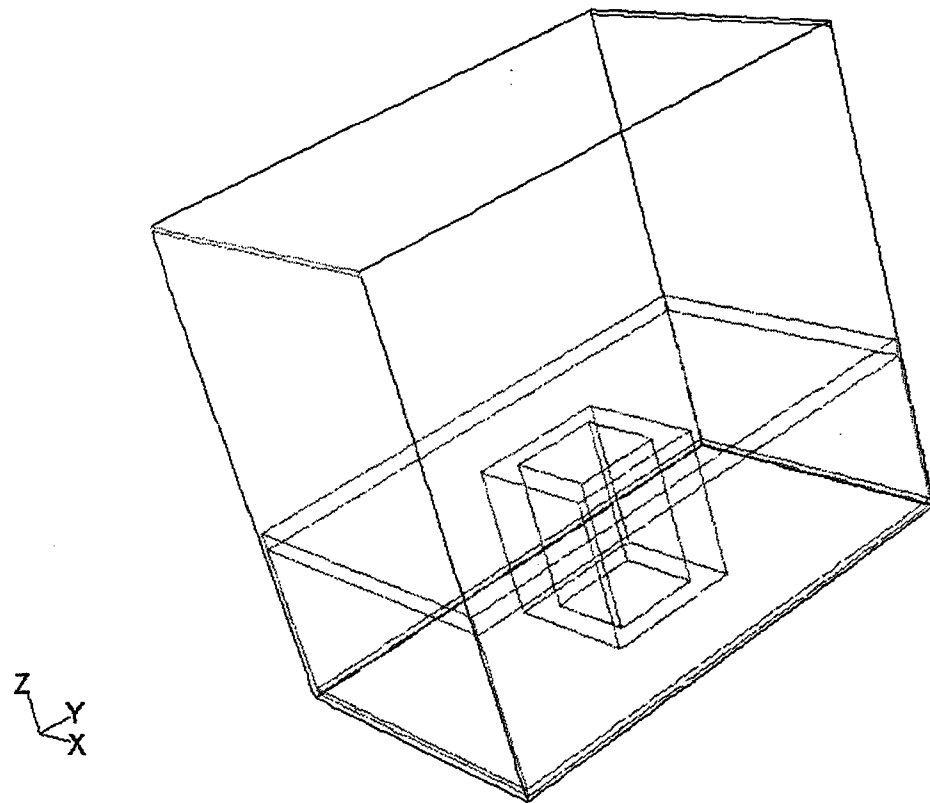
- [5.5.1] USNRC Standard Review Plan 9.1.3, Spent Fuel Pool Cooling and Cleanup System, Revision 1, July 1981.
- [5.5.2] USNRC OT Position Paper for Review and Acceptance of Spent Fuel Storage and Handling Applications, 14 April 1978.
- [5.5.3] Turkey Point Units 3 and 4 (Docket Nos. 50-250 and 50-251) Proposed License Amendments, "Addition of Cask Area Spent Fuel Storage Racks," Florida Power and Light Document L-2002-214, dated 26 November 2002.
- [5.5.4] Batchelor, G.K., "An Introduction to Fluid Dynamics", Cambridge University Press, 1967.
- [5.5.5] "Validation of FLUENT Version 6.1.18", Holtec Report HI-2032998, Revision 0.

[5.5.6] Incropera and DeWitt, "Fundamentals of Heat and Mass Transfer," John Wiley and Sons, Fourth Edition.

| <b>Table 5.2.1</b>                                     |                            |
|--|----------------------------|
| <b>Key Input Data for Local Temperature Evaluation</b> |                            |
| <b>Parameter</b>                                       | <b>Value</b>               |
| SFP Bulk Temperature                                   | 150°F                      |
| Total Decay Heat Generation Rate                       | $31.48 \times 10^6$ Btu/hr |
| Hottest Reload Batch Decay Heat Rate                   | $17.43 \times 10^6$ Btu/hr |
| Balance of Full Core Decay Heat Rate                   | $10.05 \times 10^6$ Btu/hr |
| Maximum Assembly Power Factor                          | 1.515                      |
| Assembly Total Peaking Factor                          | 1.75                       |
| Fuel Rod Outer Diameter                                | 0.422 inches               |
| Active Fuel Length                                     | 144 inches                 |
| Number of Rods per Assembly                            | 204                        |
| Minimum Rack Cell Inner Dimension                      | 8.75 inches                |
| Minimum Metamic Insert Inner Dimension                 | 8.45 inches                |
| Rack Cell Length                                       | 165.61 inches              |
| Modeled Bottom Plenum Height                           | 2.81 inches                |

Note: The total decay heat generation rate occurs at the point in time when the bulk temperature reaches 150°F following a full core offload. The hottest reload batch decay heat rate occurs three days after reactor shutdown following the offload of a maximum burnup 64-assembly refueling batch. The balance of full core decay heat rate is the value that is added to the hottest reload batch decay heat rate to obtain the total full core decay heat rate at the point in time when the bulk temperature reaches 150°F following a full core offload. All of these values are consistent with the Turkey Point Unit 3 and 4 cask area rack license amendment [5.5.3].

| <b>Table 5.4.1</b>  |                       |
|---|-----------------------|
| <b>Results of Maximum Local Water and Fuel Cladding Temperature Evaluations</b> |                       |
| <b>Parameter</b>  | <b>Value</b>          |
| Peak Local Water Temperature  | 206°F                 |
| Peak Cladding Heat Flux   | 3177 W/m <sup>2</sup> |
|   |                       |



Grid May 24, 2004  
FLUENT 6.1 (3d, dp, segregated, ske)

Figure 5.2.1 –CFD Model Isometric View

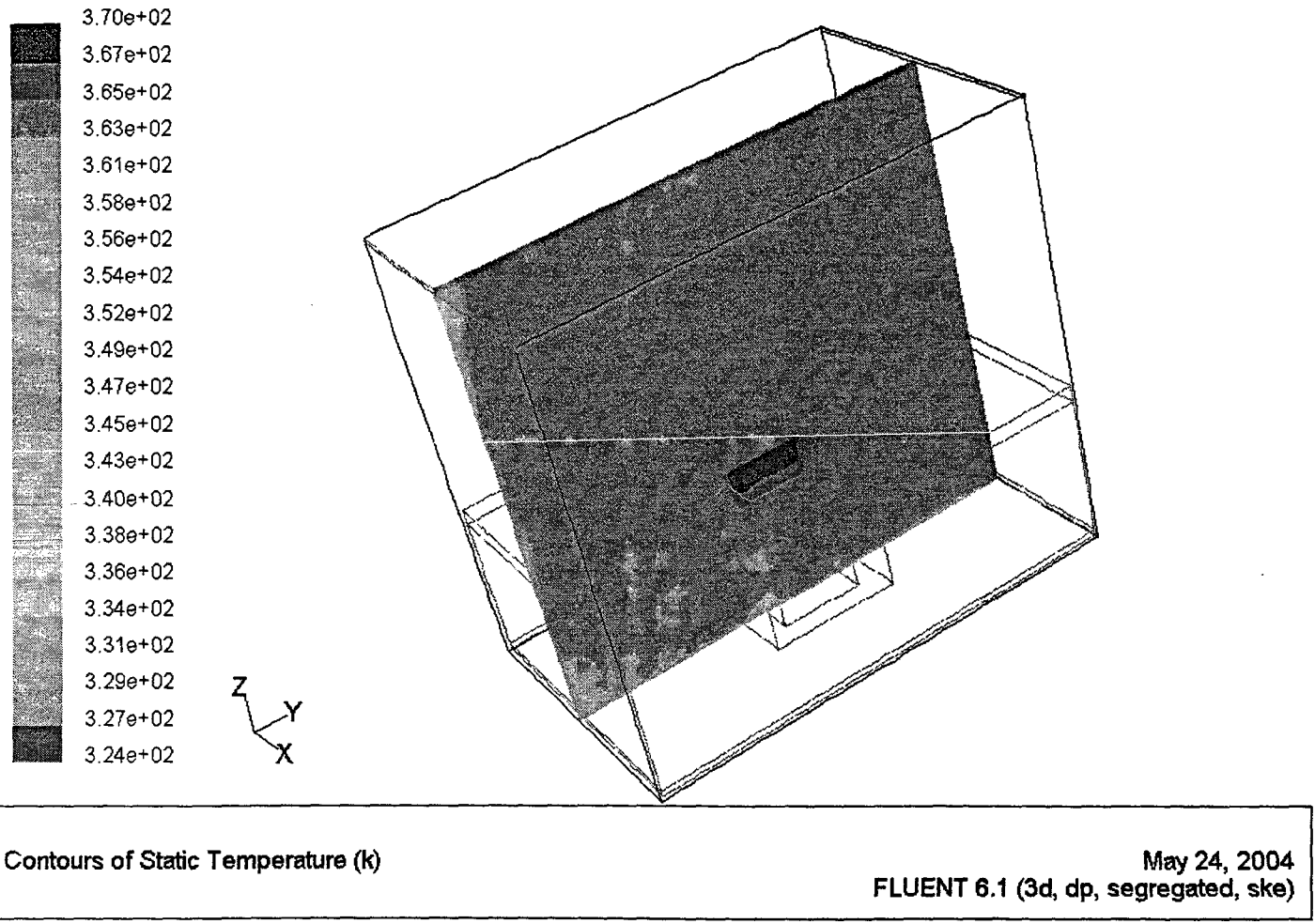


Figure 5.4.1 –CFD Model with Converged Temperature Contours

## 6.0 EXISTING RACK STRUCTURAL/SEISMIC CONSIDERATIONS

### 6.1 Introduction

This section examines the structural adequacy of the Turkey Point Spent Fuel Pool (SFP) racks, after Metamic™ inserts have been added to all existing racks, other than the Cask Area rack. Loadings postulated to occur during normal, seismic, and accident conditions have been considered. The analyzed storage rack configurations for Unit 3 and Unit 4 are depicted in Figures 1.1.1 and 1.1.2, respectively. Except for the cask rack, loads on these fuel storage racks were analyzed and the racks licensed for use during the 1980's, prior to their installation at Turkey Point. The design basis seismic analysis for racks other than the Cask Area rack, originally performed by Westinghouse, yielded substantial margins of safety. The net effect of the proposed modification to add Metamic™ inserts is that the weight of the racks, when loaded with fuel, increases by approximately 1%. Considering a change of this magnitude, and the existing design margin, seismic response of the as-modified fuel storage racks can also be expected to yield acceptable results. Therefore, the seismic analyses documented in this section serve primarily to validate the conclusions reached in earlier analyses and licensing documents. Re-analysis of the racks' seismic performance using the more rigorous Whole-Pool Multi-Rack (WPMR) analysis technique, consistent with contemporary practice, also better quantifies the available margin to design limits.

The analyses undertaken to confirm the structural integrity of the racks are performed in compliance with the USNRC Standard Review Plan [6.14.1] and the OT Position Paper [6.14.2]. For each of the analyses, an abstract of the methodology used, the modeling assumptions, key results, and a summary of parametric evaluations are presented. Delineation of the relevant criteria is discussed in the text associated with each analysis.

### 6.2 Overview of Rack Structural Analysis Methodology

The response of a free-standing rack module to seismic inputs is highly nonlinear and it involves a complex combination of motions (sliding, rocking, twisting, and turning), resulting in impacts

and friction effects. Some of the unique attributes of the rack's dynamic behavior include a large fraction of the total structural mass engaged in a confined rattling motion, friction support of rack pedestals resisting lateral motion, large fluid coupling effects due to deep submergence in water and the independent motion of closely spaced adjacent structures.

Linear methods, such as modal analysis and response spectrum techniques, cannot accurately simulate the response of such a highly nonlinear structure to seismic excitation. An accurate simulation is obtained only by direct integration of the nonlinear equations of motion with the three orthogonal pool slab acceleration time-histories applied as the forcing functions acting simultaneously.

The DYNARACK solver [6.14.6] is the vehicle utilized in this project to simulate the dynamic behavior of complex storage rack structures. The following sections provide the basis for selecting this tool and discuss development of the methodology used.

#### 6.2.1 Background of Analysis Methodology

Reliable assessment of the stress field and the kinematic behavior of rack modules calls for a conservative dynamic model incorporating all *key attributes* of the actual structure. This means that the model must feature the ability to execute concurrent motion forms compatible with the free-standing nature of the racks. The selected model must also possess the capability to effect momentum transfers which occur as a result of fuel assembly rattling inside storage cells and the capability to simulate the lift-off and subsequent impact of support pedestals with bearing pads. The contribution of the water mass in interstitial spaces around the rack modules and within the storage cells must also be modeled in an accurate manner, since erring in quantification of fluid coupling on either side of the actual value is no guarantee of conservatism.

The Coulomb friction coefficient at the pedestal-to-bearing pad interface may lie in a rather wide range and a conservative value of friction cannot be prescribed *a priori*. In fact, a perusal of results of rack dynamic analyses in numerous dockets (see Table 6.2.1) indicates that an upper

bound value of the coefficient of friction often maximizes the computed rack displacements as well as the equivalent elastostatic stresses.

In short, there are a large number of parameters with potential influence on the rack kinematics. The comprehensive structural evaluation must deal with all of these without sacrificing conservatism.

Briefly, the 3-D rack model dynamic simulation, involving one or more spent fuel racks, handles the array of variables as follows:

Interface Coefficient of Friction: Parametric runs are made with upper bound and lower bound values of the coefficient of friction. The limiting values are based on experimental data which have been found to be bounded by the values 0.2 and 0.8. Simulations are also performed with the array of pedestals having randomly chosen coefficients of friction drawn from a Gaussian distribution with a mean value of 0.5 and lower and upper limits of 0.2 and 0.8, respectively. In the fuel rack simulations, the Coulomb friction interface between rack support pedestal and bearing pad is simulated by piecewise linear (friction) elements. These elements function only when the pedestal is physically in contact with the bearing pad.

Rack Beam Behavior: Rack elasticity, relative to the rack base, is included in the model by introducing linear springs to represent the elastic bending action, twisting, and extensions.

Impact Phenomena: Compression-only gap elements are used to provide for the opening and closing of interfaces such as the pedestal-to-bearing pad interface, and the fuel assembly-to-cell wall interface. These interface gaps are modeled using nonlinear spring elements. The term "nonlinear spring" is a generic term used to denote the mathematical representation of the condition where a restoring force is not linearly proportional to displacement.

Fuel Loading Scenarios: The fuel assemblies are conservatively assumed to rattle in unison; this exaggerates the contribution of impact against the cell wall.

Fluid Coupling: Holtec International extended Fritz's classical two-body fluid coupling model to multiple bodies and utilized it to perform the first two-dimensional multi-rack analysis (Diablo Canyon, ca. 1987). Subsequently, laboratory experiments were conducted to validate fluid coupling theory. This technology was incorporated in the computer code DYNARACK [6.14.6]. This development was first utilized in the Chin Shan, Oyster Creek, and Shearon Harris plants [6.14.3, 6.14.5] in the 1980's and, subsequently, in numerous other rerack projects.

### 6.3 Description of Racks

The rack layouts for the Turkey Point Unit 3 and Unit 4 SFPs are illustrated in Figures 1.1.1 and 1.1.2. Including the Cask Area rack, there are four Region I and nine Region II racks in each unit. Due to the similarity in configuration of the two units (one unit is a mirror image of the other), a model prepared for one of the two units also applies to the other unit. For this evaluation, Unit 3 was modeled. For the purpose of analytical modeling, the racks in all cases addressed are numbered. Rack #1 is in the southwest corner of the SFP. The numbering progresses south to north, continuing with the southern most rack in the next row to the east, etc.. Thus rack module 13, as identified in Figure 1.1.1, is in the northeast corner of the Unit 3 SFP.

At Turkey Point, the Metamic™ inserts will only be installed in Region II racks. The criticality analyses, discussed in Section 4.0, consider Metamic™ inserts installed in a two-out-of-every-four cell array as the highest density of inserts loaded into any rack module. However, inserts could be loaded into one or more racks at a higher density for storage purposes, with the incremental inserts not credited for reactivity control. Therefore, the rack structural analyses considered conditions where inserts are loaded into every other Region II cell, and additional sensitivity analyses were performed considering an insert to be present in every Region II cell. The assumption that an insert is present in every cell is considered conservative because it maximizes the total weight of the rack, which in turn maximizes the rack pedestal loads. The results, as discussed below, indicate that the differences between cases where racks are assumed to be fully loaded with inserts and cases where racks contain inserts in only 50% of cells are

insignificant. This result is expected, because the insert mass is negligible when compared to the mass of a loaded rack.

The material used in the existing racks is identified in Table 6.3.1.

The cartesian coordinate system utilized within the rack dynamic model has the following nomenclature:

x = Horizontal axis along plant North  
y = Horizontal axis along plant West  
z = Vertical axis upward from the rack base

### 6.3.1 Fuel and Metamic™ Insert Weights

The weight of a fuel assembly (with rod cluster control assembly - RCCA) is approximately 1608 lb. A bounding weight of approximately 24 lb is derived for each Metamic™ insert. Where inserts are assumed to be loaded into one-half of the storage cells in each rack, the total combined (i.e., per cell) weight of a stored fuel assembly plus a Metamic™ insert credits one-half the weight of the insert and is taken as 1620 lb. The total combined weight of a stored fuel assembly plus a Metamic™ insert is taken as 1632 lb for analyses where an insert is assumed to be present in every cell.

### 6.4 Synthetic Time-Histories

The synthetic time-histories in three orthogonal directions (N-S, E-W, and vertical) are generated in accordance with the provisions of SRP Section 3.7.1 [6.14.1]. In order to prepare an acceptable set of acceleration time-histories, Holtec International's proprietary code GENEQ [6.14.7] is utilized.

A preferred criterion for the synthetic time-histories in SRP 3.7.1 calls for both the response spectrum and the power spectral density corresponding to the generated acceleration time-history to envelop their target (design basis) counterparts with only finite enveloping inflections. The time-histories for the pools have been generated to satisfy this preferred criterion. The seismic files also satisfy the requirements of statistical independence mandated by SRP 3.7.1.

Figures 6.4.1 through 6.4.3 provide plots of the time-history accelerograms which were generated over a 20 second duration for the SSE event. The time-history accelerograms for the OBE event are obtained by multiplying the SSE time-histories by a scale factor of 1/3. These artificial time-histories are used in all non-linear dynamic simulations of the racks.

Results of the correlation function of the three time-histories are given in Table 6.4.1. Absolute values of the correlation coefficients are shown to be less than 0.15, indicating that the desired statistical independence of the three data sets has been met.

## 6.5 WPMR Methodology

Recognizing that the analytical work must deal with both stress and displacement criteria, the sequence of model development and analysis steps that are undertaken are summarized in the following:

- a. Prepare 3-D dynamic models suitable for a time-history analysis of the Region II racks with Metamic™ inserts. These models include the assemblage of all rack modules in each pool. Include all fluid coupling interactions and mechanical coupling appropriate to performing an accurate non-linear simulation. This 3-D simulation is referred to as a Whole Pool Multi-Rack model.
- b. Perform 3-D dynamic analyses parametric in various physical conditions (such as coefficient of friction and extent of Region II cells containing Metamic™ inserts). Archive appropriate displacement and load outputs from the dynamic model for post-processing.

- c. Perform stress analysis of high stress areas for the limiting case of all the rack dynamic analyses. Demonstrate compliance with ASME Code Section III, Subsection NF limits on stress and displacement.

### 6.5.1 Model Details for Spent Fuel Racks

The dynamic modeling of the rack structure is prepared with special consideration of all nonlinearities and parametric variations. Particulars of modeling details and assumptions for the Whole Pool Multi-Rack analysis of Turkey Point racks are given in the following:

#### 6.5.1.1 Assumptions

- a. Motion of the fuel rack is captured by modeling the rack as a 12 degree-of-freedom structure. Movement of the rack cross-section at any height is described by six degrees-of-freedom of the rack base and six degrees-of-freedom at the rack top. In this manner, the response of the module, relative to the base-plate, is captured in the dynamic analyses once suitable springs are introduced to couple the rack degrees-of-freedom and simulate rack stiffness.
- b. Rattling fuel assemblies within a rack module are simulated by five lumped masses located at H, .75H, .5H, .25H, and at the rack base (H is the rack height measured above the base-plate). Each lumped fuel mass has two horizontal displacement degrees-of-freedom. Vertical motion of the fuel assembly mass is assumed equal to rack vertical motion at the base-plate level. The centroid of each fuel assembly mass can be located off-center, relative to the rack structure centroid at that level, to simulate a partially loaded rack.
- c. Seismic motion of a fuel rack is characterized by the random rattling of fuel assemblies in their individual storage locations. All fuel assemblies are assumed to move in-phase within a rack. This exaggerates computed dynamic loading on the rack structure and, therefore, yields conservative results.
- d. Fluid coupling between the rack and fuel assemblies, and between the rack and wall, is simulated by appropriate inertial coupling in the system kinetic energy equations. Inclusion of these effects uses the methods of [6.14.9, 6.14.10] for rack/assembly coupling and for rack-to-rack coupling.
- e. Fluid damping and form drag are conservatively neglected.
- f. Sloshing is found to be negligible at the top of the rack and is, therefore, neglected in the analysis of the rack.

- g. Potential impacts between the cell walls of the racks and the contained fuel assemblies are accounted for by appropriate compression-only gap elements positioned between the masses involved. The possible incidence of rack-to-wall or rack-to-rack impact is simulated by gap elements at the top and bottom of the rack in two horizontal directions. Bottom gap elements are located at the baseplate elevation. The initial gaps reflect the presence of baseplate extensions, and the rack stiffness values chosen are selected to simulate local structural detail.
- h. Pedestals are modeled by gap elements in the vertical direction and as "rigid links" for transferring horizontal stress. The base of each pedestal support is linked to the pool liner (or bearing pad) by two friction springs. The spring rate for the friction springs includes any lateral elasticity of the pedestals. Local pedestal vertical spring stiffness accounts for floor elasticity and for local rack elasticity just above the pedestal.
- i. Rattling of fuel assemblies inside storage locations causes the gap between fuel assemblies and the cell wall to change from a maximum of twice the nominal gap to a zero gap. Fluid coupling coefficients are based on the nominal gap in order to provide a conservative measure of fluid resistance to gap closure.
- j. The model for the rack is considered supported, at the base level, on four pedestals modeled as non-linear compression-only gap spring elements and eight piecewise linear friction spring elements. These elements are properly located with respect to the centerline of the rack beam, and allow for arbitrary rocking and sliding motions.

#### 6.5.1.2 Element Details

Figure 6.5.1 shows a schematic of the dynamic model of a single rack. The schematic depicts many of the characteristics of the model including all of the degrees-of-freedom and some of the spring restraint elements.

Table 6.5.1 provides a complete listing of each of the 22 degrees-of-freedom for a rack model. Six translational and six rotational degrees-of-freedom (three of each type on each end) describe the motion of the rack structure. Rattling fuel mass motions (shown at nodes 1\*, 2\*, 3\*, 4\*, and 5\* in Figure 6.5.1) are described by ten horizontal translational degrees-of-freedom (two at each of the five fuel masses). The vertical fuel mass motion is assumed (and modeled) to be the same as that of the rack baseplate.

Figure 6.5.2 depicts the fuel to rack impact springs (used to develop potential impact loads between the fuel assembly mass and rack cell inner walls) in a schematic isometric. Only one of the five fuel masses is shown in this figure. Four compression only springs, acting in the horizontal direction, are provided at each fuel mass.

Figure 6.5.3 provides a 2-D schematic elevation of the storage rack model, discussed in more detail in Section 6.5.3. This view shows the vertical location of the five storage masses and some of the support pedestal spring members.

Figure 6.5.4 shows the modeling technique and degrees-of-freedom associated with rack elasticity. In each bending plane, a shear and bending spring simulate elastic effects [6.14.11]. Linear elastic springs coupling rack vertical and torsional degrees-of-freedom are also included in the model.

Figure 6.5.5 depicts the inter-rack impact springs (used to develop potential impact loads between racks or between a rack and the wall).

### 6.5.2 Fluid Coupling Effect

In its simplest form, the so-called "fluid coupling effect" [6.14.9, 6.14.10] can be explained by considering the proximate motion of two bodies under water. If one body (mass  $m_1$ ) vibrates adjacent to a second body (mass  $m_2$ ), and both bodies are submerged in frictionless fluid, then Newton's equations of motion for the two bodies are:

$$(m_1 + M_{11}) A_1 + M_{12} A_2 = \text{applied forces on mass } m_1 + O(X_1^2)$$

$$M_{21} A_1 + (m_2 + M_{22}) A_2 = \text{applied forces on mass } m_2 + O(X_2^2)$$

$A_1$  and  $A_2$  denote absolute accelerations of masses  $m_1$  and  $m_2$ , respectively, and the notation  $O(X^2)$  denotes nonlinear terms.

$M_{11}$ ,  $M_{12}$ ,  $M_{21}$ , and  $M_{22}$  are fluid coupling coefficients which depend on body shape, relative disposition, etc. Fritz [6.14.10] gives data for  $M_{ij}$  for various body shapes and arrangements.

The fluid adds mass to the body ( $M_{11}$  to mass  $m_1$ ), and an inertial force proportional to acceleration of the adjacent body (mass  $m_2$ ). Thus, acceleration of one body affects the force field on another. This force field is a function of inter-body gap, reaching large values for small gaps. Lateral motion of a fuel assembly inside a storage location encounters this effect. For example, fluid coupling behavior will be experienced between nodes 2 and 2\* in Figure 6.5.1. The rack analysis also contains inertial fluid coupling terms, which model the effect of fluid in the gaps between adjacent racks.

Terms modeling the effects of fluid flowing between adjacent racks in a single rack analysis suffer from the inaccuracies described earlier. These terms are usually computed assuming that all racks adjacent to the rack being analyzed are vibrating in-phase or  $180^\circ$  out of phase. The WPMR analyses do not require any assumptions with regard to phase.

Rack-to-rack gap elements have initial gaps set to 100% of the physical gap between the racks or between outermost racks and the adjacent pool walls.

#### 6.5.2.1 Multi-Body Fluid Coupling Phenomena

During the seismic event, all racks in the pool are subject to the input excitation simultaneously. The motion of each free-standing module would be autonomous and independent of others as long as they did not impact each other and no water were present in the pool. While the scenario of inter-rack impact is not a common occurrence and depends on rack spacing, the effect of water (the so-called fluid coupling effect) is a universal factor. As noted in References 6.5.2 and 6.5.4, the fluid forces can reach rather large values in closely spaced rack geometries. It is therefore essential that the contribution of the fluid forces be included in a comprehensive manner. This is possible only if all racks in the pool are *allowed* to execute 3-D motion in the mathematical model. For this reason, single rack or even multi-rack models involving only a portion of the racks in the pool, are inherently inaccurate. The Whole Pool Multi-Rack model removes this intrinsic limitation of the rack dynamic models by simulating the 3-D motion of all modules simultaneously. The fluid coupling effect, therefore, encompasses interaction between

every set of racks in the pool, i.e., the motion of one rack produces fluid forces on all other racks and on the pool walls. Stated more formally, both near-field and far-field fluid coupling effects are included in the analysis.

The derivation of the fluid coupling matrix [6.14.12] relies on the classical inviscid fluid mechanics principles, namely the principle of continuity and Kelvin's recirculation theorem. The derivation of the fluid coupling matrix has been verified by an extensive set of shake table experiments [6.14.12].

### 6.5.3 Stiffness Element Details

Three element types are used in the rack models. Type 1 are linear elastic elements used to represent the beam-like behavior of the integrated rack cell matrix. Type 2 elements are the piece-wise linear friction springs used to develop the appropriate forces between the rack pedestals and the supporting bearing pads. Type 3 elements are non-linear gap elements, which model gap closures and the subsequent impact loadings i.e., between fuel assemblies and the storage cell inner walls, and rack outer periphery spaces.

If the simulation model is restricted to two dimensions (one horizontal motion plus one vertical motion, for example), for the purposes of model clarification only, then Figure 6.5.3 describes the configuration. This simpler model is used to elaborate on the various stiffness modeling elements.

Type 3 gap elements modeling impacts between fuel assemblies and racks have local stiffness  $K_i$  in Figure 6.5.3. Support pedestal spring rates  $K_S$  are modeled by type 3 gap elements. Local compliance of the concrete floor is included in  $K_S$ . The type 2 friction elements are shown in Figure 6.5.3 as  $K_f$ . The spring elements depicted in Figure 6.5.4 represent linear type 1 elements.

Friction at support/liner interface is modeled by the piecewise linear friction springs with suitably large stiffness  $K_f$  up to the limiting lateral load  $\mu N$ , where  $N$  is the current compression

load at the interface between support and liner and  $\mu$  is the coefficient of friction. At every time-step during transient analysis, the current value of N (either zero if the pedestal has lifted off the liner/bearing pad, or a compressive finite value) is computed.

The gap element  $K_s$ , modeling the effective compression stiffness of the structure in the vicinity of the support, includes stiffness of the pedestal, local stiffness of the underlying pool slab, and local stiffness of the rack cellular structure above the pedestal.

The previous discussion is limited to a 2-D model solely for simplicity. Actual analyses incorporate 3-D motions.

#### 6.5.4 Coefficients of Friction

To eliminate the last significant element of uncertainty in rack dynamic analyses, multiple simulations are performed to adjust the friction coefficient ascribed to the support pedestal/pool bearing pad interface. These friction coefficients are chosen consistent with the two bounding extremes from Rabinowicz's data [6.14.8]. Simulations are also performed by imposing intermediate value friction coefficients, both 0.5 and those developed by a random number generator with Gaussian distribution characteristics. The assigned values are then held constant during the entire simulation in order to obtain reproducible results.<sup>†</sup> Thus, in this manner, the WPMR analysis results are brought closer to the realistic structural conditions.

The coefficient of friction ( $\mu$ ) between the pedestal supports and the pool floor is indeterminate. According to Rabinowicz [6.14.8], results of 199 tests performed on austenitic stainless steel plates submerged in water show a mean value of  $\mu$  to be 0.503 with standard deviation of 0.125. Upper and lower bounds (based on twice standard deviation) are 0.753 and 0.253, respectively. Analyses are therefore performed for coefficient of friction values of 0.2 (lower limit), 0.5 and 0.8 (upper limit), as well as for random coefficient of friction values clustered about a mean of

---

<sup>†</sup> It is noted that DYNARACK has the capability to change the coefficient of friction at any pedestal at each instant of contact based on a random reading of the computer clock cycle. However, exercising this option would yield results that could not be reproduced. Therefore, the random choice of coefficients is made only once per run.

0.5. The bounding values of  $\mu = 0.2$  and  $0.8$  have been found to envelop the upper limit of module response in previous spent fuel rack projects.

### 6.5.5 Governing Equations of Motion

Using the structural model discussed in the prior sections, equations of motion corresponding to each degree-of-freedom are obtained using Lagrange's Formulation [6.14.11]. The system kinetic energy includes contributions from solid structures and from trapped and surrounding fluid. The final system of equations obtained have the matrix form:

$$[M] \left[ \frac{d^2 q}{dt^2} \right] = [Q] + [G]$$

where:

- [M] - total mass matrix (including structural and fluid mass contributions). The size of this matrix will be  $22n \times 22n$  for a WPMR analysis ( $n$  = number of racks in the model).
- q - the nodal displacement vector relative to the pool slab displacement (the term with q indicates the second derivative with respect to time, i.e., acceleration)
- [G] - a vector dependent on the given ground acceleration
- [Q] - a vector dependent on the spring forces (linear and nonlinear) and the coupling between degrees-of-freedom

The above column vectors have length  $22n$ . The equations can be rewritten as follows:

$$\left[ \frac{d^2 q}{dt^2} \right] = [M]^{-1}[Q] + [M]^{-1}[G]$$

This equation set is mass uncoupled, displacement coupled at each instant in time. The numerical solution uses a central difference scheme built into the proprietary computer program DYNARACK [6.14.6].

## 6.6 Structural Evaluation of Spent Fuel Rack Design

### 6.6.1 Kinematic and Stress Acceptance Criteria

There are two sets of criteria to be satisfied by the rack modules:

#### a. Kinematic Criteria

An isolated fuel rack situated in the middle of the storage cavity is most vulnerable to overturning because such a rack would be hydrodynamically uncoupled from any adjacent structures. Therefore, to assess the margin against overturning, a single rack module is evaluated. Section IV(6) of Reference [6.14.2] refers to the SRP for safety factors against rack overturning. According to SRP Section 3.8.5.II-5 [6.14.1], the minimum required safety margins under the OBE and SSE events are 1.5 and 1.1, respectively. In order to ensure that these safety factors are met, the simulations resulting in the highest top of rack displacement were re-performed with an earthquake excitation multiplier of 1.5 for both the OBE and SSE. The maximum rotations of the rack (about the two principal axes) are obtained from a post processing of the rack time history response output. The ratio of the rotation required to produce incipient tipping in either principal plane to the actual maximum rotation in that plane from the time history solution is the margin of safety. Since the factors of safety are conservatively embedded in the earthquake multipliers, meeting the acceptance criteria is established when the ratio of rotation described above is greater than 1.0.

b. Stress Limit Criteria

Stress limits must not be exceeded under the postulated load combinations provided herein.

6.6.2 Stress Limit Evaluations

The stress limits presented below apply to the rack structure and are derived from the ASME Code, Section III, Subsection NF [6.14.13]. Parameters and terminology are in accordance with the ASME Code. Material properties are obtained from the ASME Code Appendices [6.14.14], and are listed in Table 6.3.1.

(i) Normal Conditions (Level A)

- a. Allowable stress in tension on a net section is:

$$F_t = 0.6 S_y$$

Where,  $S_y$  = yield stress at temperature, and  $F_t$  is equivalent to primary membrane stress.

- b. Allowable stress in shear on a net section is:

$$F_v = 0.4 S_y$$

- c. Allowable stress in compression on a net section is:

$$F_a = S_y \left( 0.47 - \frac{kl}{444r} \right)$$

where  $kl/r$  for the main rack body is based on the full height and cross section of the honeycomb region and does not exceed 120 for all sections.

$l$  = unsupported length of component

$k$  = length coefficient which gives influence of boundary conditions. The following values are appropriate for the described end conditions:

1 (simple support both ends)

2 (cantilever beam)

½ (clamped at both ends)

$r$  = radius of gyration of component

- d. Maximum allowable bending stress at the outermost fiber of a net section, due to flexure about one plane of symmetry is:

$$F_b = 0.60 S_y \quad (\text{equivalent to primary bending})$$

- e. Combined bending and compression on a net section satisfies:

$$\frac{f_a}{F_a} + \frac{C_{mx} f_{bx}}{D_x F_{bx}} + \frac{C_{my} f_{by}}{D_y F_{by}} < 1$$

where:

$f_a$  = Direct compressive stress in the section

$f_{bx}$  = Maximum bending stress along x-axis

$f_{by}$  = Maximum bending stress along y-axis

$C_{mx}$  = 0.85

$C_{my}$  = 0.85

$D_x$  =  $1 - (f_a/F'_{ex})$

$D_y$  =  $1 - (f_a/F'_{ey})$

$F'_{ex,ey}$  =  $(\pi^2 E)/(2.15 (kl/r)_{x,y}^2)$

$E$  = Young's Modulus

and subscripts x,y reflect the particular bending plane.

- f. Combined flexure and compression (or tension) on a net section:

$$\frac{f_a}{0.6 S_y} + \frac{f_{bx}}{F_{bx}} + \frac{f_{by}}{F_{by}} < 1.0$$

The above requirements are to be met for both direct tension or compression.

- g. Welds

Allowable maximum shear stress on the net section of a weld is given by:

$$F_w = 0.3 S_u$$

where  $S_u$  is the weld material ultimate strength at temperature. The shear stress on the adjoining base metal is limited to  $F_v = 0.4 S_y$ , where  $S_y$  is the base material yield strength at temperature.

h. Bearing

Allowable maximum stress for bearing on a contact area is given by:

$$F_p = 0.9 S_u$$

(ii) Level B Service Limits (Upset Conditions, including OBE)

Section NF-3321 (ASME Section III, Subsection NF [6.14.13]) states that, for the Level B condition, the allowable stresses for those given above in (i) may be increased by a factor of 1.33.

(iii) Level D Service Limits (including SSE)

Section F-1334 (ASME Section III, Appendix F [6.14.14]), states that limits for the Level D condition are the smaller of 2 or  $1.167S_u/S_y$  times the corresponding limits for the Level A condition if  $S_u > 1.2S_y$ , or 1.4 if  $S_u$  less than or equal  $1.2S_y$  except for requirements specifically listed below.  $S_u, S_y$  are the ultimate strength and yield strength at the specified rack design temperature. Examination of material properties for 304L stainless demonstrates that 1.2 times the yield strength is less than the ultimate strength. Therefore, the Level D stress limits are double the corresponding Level A limits.

Exceptions to the above general multiplier are the following:

- a) Stresses in shear shall not exceed the lesser of  $0.72S_y$  or  $0.42S_u$ . In the case of the Austenitic Stainless material used here,  $0.72S_y$  governs.
- b) Axial Compression Loads shall be limited to  $2/3$  of the calculated buckling load.
- c) Combined Axial Compression and Bending - The equations for Level A conditions shall apply except that:

$F_a = 0.667 \times \text{Buckling Load} / \text{Gross Section Area}$ ,  
and the terms  $F'_{ex}$  and  $F'_{ey}$  may be increased by the factor 1.65.

- d) For welds, the Level D allowable maximum weld stress is not specified in Appendix F of the ASME Code. An appropriate limit for weld throat stress is conservatively set here as:

$$F_w = (0.3 S_u) \times \text{factor}$$

where:

$$\begin{aligned} \text{factor} &= (\text{Level D shear stress limit}) / (\text{Level A shear stress limit}) \\ &= 0.72 S_y / 0.4 S_y = 1.8 \end{aligned}$$

### 6.6.3 Dimensionless Stress Factors

For convenience, the stress results are presented in a dimensionless form. Dimensionless stress factors are defined as the ratio of the actual developed stress to the specified limiting stress value. The limiting value of each stress factor is 1.0. Stress factors are determined as follows:

- $R_1$  = Ratio of direct tensile or compressive stress on a net section to its allowable value (note that pedestals only resist compression)
- $R_2$  = Ratio of gross shear on a net section in the x-direction to its allowable value
- $R_3$  = Ratio of maximum x-axis bending stress to its allowable value for the section
- $R_4$  = Ratio of maximum y-axis bending stress to its allowable value for the section
- $R_5$  = Combined flexure and compressive factor (as defined in the foregoing)
- $R_6$  = Combined flexure and tension (or compression) factor (as defined in the foregoing)
- $R_7$  = Ratio of gross shear on a net section in the y-direction to its allowable value

#### 6.6.4 Loads and Loading Combinations for Spent Fuel Racks

The applicable loads and their combinations, which must be considered in the seismic analysis of rack modules, are excerpted from the OT Position [6.14.2] and SRP, Section 3.8.4 [6.14.1]. The load combinations considered are identified below:

| Loading Combination                           | Service Level  |
|---|--|
| $D + L$<br>$D + L + T_o$<br>$D + L + T_o + E$ | Level A  |
| $D + L + T_a + E$<br>$D + L + T_o + P_f$      | Level B  |
| $D + L + T_a + E'$<br>$D + L + T_o + F_d$     | Level D<br><br>The functional capability of the fuel racks must be demonstrated. † |

Where:

- D = Dead weight-induced loads (including fuel assembly weight)
- L = Live Load (not applicable for the fuel rack, since there are no moving objects in the rack load path)
- $P_f$  = Upward force on the racks caused by postulated stuck fuel assembly
- $F_d$  = Impact force from accidental drop of the heaviest load from the maximum possible height.
- E = Operating Basis Earthquake (OBE)
- $E'$  = Safe Shutdown Earthquake (SSE)
- $T_o$  = Differential temperature induced loads (normal operating or shutdown condition based on the most critical transient or steady state condition)
- $T_a$  = Differential temperature induced loads (the highest temperature associated with the postulated abnormal design conditions)

† The addition of Metamic™ inserts does not change the existing rack capability to withstand fuel assembly drops. Therefore, the racks need not be re-evaluated for this case.

$T_a$  and  $T_o$  produce local thermal stresses. The worst thermal stress field in a fuel rack is obtained when an isolated storage location contains a fuel assembly generating heat at the maximum postulated rate and surrounding storage locations contain no fuel. Heated water makes unobstructed contact with the inside of the storage walls, thereby maximizing the temperature difference between adjacent cells. Secondary stresses produced are limited to the body of the rack; that is, support pedestals do not experience secondary (thermal) stresses.

### 6.7 Parametric Simulations

The multiple rack models employ the fluid coupling effects for all racks in the pool, as discussed above, and these simulations are referred to as WPMR evaluations.

Ten simulations are performed to investigate the structural integrity of the racks with Metamic™ inserts. OBE and SSE seismic events were considered as input loading for the racks with friction coefficients of 0.8, 0.2, and using random  $\mu$  values drawn from a Gaussian distribution with a mean of 0.5 (i.e., random coefficient of friction (COF) with upper and lower limits of 0.8 and 0.2, respectively). A bounding model is synthesized that is applicable to both units, using the layout of Turkey Point Unit 3. Where dimensional differences exist, a conservative value for the parameter is chosen. For example, for mass matrix-related data, dimensions are maximized, while for impact clearance-related data, minimum dimensions are selected.

The following table presents a complete listing of the simulations discussed herein. The results from DYNARACK solver simulations may be seen in the raw data output and solver summary files. However, due to the quantity of output data, a post-processor (DYNAPOST) is used to scan for worst case conditions and to develop the stress factors.

The sensitivity of results to the density of Metamic™ inserts in a rack module is examined by considering three different COF SSE cases that assume an insert is present in every storage cell, but where no reduction in assembly-cell wall gap (due to the Metamic™ insert) is credited.

These runs (7, 8 and 9) are denoted with “f” in the following table. The tenth and final run is identical to run # 8, except that the Cask Area rack (rack # 11) has effectively been removed from the WPMR model.

Consideration of the parameters described above resulted in the following 10 runs.

| <u>Run</u> | <u>Rack Fuel Loading Pattern</u> | <u>COF</u> | <u>Event</u> |
|------------|----------------------------------|------------|--------------|
| 1          | 13 racks, fully loaded           | 0.2        | SSE          |
| 2          | 13 racks, fully loaded           | 0.8        | SSE          |
| 3          | 13 racks, fully loaded           | Random     | SSE          |
| 4          | 13 racks, fully loaded           | 0.2        | OBE          |
| 5          | 13 racks, fully loaded           | 0.8        | OBE          |
| 6          | 13 racks, fully loaded           | Random     | OBE          |
| 7          | 13 racks, fully loaded “f”       | 0.2        | SSE          |
| 8          | 13 racks, fully loaded “f”       | 0.8        | SSE          |
| 9          | 13 racks, fully loaded “f”       | Random     | SSE          |
| 10         | 12 racks, fully loaded “f”       | 0.8        | SSE          |

where:

Random = drawn from a Gaussian distribution with a mean of 0.5. COF = Coefficient of friction (upper and lower limits of 0.8 and 0.2). “f” denotes sensitivity cases run with Metamic™ inserts in every cell.

## 6.8 Time History Simulation Results

The results from the DYNARACK runs may be seen in the raw data output files. However, due to the huge quantity of output data, a post-processor is used to scan for worst case conditions and develop the stress factors discussed in Subsection 6.6.3. Further reduction in this bulk of information is provided in this section by extracting the worst case values from the parameters of interest; namely displacements, support pedestal forces, impact loads, and stress factors. This section also summarizes additional analyses performed to develop and evaluate structural member stresses which are not determined by the post processor.

The following table presents the results for the major parameters of interest. The table is followed by a discussion of those parameters, after which additional analyses are addressed.

RESULT TABLE

| Run | Max. Disp. (in) | Rack No. | Max. Stress Factor † | R5/R6 /Rack | Max. Vertical Load (lbf) /Rack | Max. Friction Load (lbf) (X or Y) /Rack | Max. Thread Engagement Stress (psi) /Rack | Max. Impact Force (lbf) /Rack |
|-----|-----------------|----------|----------------------|-------------|--------------------------------|---|---|-------------------------------|
| 1   | 0.229           | 10       | 0.154                | R5,R6/4     | 102,000/11                     | 18,600/6                                | 4,293/11                                  | 303/12                        |
| 2   | 0.218           | 10       | 0.155                | R5,R6/3     | 102,000/8                      | 15,400/6                                | 4,293/8                                   | 303/12                        |
| 3   | 0.218           | 10       | 0.155                | R5,R6/3     | 101,000/8                      | 17,500/6                                | 4,251/8                                   | 303/12                        |
| 4   | 0.108           | 10       | 0.171                | R5/3        | 77,900/10                      | 6,310/5                                 | 3,279/10                                  | 0                             |
| 5   | 0.108           | 10       | 0.171                | R5/3        | 77,900/10                      | 10,200/8                                | 3,279/10                                  | 0                             |
| 6   | 0.108           | 10       | 0.171                | R5/3        | 77,900/10                      | 9,810/7                                 | 3,279/10                                  | 0                             |
| 7   | 0.223           | 10       | 0.157                | R5/1        | 107,000/10                     | 16,400/10                               | 4,504/12                                  | 286/5                         |
| 8   | 0.253           | 10       | 0.158                | R5/1        | 105,000/10                     | 18,000/10                               | 4,420/10                                  | 308/4                         |
| 9   | 0.255           | 10       | 0.157                | R5,R6/1     | 105,000/10                     | 17,300/10                               | 4,420/10                                  | 309/5                         |
| 10  | 0.249           | 10       | 0.150                | R5/1        | 105,000/10                     | 15,400/10                               | 4,420/10                                  | 310/6                         |

### 6.8.1 Rack Displacements

The maximum rack displacements are obtained from time histories of the motion of the upper and lower four corners of each rack in each simulation. The maximum absolute value of

† Stress Factor is the inverse of "factor of safety".

displacement in the two horizontal directions, relative to the pool slab, is determined by the post-processor for each rack, at the top and bottom corners. As expected from the tipping and bending behavior of the rack module, displacements at the tops of the storage racks are much larger than at the baseplate level. For the same seismic excitation, SSE or OBE, most rack simulations have similar displacements in both x and y directions. It is obvious from the small maximum displacement, as shown in the result table above, that the safety factors for tipping are met. Furthermore, since the typical spacing between rack modules is approximately 2.5", it is equally clear that the racks will not impact one another.

#### 6.8.2 Pedestal Vertical Forces

The highest compressive pedestal load is based on the conservative modeling assumption that each rack has only 4 pedestals. In reality, some of the Region I racks have eight pedestals. Despite this obvious conservatism, the maximum computed force given in the table above is used to determine the stresses in the pedestal and its connecting welds. The summary table provided above shows that the maximum vertical pedestal load is 107,000 lbs.

#### 6.8.3 Pedestal Friction Forces

The maximum (x and y direction) friction load indicated by the summary table above is 18,600 lbs. This load has been considered in the female pedestal-to-baseplate weld evaluation discussed below.

#### 6.8.4 Rack Impact Loads

A freestanding rack, by definition, is a structure subject to potential impacts during a seismic event. Stresses arise, in some instances, from localized impacts between the racks, or between a peripheral rack and the pool wall and from rattling of fuel assemblies inside the storage rack. The following sections discuss the bounding values of these impact loads.

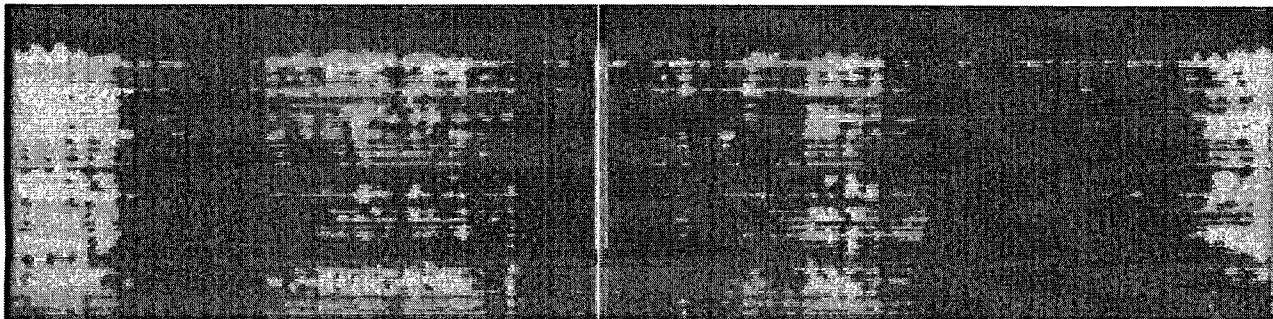
#### 6.8.4.1 Impacts External to the Rack

Gap elements track the potential for rack-to-rack or rack-to-pool wall impacts. The impact force associated with each gap spring element is printed in a list format in the output file produced by the DYNARACK program. The lists from each simulation are scanned for non-zero values. A non-zero value indicates an impact and vice versa. Rack-to-wall or rack-to-rack impacts did not occur during any of the simulations.

#### 6.8.4.2 Impacts Internal to the Rack

A review of all simulations performed allows determination of the maximum instantaneous impact load between a fuel assembly and the storage cell wall at any modeled impact site. The maximum fuel/cell wall impact load is 310 lbf. The integrity of a storage cell wall following a 310 lbf impact load has been evaluated and the cell has been shown to remain intact with no permanent damage. The physical integrity of Metamic™ inserts (a non-structural rack component) has also been evaluated for this impact load; results indicate integrity of the insert is maintained with a large margin of safety (over four).

The permissible lateral load on an irradiated spent fuel assembly has been studied by the Lawrence Livermore National Laboratory. The LLNL report [6.14.15] states that "...for the most vulnerable fuel assembly, axial buckling varies from 82g's at initial storage to 95g's after 20 years' storage. In a side drop, no yielding is expected below 63g's at initial storage to 74g's after 20 years' [dry] storage". The most significant load on the fuel assembly arises from rattling during the seismic event.



$a =$  permissible lateral acceleration in g's ( $a = 63$ )

Therefore, the limiting lateral load,  $F_e = 25,704$  lb

The maximum fuel-to-storage cell rattling force from the WPMR runs is only 310 lb. Therefore, the nominal factor of safety against fuel failure is computed to be more than 80.

## 6.9 Rack Structural Evaluation

### 6.9.1 Rack Stress Factors

The time history results from the DYNARACK solver provide the pedestal normal and lateral interface forces, which may be converted to the limiting bending moment and shear force at the bottom baseplate-pedestal interface. In particular, maximum values for the previously defined stress factors are determined for every pedestal in the array of racks. With this information available, the structural integrity of the pedestal can be assessed and reported. The net section maximum (as a function of time) bending moments and shear forces can also be determined at the bottom baseplate-rack cellular structure interface for each rack module in the pool. Using these forces and moments, the maximum stress in the limiting rack cell (box) can be evaluated.

The stress factor results for male and female pedestals, and for the entire spent fuel rack cellular cross-section just above the bottom casting has been determined. These factors are reported for every rack in each simulation, and for each pedestal in every rack. These locations are the most heavily loaded net sections in the structure so that satisfaction of the stress factor criteria at these locations ensures that the overall structural criteria set forth in Section 6.6 are met.

A review of stress factors from all of the simulations performed leads to the conclusion that all stress factors are less than the mandated limit of 1.0 for the load cases examined. The bounding stress factor from all runs is 0.171 for module 3. Therefore, the requirements of Section 6.6.2 are indeed satisfied for the load levels considered at every limiting location in the racks.

### 6.9.2 Pedestal Thread Shear Stress

The ultimate strength of the female part of the pedestal is 66,200 psi. The yield stress for this material is 21,300 psi. These values are conservatively taken at 200<sup>0</sup>F, which is only a few degrees less than the peak local water temperature reported in Table 5.4.1 which occurs near the top of the rack, well above the pedestals. The allowable shear stress for Level A conditions is 0.4 times the yield stress, which gives a value of 8,520 psi. The allowable shear stress for Level D conditions is 0.72 times the yield stress, which gives a value of 15,336 psi. The maximum pedestal thread stress shown in the result table above is 4,504 psi, which is below each of these values. Therefore, the stresses on female pedestal threads are shown to be acceptable. The thread shear allowable value for the male pedestal threads is the same or larger and therefore the stresses imposed on male threads are also acceptable.

### 6.9.3 Local Stresses Due to Impacts

Impact loads at the pedestal base produce stresses in the pedestal for which explicit stress limits are prescribed in the Code. However, impact loads on the cellular region of the racks, as discussed in Subsection 6.8.4.2 above, produce stresses which attenuate rapidly away from the loaded region. This behavior is characteristic of secondary stresses.

Even though limits on secondary stresses are not prescribed in the Code for Class 3 NF structures, evaluations are performed to ensure that localized impacts do not cause plastic deformation in the storage cells, which could adversely affect neutron multiplication of the stored fuel array.

Local cell wall integrity is conservatively estimated from peak impact loads. Plastic analysis is used to obtain the minimum impact load that would cause gross permanent deformation. The limiting impact load (determined to be 3,204 lbf, including a safety factor of 2.0) is much greater

than the highest calculated impact load value (310 lbf, see Subsection 6.8.4.2) obtained from any of the rack analyses. Therefore, fuel impacts do not represent a significant concern with respect to fuel rack cell deformation.

#### 6.9.4 Weld Stresses

Weld locations subjected to significant seismic loading are the bottom of the rack at the baseplate-to-cell connection, the top of the pedestal support at the baseplate connection, and cell-to-cell connections. Bounding values of resultant loads are used to qualify the connections. The ultimate strength of SA 240 grade 304L at 200<sup>0</sup>F is 66,200 psi.

##### a. Baseplate-to-Rack Cell Welds

ASME Code Section III, Subsection NF [6.14.13] permits, for Level A or B conditions, an allowable weld stress  $\tau = .3 S_u$ . Conservatively assuming that the weld strength is the same as the lower base metal ultimate strength, the allowable stress is given by;  $\tau = .3 * (66,200) = 19,860$  psi. As stated in Subsection 6.6.2, the allowable may be increased for Level D by the ratio of 1.8, giving an allowable of 35,748 psi. However, this increase is not credited here, which provides an additional safety factor of 1.8.

Weld stresses are determined through the use of a simple conversion (ratio) factor applied to the corresponding stress factor in the adjacent rack material. A cell wall-to-weld stress conversion value of 2.15 is developed from the differences in material thickness and width versus weld throat dimension and length:

$$Ratio = \frac{0.075 * 8.875}{0.0625 * 0.7071 * 7.0} = 2.15$$

where 0.075 in. is the wall thickness and 8.875 in. is the average cell wall width.

The highest predicted cell to baseplate weld stress is calculated based on the highest R5 value for the rack cell region tension stress factor and R2 and R7 values for the rack cell region shear stress factors from all the simulations. Refer to Subsection 6.6.3 for definition of these factors. These cell wall stress factors may be converted into weld stress values as follows:

$$\begin{aligned} & [R5 + R2 + R7] * [2 (0.6) S_y] * \text{Ratio} \\ & = [(0.140 + 0.011 + 0.014)/0.888] * [2 (0.6) 21,300] * 2.15 \\ & = 10,211 \text{ psi} \end{aligned}$$

This calculation is conservative for the following reasons:

- 1) The actual shear stress computed from the R2 and R7 stress factors should use an allowable of  $0.72 * S_y$  instead of  $1.2 * S_y$ .
- 2) The directional stresses associated with the normal stress  $\sigma_y$  and the two shear stresses  $\tau_x$  and  $\tau_y$  should be combined using the square root of the sum of the squares (SRSS) instead of direct summation.
- 3) The maximum stress factors used above do not all occur at the same time instant, in the same storage rack, or during the same simulation.

The value presented above is less than the allowable weld stress value, which is 19,860 psi. Therefore, the welds are acceptable, with a safety factor of  $(19,860/10,211) = 1.945$ .

#### b. Baseplate-to-Pedestal Welds

The weld between the rack baseplate and a support pedestal is checked using finite element analysis to determine that the maximum stress is 5,951 psi under a Level D event. This calculated stress value is below the SSE allowable of 35,748 psi. Therefore, these welds have been determined to be acceptable with a safety factor of about 6.

### c. Cell-to-Cell Welds

Adjacent storage cells are joined together through a series of connecting welds along the vertical length (i.e., height) of the cell. Stresses in storage cell-to-cell welds develop as a result of fuel assembly impacts with the cell wall and shear flow within the storage rack from beam bending behavior. The weld stresses from fuel impacts are conservatively calculated by assuming that fuel assemblies in adjacent cells are moving out of phase so the impact loads in two adjacent cells are in opposite directions and are applied simultaneously. This analytical approach tends to separate the two cells from each other at the weld.

The maximum stress in these welds under any load case is determined to be 3,476 psi. This calculated stress from the SSE condition is below the OBE allowable of 19,860 psi with a safety factor of more than 5.7.

### 6.10 Level A Evaluation

The Level A condition is not a governing condition for spent fuel racks since the general level of imposed loading is far less than during Level B or Level D loading. The stress allowable for Level B loading is only approximately 1/3 greater than the corresponding Level A stress allowable. However, the ratio of loading increase from Level A to B loading far exceeds this 1/3 value. Therefore, Level A is acceptable by comparison.

### 6.11 Hydrodynamic Loads on Pool Walls

The hydrodynamic pressures that develop between adjacent racks and the pool walls can be developed from the archived results produced by the WPMR analysis. Of the racks located next to the SFP walls, the one that experienced the maximum displacement generates the maximum hydrodynamic load on its adjacent wall.

## 6.12 Local Stress Considerations

This section presents the results of evaluations for the possibility of cell wall buckling and the secondary stresses produced by temperature effects.

### 6.12.1 Cell Wall Buckling

The allowable local buckling stresses in the fuel cell walls are obtained by using classical plate buckling analysis and a model as shown in Figure 6.12.1. The evaluation for cell wall buckling is based on the applied stress being uniform along the entire length of the cell wall. In the actual fuel rack, the compressive stress comes from consideration of overall bending of the rack structures during a seismic event, and as such is negligible at the rack top, and maximum at the rack bottom.

The critical buckling stress is determined to be 6,932 psi. The computed compressive stress in the cell wall, based on the R5 stress factor, is 2,015 psi. Therefore, there is a margin of safety of more than 3 against local cell wall buckling.

## 6.13 Conclusion

A comprehensive Whole-Pool Multi-Rack (WPMR) time history analysis of the existing array of racks in the Turkey Point Unit 3 pool was performed considering the scenario that the Region II racks are loaded with Metamic™ inserts at different densities (i.e., fully loaded and 50% loaded). The Unit 4 pool is bounded by the results for Unit 3 since the two pools, including the spent fuel rack layouts, are mirror images of one another. The analysis procedure utilizes well established methodology appropriate to free standing deeply submerged rack modules and gives proper consideration of fluid coupling effects. The results show that stress levels in the rack modules are considerably less than the corresponding ASME Section III Subsection NF limits for linear structures under the load combinations specified in NRC's OT Position Paper [6.14.2]. The analyses reported in this section further serve to confirm that Metamic™ inserts and fuel

assemblies from Turkey Point may be placed in spent fuel storage cells as needed to control neutron multiplication, consistent with the requirements of Section 4 of this report, without exceeding any of these stress levels. Additionally, the analyses discussed in this section (Section 6) support the conclusions reached by FPL in the original license amendment request under which the existing racks, not including the Cask Area rack, were installed in the mid 1980's.

#### 6.14 References

- [6.14.1] USNRC NUREG-0800, Standard Review Plan, June 1987.
- [6.14.2] (USNRC Office of Technology) "OT Position for Review and Acceptance of Spent Fuel Storage and Handling Applications", dated April 14, 1978, and January 18, 1979 amendment thereto.
- [6.14.3] Soler, A.I. and Singh, K.P., "Seismic Responses of Free Standing Fuel Rack Constructions to 3-D Motions", Nuclear Engineering and Design, Vol. 80, pp. 315-329 (1984).
- [6.14.4] Soler, A.I. and Singh, K.P., "Some Results from Simultaneous Seismic Simulations of All Racks in a Fuel Pool", INNEM Spent Fuel Management Seminar X, January, 1993.
- [6.14.5] Singh, K.P. and Soler, A.I., "Seismic Qualification of Free Standing Nuclear Fuel Storage Racks - the Chin Shan Experience, Nuclear Engineering International, UK (March 1991).
- [6.14.6] Holtec Proprietary Report HI-961465 - WPMR Analysis User Manual for Pre&Post Processors & Solver, August, 1997.
- [6.14.7] Holtec Proprietary Report HI-89364 - Verification and User's Manual for Computer Code GENEQ, January, 1990.
- [6.14.8] Rabinowicz, E., "Friction Coefficients of Water Lubricated Stainless Steels for a Spent Fuel Rack Facility," MIT, a report for Boston Edison Company, 1976.

- [6.14.9] Singh, K.P. and Soler, A.I., "Dynamic Coupling in a Closely Spaced Two-Body System Vibrating in Liquid Medium: The Case of Fuel Racks," 3rd International Conference on Nuclear Power Safety, Keswick, England, May 1982.
- [6.14.10] Fritz, R.J., "The Effects of Liquids on the Dynamic Motions of Immersed Solids," Journal of Engineering for Industry, Trans. of the ASME, February 1972, pp 167-172.
- [6.14.11] Levy, S. and Wilkinson, J.P.D., "The Component Element Method in Dynamics with Application to Earthquake and Vehicle Engineering," McGraw Hill, 1976.
- [6.14.12] Paul, B., "Fluid Coupling in Fuel Racks: Correlation of Theory and Experiment", (Proprietary), NUSCO/Holtec Report HI-88243.
- [6.14.13] ASME Boiler & Pressure Vessel Code, Section III, Subsection NF, 1998.
- [6.14.14] ASME Boiler & Pressure Vessel Code, Section III, Appendices, 1998.
- [6.14.15] Chun, R., Witte, M. and Schwartz, M., "Dynamic Impact Effects on Spent Fuel Assemblies," UCID-21246, Lawrence Livermore National Laboratory, October 1987.

Table 6.2.1

## PARTIAL LISTING OF FUEL RACK APPLICATIONS USING DYNARACK

| PLANT                     | DOCKET NUMBER(s)     | YEAR |
|---------------------------|----------------------|------|
| Enrico Fermi Unit 2       | USNRC 50-341         | 1980 |
| Quad Cities 1 & 2         | USNRC 50-254, 50-265 | 1981 |
| Rancho Seco               | USNRC 50-312         | 1982 |
| Grand Gulf Unit 1         | USNRC 50-416         | 1984 |
| Oyster Creek              | USNRC 50-219         | 1984 |
| Pilgrim                   | USNRC 50-293         | 1985 |
| V.C. Summer               | USNRC 50-395         | 1984 |
| Diablo Canyon Units 1 & 2 | USNRC 50-275, 50-323 | 1986 |
| Byron Units 1 & 2         | USNRC 50-454, 50-455 | 1987 |
| Braidwood Units 1 & 2     | USNRC 50-456, 50-457 | 1987 |
| Vogtle Unit 2             | USNRC 50-425         | 1988 |
| St. Lucie Unit 1          | USNRC 50-335         | 1987 |
| Millstone Point Unit 1    | USNRC 50-245         | 1989 |
| Chin Shan                 | Taiwan Power         | 1988 |
| D.C. Cook Units 1 & 2     | USNRC 50-315, 50-316 | 1992 |
| Indian Point Unit 2       | USNRC 50-247         | 1990 |
| Three Mile Island Unit 1  | USNRC 50-289         | 1991 |
| James A. FitzPatrick      | USNRC 50-333         | 1990 |
| Shearon Harris Unit 2     | USNRC 50-401         | 1991 |
| Hope Creek                | USNRC 50-354         | 1990 |
| Kuosheng Units 1 & 2      | Taiwan Power Company | 1990 |

Table 6.2.1

## PARTIAL LISTING OF FUEL RACK APPLICATIONS USING DYNARACK

| PLANT                      | DOCKET NUMBER(s)                 | YEAR |
|----------------------------|----------------------------------|------|
| Ulchin Unit 2              | Korea Electric Power Co.         | 1990 |
| Laguna Verde Units 1 & 2   | Comision Federal de Electricidad | 1991 |
| Zion Station Units 1 & 2   | USNRC 50-295, 50-304             | 1992 |
| Sequoyah                   | USNRC 50-327, 50-328             | 1992 |
| LaSalle Unit 1             | USNRC 50-373                     | 1992 |
| Duane Arnold Energy Center | USNRC 50-331                     | 1992 |
| Fort Calhoun               | USNRC 50-285                     | 1992 |
| Nine Mile Point Unit 1     | USNRC 50-220                     | 1993 |
| Beaver Valley Unit 1       | USNRC 50-334                     | 1992 |
| Salem Units 1 & 2          | USNRC 50-272, 50-311             | 1993 |
| Limerick                   | USNRC 50-352, 50-353             | 1994 |
| Ulchin Unit 1              | KINS                             | 1995 |
| Yonggwang Units 1 & 2      | KINS                             | 1996 |
| Kori-4                     | KINS                             | 1996 |
| Connecticut Yankee         | USNRC 50-213                     | 1996 |
| Angra Unit 1               | Brazil                           | 1996 |
| Sizewell B                 | United Kingdom                   | 1996 |
| Waterford 3                | USNRC 50-382                     | 1997 |
| J.A. Fitzpatrick           | USNRC 50-333                     | 1998 |
| Callaway                   | USNRC 50-483                     | 1998 |
| Nine Mile Unit 1           | USNRC 50-220                     | 1998 |

Table 6.2.1

PARTIAL LISTING OF FUEL RACK APPLICATIONS USING DYNARACK

| PLANT                   | DOCKET NUMBER(s)                        | YEAR |
|-------------------------|---|------|
| Chin Shan               | Taiwan Power Company                    | 1998 |
| Vermont Yankee          | USNRC 50-271                            | 1998 |
| Millstone 3             | USNRC 50-423                            | 1998 |
| Byron/Braidwood         | USNRC 50-454, 50-455,<br>50-567, 50-457 | 1999 |
| Wolf Creek              | USNRC 50-482                            | 1999 |
| Plant Hatch Units 1 & 2 | USNRC 50-321, 50-366                    | 1999 |
| Harris Pools C and D    | USNRC 50-401                            | 1999 |
| Davis-Besse             | USNRC 50-346                            | 1999 |
| Enrico Fermi Unit 2     | USNRC 50-341                            | 2000 |
| Kewaunee                | USNRC 50-305                            | 2001 |
| V.C. Summer             | USNRC 50-395                            | 2001 |
| St. Lucie               | USNRC 50-335, 50-389                    | 2002 |
| Turkey Point            | USNRC 50-250, 251                       | 2002 |
| Clinton                 | USNRC 50-461                            | 2004 |

| <p style="text-align: center;">Table 6.3.1</p> <p style="text-align: center;">RACK MATERIAL DATA (200°F)</p> <p style="text-align: center;">(ASME - Section II, Part D)</p> |                               |   |  |
|---|-------------------------------|---|--|
| Stainless Steel<br>Material   | Young's Modulus<br>E<br>(psi) | Yield Strength<br>S <sub>y</sub><br>(psi) | Ultimate Strength<br>S <sub>u</sub><br>(psi) |
| SA240, Type 304L (cell boxes)   | 27.6 x 10 <sup>6</sup>        | 21,300                                    | 66,200                                       |
| SUPPORT MATERIAL DATA (200°F)   |                               |   |  |
| SA240, Type 304L<br>(upper part of support feet & Bearing Pads)   | 27.6 x 10 <sup>6</sup>        | 21,300                                    | 66,200                                       |
| SA-564-630 (lower part of support feet; age hardened at 1100°F)   | 28.5 x 10 <sup>6</sup>        | 106,300                                   | 140,000                                      |

| Table 6.4.1<br>TIME-HISTORY STATISTICAL CORRELATION RESULTS |       |
|---|-------|
| SSE & OBE   |       |
| Data1 to Data2  | 0.001 |
| Data1 to Data3  | 0.129 |
| Data2 to Data3  | 0.037 |

Data1 corresponds to the time-history acceleration values along the X axis (East)

Data2 corresponds to the time-history acceleration values along the Y axis (North)

Data3 corresponds to the time-history acceleration values along the Z axis (Vertical)

Table 6.5.1

Degrees-of-freedom

| LOCATION (Node)  | DISPLACEMENT    |                 |                | ROTATION        |                 |                 |
|--|-----------------|-----------------|----------------|-----------------|-----------------|-----------------|
|  | U <sub>x</sub>  | U <sub>y</sub>  | U <sub>z</sub> | θ <sub>x</sub>  | θ <sub>y</sub>  | θ <sub>z</sub>  |
| 1  | p <sub>1</sub>  | p <sub>2</sub>  | p <sub>3</sub> | q <sub>4</sub>  | q <sub>5</sub>  | q <sub>6</sub>  |
| 2  | p <sub>7</sub>  | p <sub>8</sub>  | p <sub>9</sub> | q <sub>10</sub> | q <sub>11</sub> | q <sub>12</sub> |
| Node 1 is assumed to be attached to the rack at the bottom most point.<br>Node 2 is assumed to be attached to the rack at the top most point.<br>Refer to Figure 6.5.1 for node identification.  |                 |                 |                |                 |                 |                 |
| 2*   | p <sub>13</sub> | p <sub>14</sub> |                |                 |                 |                 |
| 3*   | p <sub>15</sub> | p <sub>16</sub> |                |                 |                 |                 |
| 4*   | p <sub>17</sub> | p <sub>18</sub> |                |                 |                 |                 |
| 5*   | p <sub>19</sub> | p <sub>20</sub> |                |                 |                 |                 |
| 1*   | p <sub>21</sub> | p <sub>22</sub> |                |                 |                 |                 |
| where the relative displacement variables q <sub>i</sub> are defined as:<br><br>$p_i = q_i(t) + U_x(t) \quad i = 1,7,13,15,17,19,21$ $= q_i(t) + U_y(t) \quad i = 2,8,14,16,18,20,22$ $= q_i(t) + U_z(t) \quad i = 3,9$ $= q_i(t) \quad i = 4,5,6,10,11,12$ p <sub>i</sub> denotes absolute displacement (or rotation) with respect to inertial space<br>q <sub>i</sub> denotes relative displacement (or rotation) with respect to the floor slab<br><br>* denotes fuel mass nodes<br>U(t) are the three known earthquake displacements |                 |                 |                |                 |                 |                 |

Figure 6.4.1

Turkey Point Units 3&4 SFP  
Time History Accelerogram  
E/W Direction SSE (2% Damping)

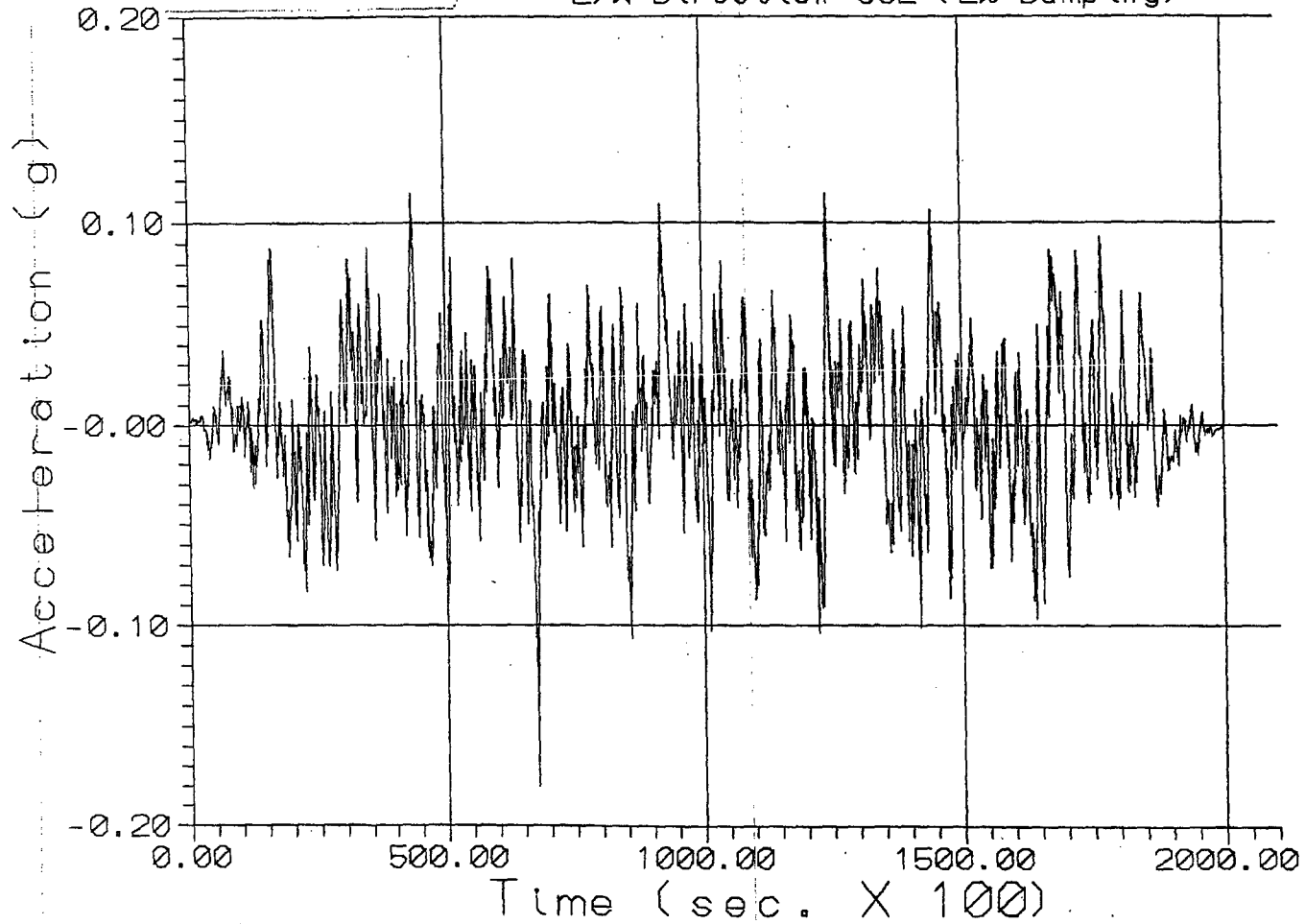


Figure 6.4.2

Turkey Point Units 3&4 SFP  
Time History Accelerogram  
N/S Direction SSE (2% Damping)

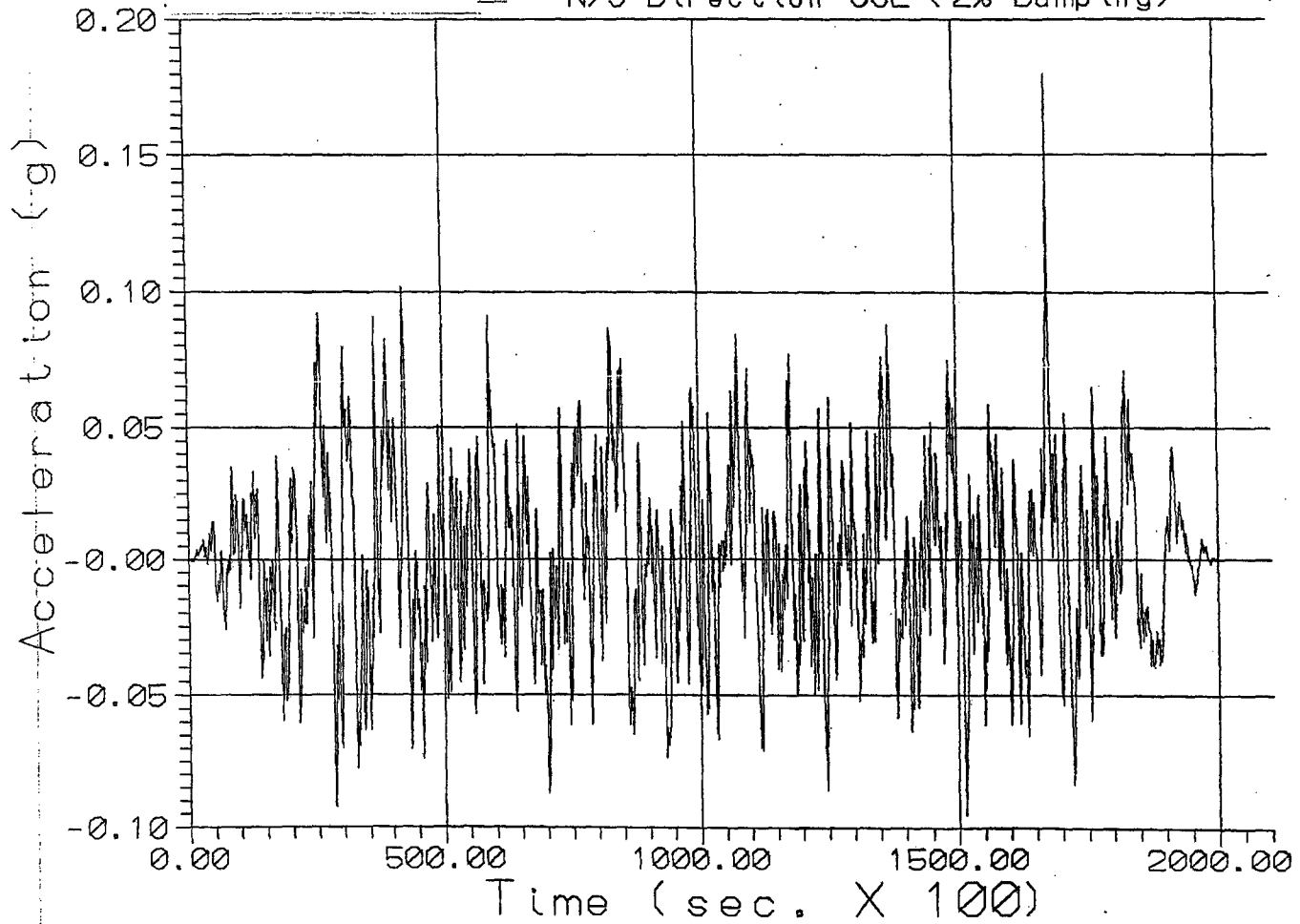
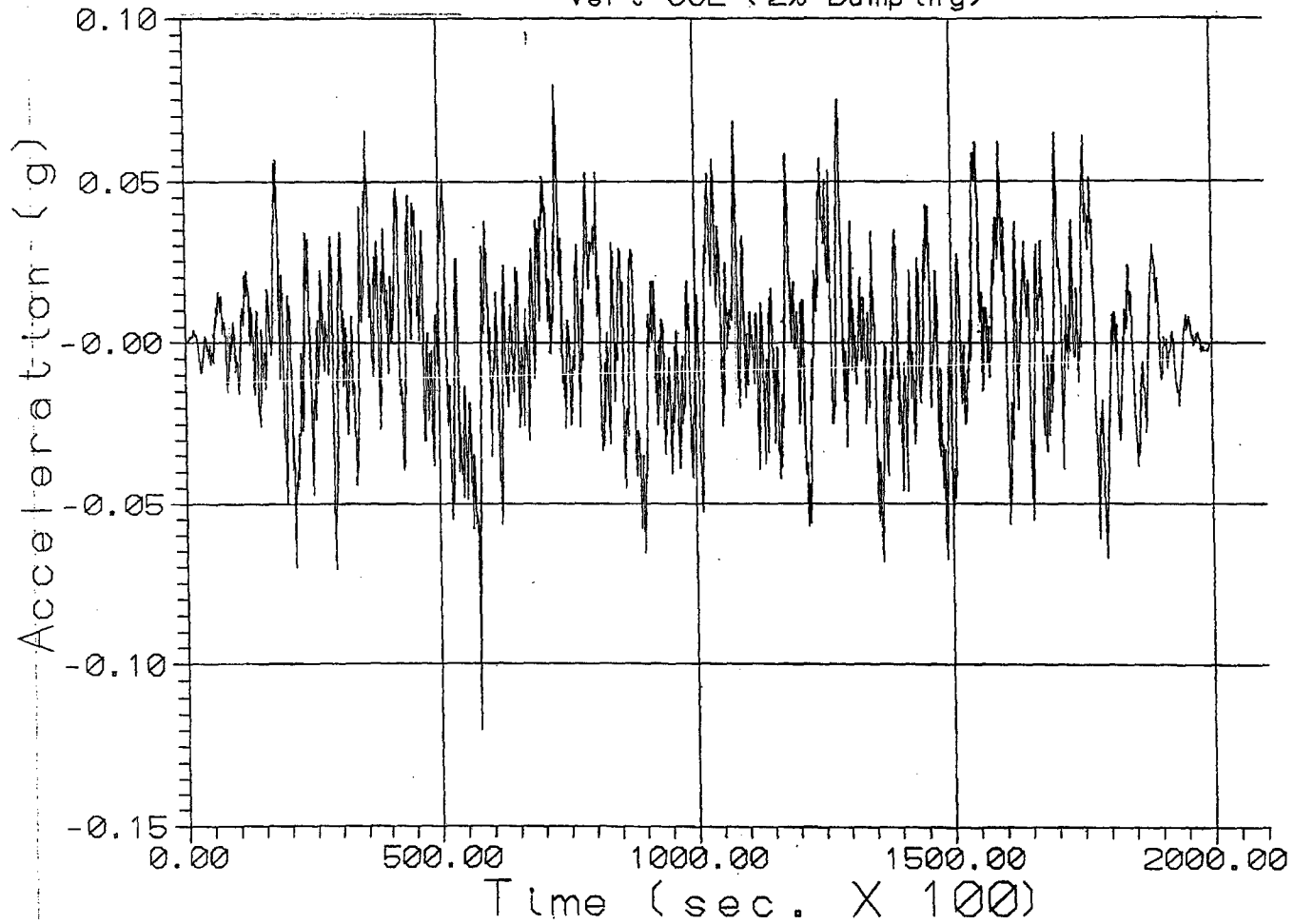


Figure 6.4.3

Turkey Point Units 3&4 SFP  
Time History Accelerogram  
Vert SSE (2% Damping)



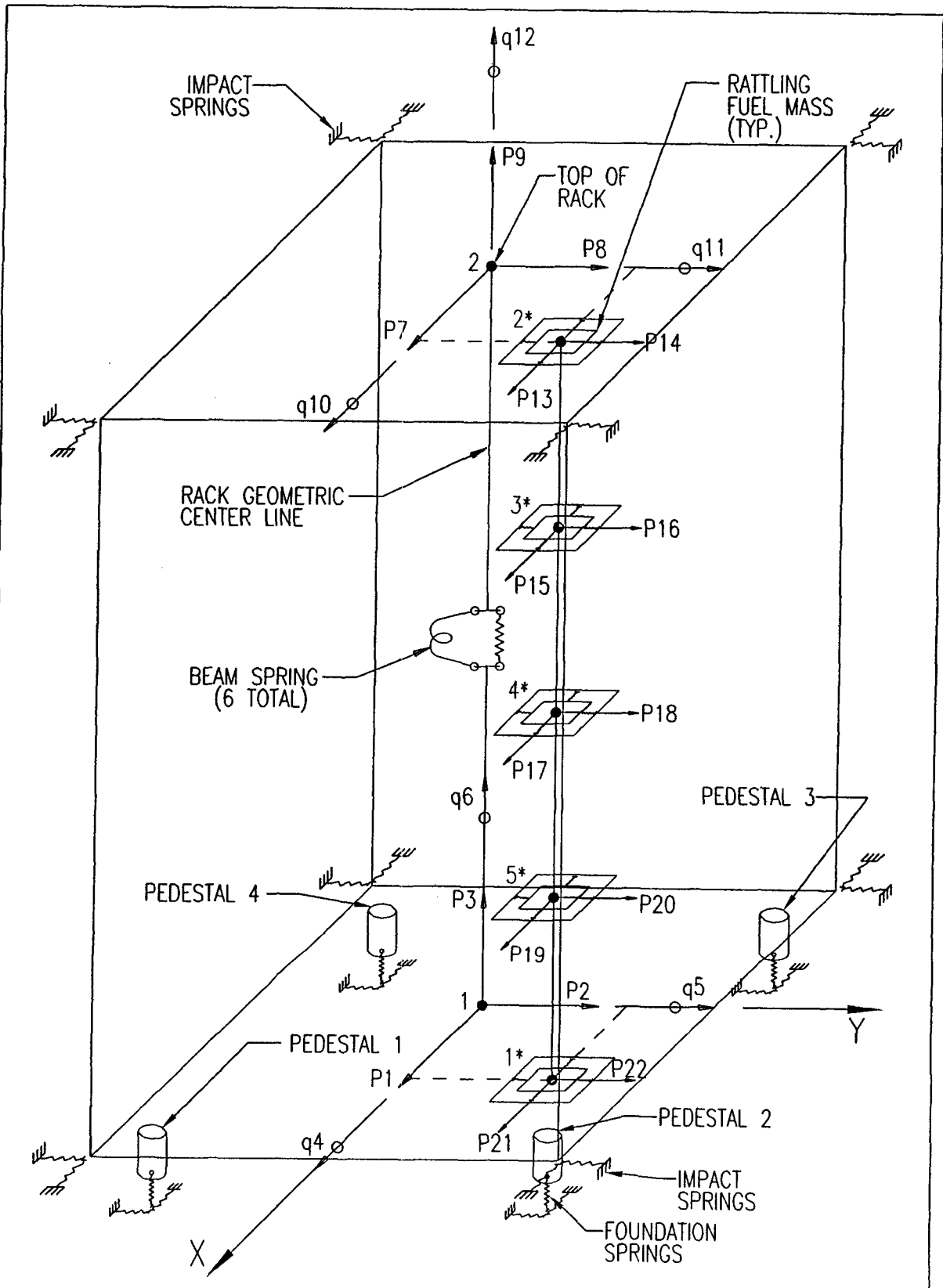


FIGURE 6.5.1; SCHEMATIC OF THE DYNAMIC MODEL OF A SINGLE RACK MODULE USED IN DYNARACK

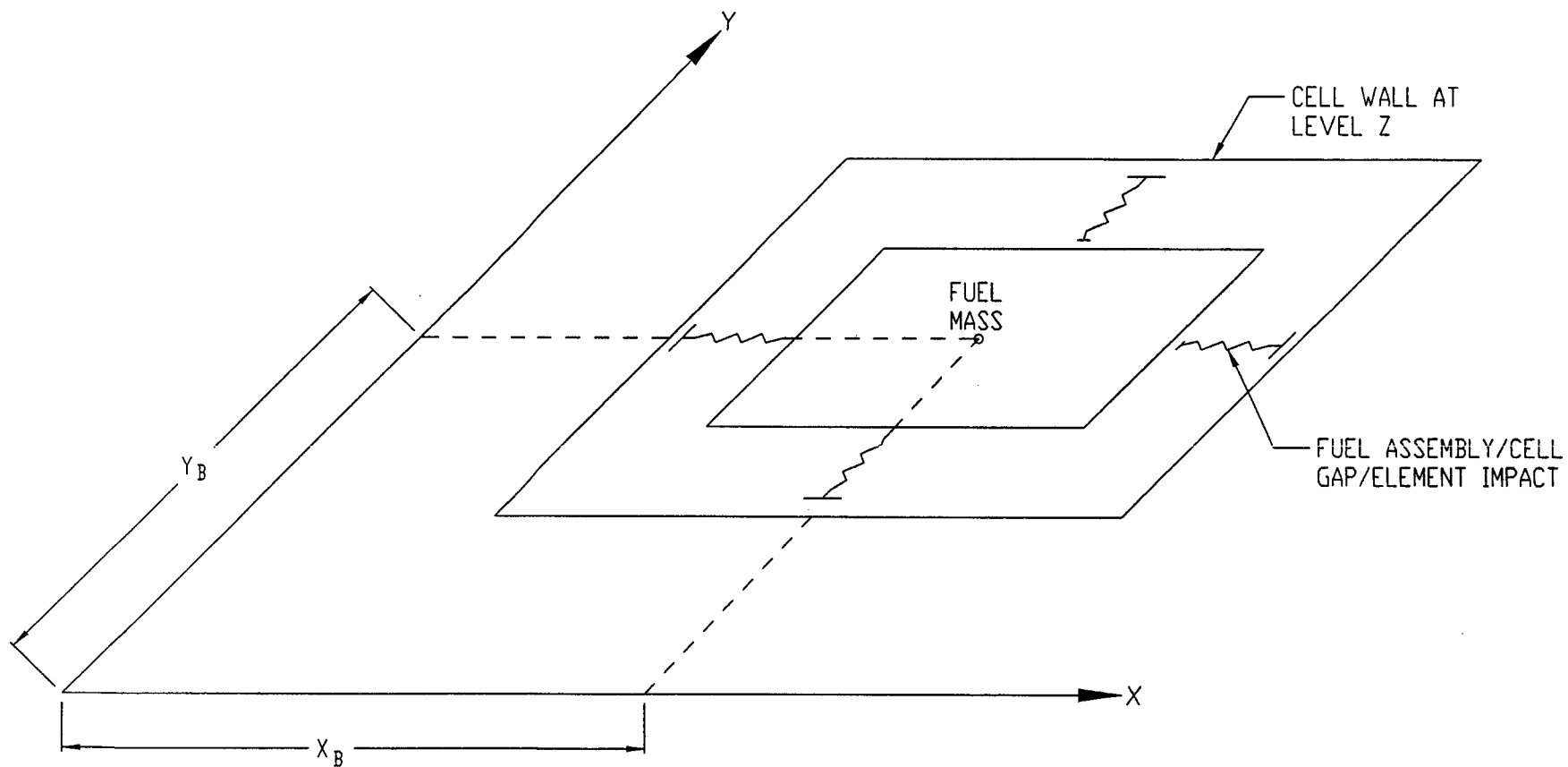


FIGURE 6.5.2; FUEL-TO-RACK GAP/IMPACT ELEMENTS AT LEVEL OF RATTLING MASS

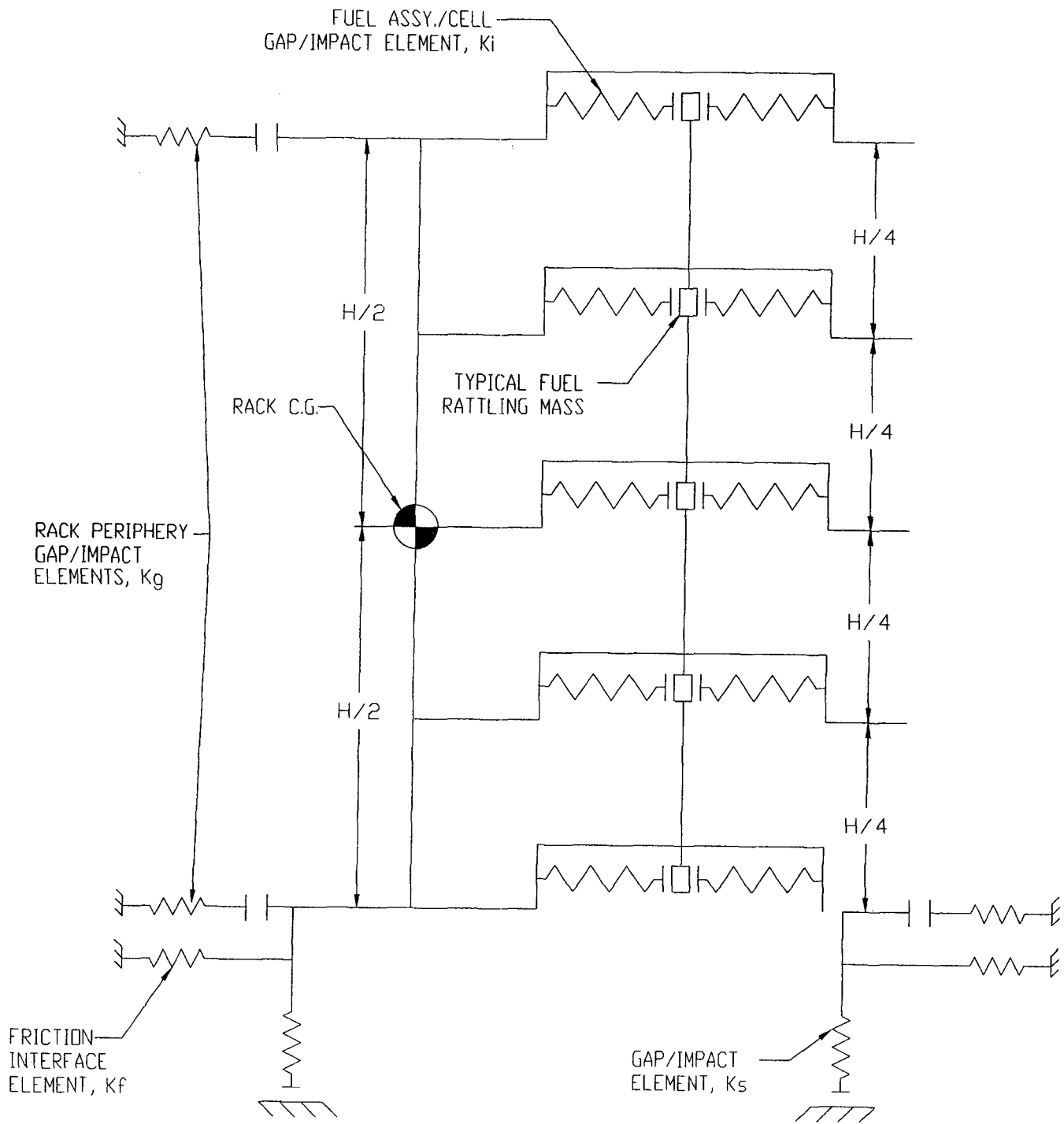
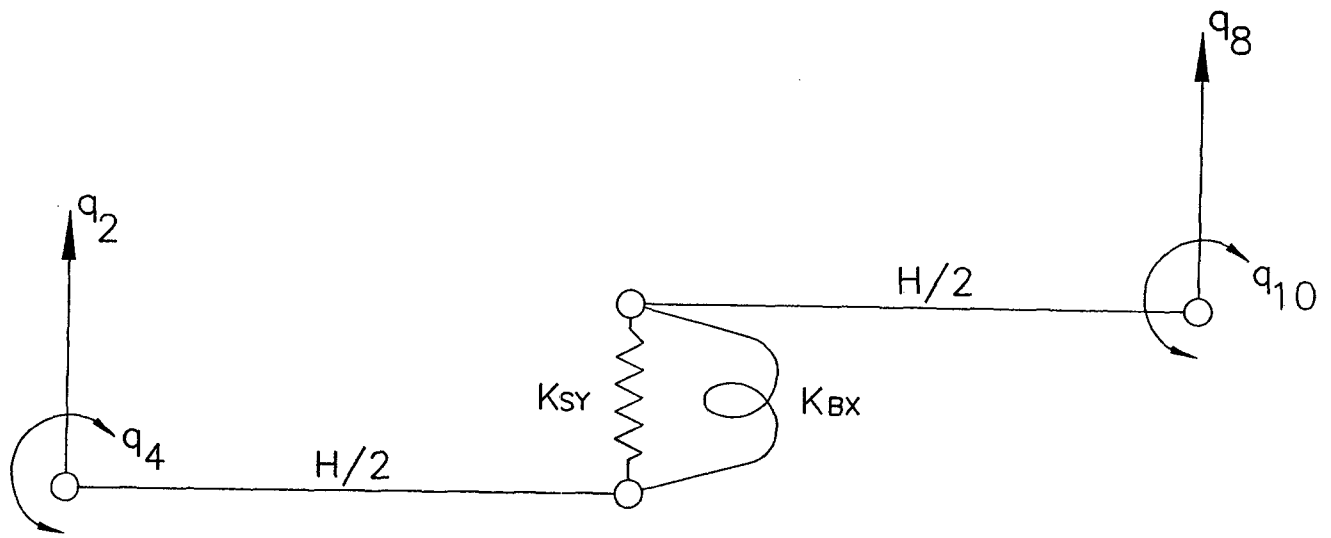
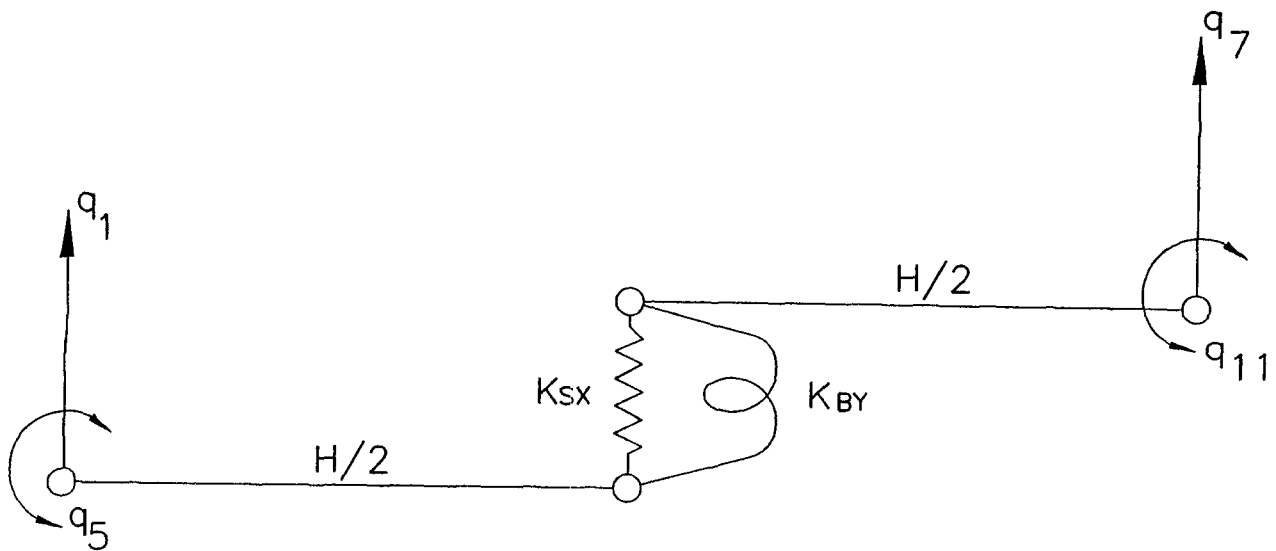


FIGURE 6.5.3; TWO DIMENSIONAL VIEW OF THE SPRING-MASS SIMULATION



FOR Y-Z PLANE BENDING



FOR X-Z PLANE BENDING

FIGURE 6.5.4; RACK DEGREES-OF-FREEDOM WITH SHEAR AND BENDING SPRINGS

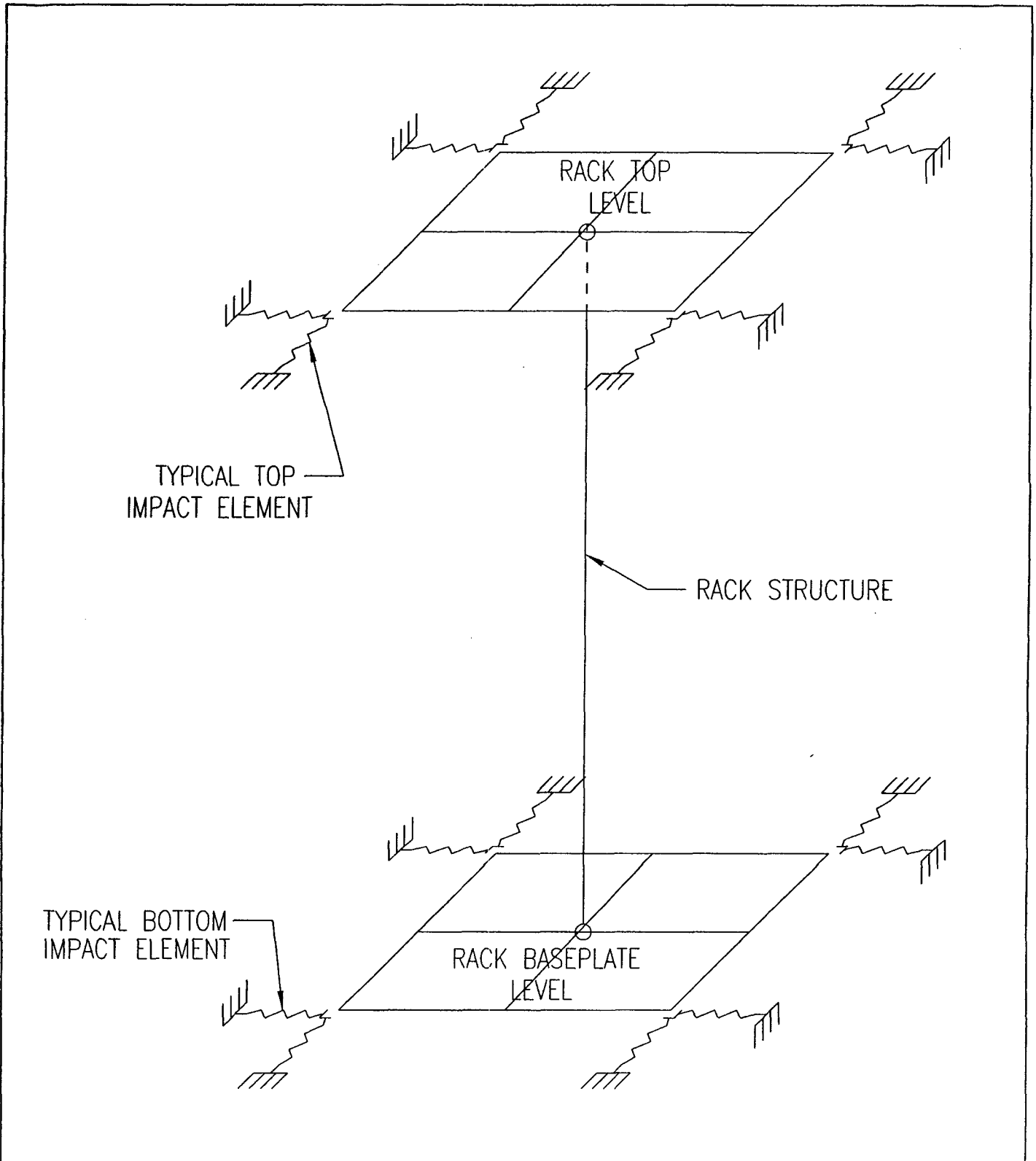


FIGURE 6.5.5; RACK PERIPHERY GAP/IMPACT ELEMENTS

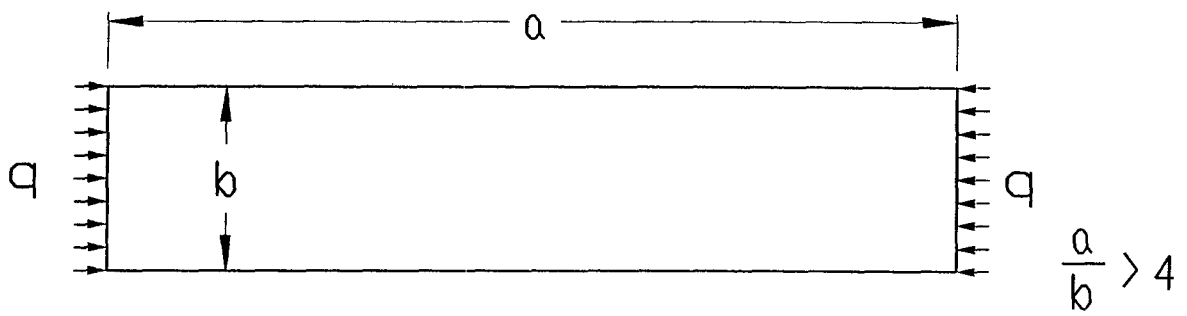


FIGURE 6.12.1; LOADING ON RACK WALL

## 7.0 STRUCTURAL INTEGRITY CONSIDERATIONS FOR THE FUEL POOL STRUCTURE

### 7.1 Introduction

This section summarizes structural integrity considerations for the Turkey Point Unit 3 & 4 fuel pools. The spent fuel structures in Units 3 and 4 are of similar design. Both pool structures are founded on grade and are designated as Seismic Category I. The inside dimensions of the spent fuel pool (SFP) of each unit are 41'-4" long by 25'-4" by 40'-0" high. The west, north, and east walls are 5'-6" thick from elevation 18'-0" to elevation 33'-0" and then change to a thickness of 3'-0" for the remainder of the height to elevation 58'-0". Both sections are flush on the side of the wall interior to the pool. This offsets the mid-planes of the lower and upper sections of the wall by 15". The south wall separates the SFP from the Transfer Canal and is 4'-0" thick over its entire 40' height. There are several walls and floors that laterally support the SFP walls.

The floor of the SFP varies in thickness. The thinnest portion is in the middle section of the pool and measures 3'-6" thick. The periphery of the pool has greater floor thickness, which measures 4'-6". The floor is supported by 19 feet of graded limestone fill that rests on bedrock. In what follows the term "pool structure" refers to both Units 3 and 4.

The pool structure at both units was recently evaluated [7.2.1] to assess the walls and floor for the proposed addition of a Region 1-style rack in the Cask Area of the SFP. The existing structures were shown to have satisfactory design margins. As discussed below, because this license amendment request does not involve an expansion of storage capacity at either unit, no new structural loadings are created.

In particular, the introduction of Metamic™ inserts into Region 2 racks will have a negligible effect on the existing pool structure, because the additional weight of inserts represents less than 0.1% of the gross weight on the pool slab. Since the bulk pool temperature is not affected by the addition of Metamic™ inserts, the thermal load cases, which represent a significant portion of the loading imposed on the structure, will not be changed. Therefore, a new structural evaluation of the Turkey Point 3 & 4 fuel pools is neither necessary nor warranted.

Specifically, the applicable load combinations for the pool structure are adapted from ACI-318 [7.2.3] and provided in Appendix 5A of the Turkey Point Units 3 and 4 UFSAR [7.2.2]. The governing load combinations evaluated for structural integrity are:

|                    |                          |
|--------------------|--------------------------|
| Load Combination 1 | $1.25*(D + E')$          |
| Load Combination 7 | $1.25*(D + E') + 1.0* T$ |
| Load Combination 8 | $1.25*D + 1.0* T$        |

In the above formulas:

- D = total dead load on the pool structure;
- T = thermal load from thru-thickness gradients and constraint of differential thermal expansion.
- E' = SSE earthquake induced loads combined in accordance with the UFSAR

The dead load (D) consists of the combined weight of the contained pool water, the fuel racks, the reinforced concrete mass and the stored fuel. Pool water mass is slightly reduced as a result of inventory displaced by the added Metamic inserts. Adding inserts to storage racks increases their mass by a minor amount. However, the preponderant component of dead weight (i.e., fuel and reinforced concrete mass) remains unchanged, so it follows that D remains essentially unchanged. A negligible change in the overall mass of the pool structure implies that the dynamic characteristics remain essentially unchanged, therefore the seismic excitation load E', likewise, is essentially unchanged.

Finally, because this license amendment request does not entail any change in the thermal-hydraulic parameters for the pool or the pool cooling system, the thermal gradient induced loadings, T, remain unchanged.

Therefore, it is concluded that the applicable factored loads on the pool structure remain unaltered, and the structural margins-of-safety computed in existing licensing bases remain applicable after Metamic™ inserts are installed in the Turkey Point fuel storage racks.

## 7.2 References

- [7.2.1] Technical Specification Amendment Request, transmitted under FPL Letter L-2002-214, dated November 26, 2002.
- [7.2.2] Turkey Point Units 3 and 4 UFSAR, latest revision.
- [7.2.3] ACI 318-63, Building Code Requirements for Reinforced Concrete, American Concrete Institute, Detroit, Michigan.

## 8.0 RADIOLOGICAL EVALUATION

### 8.1 Fuel Handling Accident

Crediting the presence of Metamic™ inserts as a replacement for Boraflex, in rack storage cells at Turkey Point, does not invalidate analysis of the fuel-handling accident, as currently described in the updated FSAR [8.6.1]. None of the parameters that affect dose, such as the depth of the pool water, the fission product inventory of stored fuel, distance to the site boundary, etc., have changed and hence a re-evaluation of fuel handling accidents is not warranted.

Handling Metamic™ inserts in the vicinity of fuel pool storage racks, such as will occur during the installation process, does not affect either the probability or the consequences of a fuel handling accident. Each insert weighs approximately 24 lbs, which is considerably less than the weight of a fuel assembly. Thus, any damage caused by dropping an insert onto fuel will be bounded by the damage that results from the limiting fuel assembly drop. Irradiated fuel and Metamic inserts will not be handled simultaneously; instead, each Metamic™ insert will be placed in its host cell after the resident fuel assembly has been seated. Insert design has been optimized to facilitate easy installation, without causing damage to rods or hardware in the co-resident fuel bundle. Also, the presence of inserts in the racks in no way adversely affects the response of a seated fuel assembly to impact by a dropped fuel assembly. The design basis radiological consequences of a fuel handling accident are determined based on non-mechanistic considerations.

### 8.2 Solid Radwaste

The installation and use of Metamic™ inserts in Turkey Point's spent fuel storage racks should not generate a significant amount of radwaste during routine plant operation. However, as Metamic inserts approach the end of their useful life, they could become classified as radioactive waste. Considering the insert's constituent materials and surface finish characteristics, it is possible that most inserts installed in fuel storage racks could be removed from the pool, decontaminated and disposed of as clean trash. Alternatively, inserts could be retained in the racks and disposed of as radioactive waste when the fuel pool or storage racks are decommissioned.

The initial installation campaign may dislodge some otherwise-settled crud/silt from fuel or from fuel storage racks, however, the amount of re-suspended material is expected to be no more than that created by a normal refueling. The installed fuel pool purification system is designed to remove suspended material, such as crud or silt, from the pool water column.

The frequency of ion exchanger resin replacement is determined primarily by the requirement for water clarity, and the resin is normally changed about once a year. Aside from the re-suspension of deposited crud or silt, there is no plausible mechanism by which the volume of solid radioactive wastes would be substantially increased due to the addition of Metamic™ inserts.

### 8.3 Gaseous Releases

Normally, the contribution from the fuel storage building is negligible compared to the other releases, and no significant increases are expected as a result of the addition of Metamic™ inserts.

### 8.4 Personnel Exposures

During normal operations, personnel on the working level of the fuel storage area are exposed to radiation from the spent fuel pool. The dose rates experienced by these personnel are not expected to increase due to the addition of Metamic™ inserts because the dose rate from the fuel in storage is negligible and Metamic™ does not constitute a new radiation source. The water column above stored irradiated fuel seated in the racks is sufficiently deep that the dose rate to personnel on the operating deck from that fuel is orders of magnitude lower than the dose rate from radionuclides in the pool water itself and the dose rate from an irradiated fuel assembly in transit.

Radionuclide concentrations in fuel pool water are not expected to increase significantly; these concentrations are determined principally from the mixing of primary system water with the pool water and the spalling of crud deposits from spent fuel assemblies as they are moved into the storage pool during refueling operations. The overall storage capacity of the pools is not being increased, and the amount of fuel movement required during any particular refueling evolution is independent

of the addition of Metamic™ inserts. No significant material spalling is expected following the installation of Metamic™ inserts, because the device is designed to make contact with the fuel assembly upper end fitting and grid straps rather than the fuel cladding.

Adding Metamic inserts to Turkey Point fuel storage racks does not change the dose rate caused by an irradiated fuel assembly in transit, as the relevant fuel parameters are not changed and the depth in water at which the assembly is transported has not changed.

At the depth of the fuel, the concrete walls of the fuel pool are 5.5 feet thick on three sides and 4 feet thick on the side facing the Transfer Canal. These walls provide sufficient shielding such that the maximum dose rate at the outside surface of the concrete, due to stored spent fuel, is 2 mrem/hr when the pool is assumed to be completely filled with irradiated fuel that has cooled for 24 hours. Shielding characteristics of these concrete walls will not be changed by the presence of Metamic™ inserts.

Operating experience has shown that there have been negligible concentrations of airborne radioactivity in the Fuel Handling Building, and no increases in the concentration of airborne radioisotopes are expected following the proposed storage rack enhancement. Job site monitoring by Health Physics personnel and the use of proven decontamination techniques ensure that there is no credible mechanism to cause an increase in airborne radioactivity during the installation campaign. Additionally, area monitors for airborne activity are available in the immediate vicinity of each fuel pool.

In summary, no increases in dose rates to operating personnel are expected following the Metamic™ insert installation campaign. Consequently, neither the current health-physics program nor the area monitoring system needs to be modified.

#### 8.5 Anticipated Exposures During the Addition of Metamic™ Inserts

All of the operations involved in the addition of Metamic™ inserts will utilize detailed procedures prepared with full consideration of ALARA principles. Similar operations have been performed in

numerous facilities in the past, including FPL's St. Lucie plant and there is every reason to believe that the addition of Metamic™ inserts can be safely and efficiently accomplished at Turkey Point, with minimum radiation exposure to plant personnel.

Total occupational exposure for the operations required to perform the initial installation of Metamic™ panels is estimated to be between 5 and 7 person-rem per Unit, as shown in Table 8.1. While individual task efforts and exposures may differ from those in Table 8.1, the total is believed to be a reasonable estimate for planning purposes.

As noted earlier, the existing radiation protection program implemented at the plant is judged adequate to control Metamic™ insertion operations. As required by the plant's radiation protection program, where there is a potential for significant airborne activity, continuous air samplers will be in operation. Personnel will wear protective clothing and, if necessary, respiratory protective equipment. Activities will be governed by Radiation Work Permits, and personnel monitoring equipment will be issued to each individual. The desirability of continuous Health Physics monitoring during critical evolutions will be evaluated. Work tasks, area access, and the movement of equipment will be monitored and controlled to minimize contamination and to assure that personnel exposures are maintained ALARA.

## 8.6 References

[8.6.1] Turkey Point Units 3 & 4 Updated Final Safety Analysis Report, latest version.

| <b>Table 8.1</b>  |                                    |              |  |
|---|------------------------------------|--------------|--|
| <b>PRELIMINARY ESTIMATE<sup>1</sup> OF PERSON-REM EXPOSURES<br/>DURING METAMIC INSERTION &amp; RELATED ACTIVITIES</b> |                                    |              |  |
| <u>Operation</u>  | <u>Number<br/>of<br/>Personnel</u> | <u>Hours</u> | <u>Estimated<br/>Person-Rem<br/>Exposure</u> |
| Initial Fuel Shuffle <sup>2</sup>   | 3                                  | 250          | 1.875 to 2.625                               |
| Installation of Metamic <sup>TM</sup> Inserts (500 Inserts)   | 4                                  | 250          | 2.5 to 3.5                                   |
| Final Fuel Shuffle <sup>3</sup>   | 3                                  | 50           | 0.375 to 0.525                               |
| TOTAL PERSON-REM EXPOSURE (per Unit)  |                                    |              | 4.75 to 6.65                                 |

<sup>1</sup> estimates will be refined during the process of engineering required implementation activities

<sup>2</sup> based on repositioning 500 irradiated fuel assemblies

<sup>3</sup> assumes a final fuel shuffle of approximately 100 assemblies

## 9.0 INSTALLATION AND OPERATION

Although the Metamic™ inserts are light in weight (less than 25 lbs), small in size (enveloped in a 8.75" square by 152" long parallelepiped) and uncomplicated in geometry, a summary of their design and operational considerations is provided in this section to elucidate safety and ALARA attributes of the proposed modification.

### 9.1 Metamic™ Insert Installation and Handling

With the exception of the Cask Area rack, Metamic™ inserts are designed to be installed in any cell of the existing Spent Fuel Pool racks. However, as discussed in Section 4.0, the inserts are only credited as neutron absorbers when installed in the Region 2 style racks. Section 4.0 also discusses the fuel and insert configurations evaluated for various storage patterns.

The inserts will be initially introduced and installed in the storage racks using the fuel bridge and the same lifting paths as are used to bring new fuel into the pool. A installation tooling will be used to lift, carry, and install the inserts. Lifting the Metamic™ insert will be accomplished by engaging the installation tool at the top of the insert.

The installation tool provides three lifting pawls at the bottom of the tool; each is inserted into one of the lift locations situated at the top of the Metamic™ insert. The pawls are configured to be inserted and then rotated 90 degrees to ensure positive engagement with the insert. Rotation is accomplished by a mechanism at the top of the installation tool that also provides visual indication of the position of the pawls. Thus, design features of the lifting mechanism ensure that the position of the pawls are correctly oriented for the installation tool engagement/disengagement and for the actual hoisting processes. Once engaged in the insert, the installation tool provides lateral, vertical, and radial control. In addition, the tool provides the rigidity necessary to apply vertical force to install the insert.

The combined load of the installation tool and the Metamic™ insert hangs vertically, due to the location of the lifting point. This ensures that the Metamic™ insert can be easily placed in any storage cell that contains a fuel assembly. The position of the insert's landing area on top of the fuel assembly and the

configuration of the installation tool will be visually verifiable from the fuel bridge. This permits an unambiguous confirmation of the orientation of any Metamic™ insert.

The insert panel length is selected to ensure that the active fuel region is covered by the neutron absorber upon insertion and seating at the top of the assembly, except for the bottom 6 inches. This 6 inch offset is considered in the criticality evaluation discussed in Section 4.0 and was chosen to avoid interference between insert panels and the lower grid strap. The vertical location of the top of the insert provides easy visual indication that the insert is seated properly and resting on the fuel assembly. This visual indication, coupled with the physical contact resistance, provides assurance that the insert is correctly positioned to provide neutron attenuation.

The differences between nominal fuel assembly dimensions (8.426 inches square) and the inside dimension of a Region 2 storage cell (8.80 inches square) provide a sufficient gap (0.374 inches nominal) for the 0.073 inch thick Metamic™ panels to be easily inserted. The base of each panel is skew cut and beveled to ensure that the panels will readily slide into this gap and not snag on any fuel rods, grid straps or other assembly hardware.

## 9.2 Operation

The Metamic™ inserts are passive devices that perform their neutron attenuation function by their mere presence at the proper location in the fuel storage cell. Inserts contain no moving parts, mechanical or electrical devices credited for neutron absorption or to promote longevity. However, the inserts do experience mechanical loads during movement and seismic conditions. The capability of the inserts to withstand these loads has been evaluated and a summary of the evaluation is discussed below.

### 9.2.1 Seismic Loads

Metamic™ inserts are subjected to loads during the seismic events postulated for the Turkey Point plant. During these events, the fuel assembly rattles within the storage cell and consequently, it impacts the insert and the inside of the cell wall. This amplitude of motion and the corresponding impact loads are reduced with an insert in place within the storage cell, due to a reduction in free space available to the fuel assembly. Loads on rack storage cell walls have been re-evaluated to quantify the fuel assembly's seismically-induced impacts, both with and without consideration of Metamic™ inserts, as discussed in Section 6.9.3. The Metamic™ inserts have also been evaluated for the impact load of a fuel assembly. As stated in Section 6.8.4.2, the maximum seismic impact load that could be experienced by an insert has been determined from the DYNARACK rack seismic/structural simulations to be 310 lbs. The Metamic™ inserts have been shown to be able to withstand this loading with a factor of safety of more than four.

Based on the small clearances between the fuel assembly, cell wall, and the Metamic™ insert, there is no significant risk of vertical motions temporarily displacing an insert above its seated position. Since the upward seismic accelerations do not exceed gravity (i.e., 1.0g), inserts are expected to remain seated and have a vertical displacement consistent with the adjacent rack and fuel assembly. However, even if differential motion could occur, each individual insert would move independently of the inserts stored in adjacent cells, yielding random (i.e., chaotic) changes in vertical position. In other words, the presence of unseated inserts would likely be a localized, temporary (i.e., until they could be re-seated in their storage location) phenomenon, not global throughout all rack cells. Cumulatively, these displacements would not be expected to uncover a significant portion of the active fuel region. The corresponding change in reactivity of the stored fuel array would be less than the effects already quantified for the misplaced or misloaded fuel assembly events discussed in Section 4.6.13.4.

### 9.2.2 Movement Loads

The Metamic™ inserts are also subjected to loads during lifting, insertion, and travel through the pool, due to frictional drag forces.

### 9.2.2.1 Insertion/Withdrawal Loads

The insertion and removal forces experienced by the inserts produce axial compression or tension stresses along the long axis of the insert. FPL has imposed a maximum value of 150 lbs on the insertion and withdrawal load (after considering the tool and insert weights). This maximum load will be monitored by the crane operator during installation. Exceeding this load limit will prompt the operator to stop and determine the cause of the problem and implement corrective actions.

The weight of the insert is approximately 24 lbs and the weight of the tool is less than 150 lbs. The combined weight of less than 200 lbs is far below the weight (approximately 2,000 lbs) of an individual fuel assembly and its handling tool. Therefore, a re-evaluation of the fuel bridge loads while handling an insert is not necessary. Likewise, re-evaluation of the fuel assembly accidents is not necessary, because a fuel assembly is a bounding load.

### 9.2.2.2 Horizontal Movement Loads

The forces on an insert while traveling through the pool water result from the drag of the insert passing horizontally through the pool water medium. The applied force is a function of the velocity and surface area of the insert and the maximum force has been determined from an evaluation of the forces developed at the highest speed of the fuel bridge. The applied force is experienced as stresses along the Metamic™ panels, and at lift locations and welds (if welded). These components have been evaluated for the corresponding stresses and have been determined to have satisfactory design margins.

Operational loads have been quantitatively determined for all possible in-service and movement scenarios. Both the Metamic™ inserts and their installation tool have been evaluated and both are shown to be adequate to withstand the operational loads experienced during seismic events, insert handling, installation, and removal.

### 9.3 Safety, Health Physics, and ALARA Methods

#### 9.3.1 Safety

During the installation and manipulation of the Metamic™ inserts, personnel safety is of paramount importance. All work shall be carried out in compliance with applicable approved procedures.

#### 9.3.2 Health Physics

Health Physics monitoring and the related controls on performing work tasks in the Turkey Point Radiation Control Area (RCA) are implemented consistent with requirements of the site Radiation Protection Program. All work in the vicinity of or within the Spent Fuel Pool is performed as directed by the applicable Radiation Work Permit (RWP). Additional procedures, such as those controlling Foreign Material Exclusion (FME), hot particles, and fuel movement will be used to maintain personnel exposures ALARA, to ensure configuration control and to ensure safe implementation of the storage rack enhancement project.

#### 9.3.3 ALARA

The key factors in maintaining project dose As Low As Reasonably Achievable (ALARA) are time, distance, and shielding. These factors are influenced by many mechanisms with respect to project planning and execution.

##### Time

Each member of the project team will be trained and provided with an appropriate understanding of critical evolutions. Additionally, daily pre-job briefings are employed to acquaint each team member with the scope of work to be performed and the proper means of executing such tasks. Such pre-planning devices reduce worker time within the radiological controlled area and therefore, project dose.

## Distance

Remote tooling such as lift fixtures and a lift rod disengagement device have been developed to execute numerous activities from the SFP surface, where dose rates are relatively low.

## Shielding

During the course of the Metamic™ insert project, primary shielding is provided by the water in the Spent Fuel Pool. The water column between an individual above the surface and a submerged irradiated fuel assembly is an essential shield that reduces personnel dose. Additionally, other shielding may be employed to reduce exposure when work is performed around high dose rate sources. If necessary, additional activity specific shielding may be utilized to meet ALARA principles.

### 9.4 Radwaste Material Control

Radioactive waste generated during the Metamic™ insert installation campaign will be controlled in accordance with established Turkey Point procedures. Only small quantities of liquid, gaseous, and solid radwaste should be generated by the installation process, based on FPL's experience with similar activities at St. Lucie, and because no plant components are being permanently removed from the SFP.

As noted elsewhere in this report, if decontamination techniques supporting their free-release are unsuccessful, some fraction of the installed Metamic™ inserts may be classified as radioactive waste upon decommissioning of the Turkey Point Fuel Handling Building or upon disposal of the currently-installed spent fuel storage racks.

## 10.0 ENVIRONMENTAL AND COST / BENEFIT ASSESSMENT

### 10.1 Introduction

Article V of the USNRC OT Position Paper [10.7.1] requires submittal of a cost/benefit analysis for fuel storage capacity enhancement projects. Although the licensed pool storage capacity at Turkey Point is not being increased, information requested in this portion of the Position Paper is provided by the material summarized in this section. This material provides justification for selecting the installation of Metamic™ inserts in the Turkey Point spent fuel storage racks as the most cost effective alternative to maintain continued use of all fuel storage locations, without reliance on Boraflex.

### 10.2 Imperative for Metamic™ Inserts

The criticality analysis of record for the existing storage racks at each unit credits the presence of Boraflex, and also credits a portion of the soluble boron present during normal operating conditions. Due to continuing dissolution of Boraflex, some spent fuel storage locations have become significantly degraded. The margin to the analyzed amount of allowed dissolution has become a cause for immediate concern and significant numbers of storage locations may become unavailable for fuel storage in the near future, unless fuel pool soluble boron concentrations greater than those currently approved for use are credited. In rare instances, control rods (RCCAs) could be used to recover degraded cells by requiring the presence of an RCCA in the stored assembly, when an RCCA is available. The specific need to recapture licensed storage capacity in the SFP is based on the continually increasing inventory of irradiated fuel, the prudent requirement to maintain full-core offload capability, and a lack of viable economic alternatives.

### 10.3 Appraisal of Alternative Options

The key considerations in evaluating the alternative options included:

- Safety: Minimize the risk to the public and to plant personnel.
- Economy: Optimize capital and O&M expenditures.

- Security: No degradation of protection from potential saboteurs or natural phenomena.
- Ease of Implementation: Minimize required modifications to existing plant systems.
- Maturity: Extent of industry experience with the technology and implementation protocol.
- ALARA: Minimize cumulative dose.
- Interface with Future Fuel Storage Plans: How will this activity affect implementation of on-site dry storage or the shipment off-site of spent nuclear fuel (SNF)?
- Effectiveness: Likelihood that implementing the proposed modification will fully resolve issues with reactivity control in fuel storage racks.

The four options that were considered are (i) no action, (ii) rod consolidation, (iii) spent fuel pool reracking and (iv) dry fuel storage. Section 10.3.1 summarizes the anticipated costs for each option. Other options such as Modular Vault Dry Storage or a new spent fuel storage pool were judged overly expensive and more complex than necessary at this point in time. Furthermore, due to the complexity of implementation, some of these options could not meet the required schedule for extending full-core offload capability.

(i) No Action Option

The no action alternative is simply what is stated, no advance remedy is implemented to address the potential consequences of future Boraflex degradation. The current criticality analysis credits the presence of Boraflex, in its degraded state, and credits part of the available soluble boron during normal operation. As a result of future fuel discharges and degradation of the Boraflex material, stored fuel would eventually need to be configured in a checkerboard pattern of 2 assemblies per 4 cell array. Due to the reduced fuel pool storage capacity this checkerboard configuration could not accommodate all irradiated Turkey Point fuel. The imminent de-rate of fuel storage capacity would require a dry fuel storage program to be implemented as quickly as possible to relieve fuel pool storage congestion and permit continued operation of the units. Contemporaneously, interim credit for additional fuel pool soluble boron could be taken, following the guidance of NRC Generic Letter 91-18. From this point forward, Turkey Point would in essence rely on dry storage casks to maintain the spent fuel pool inventory at levels conducive to continued plant operation.

(ii) Rod Consolidation Option

Rod consolidation involves disassembly of a fuel bundle, the removal of fuel rods and subsequent disposal of the fuel assembly skeleton outside the pool. The rods are stored in stainless steel cans having the approximate outer dimensions of a fuel assembly. Each can is stored in the spent fuel racks. The top of the can has an end fixture that matches up with the spent fuel handling tool. This permits repositioning the cans when necessary.

Rod consolidation pilot project campaigns in the past have utilized underwater tooling that is manipulated by an overhead crane and operated by a maintenance worker. Historically, rod removal has been a slow process.

The principal advantages of this technology are: the ability to increase storage capacity in small increments, moderate cost per unit of incremental storage, no need of additional land and no additional required surveillance. The disadvantages are: the potential release of gap fission product inventory as a result of rod breakage due to handling, a potential for increased fuel clad corrosion due to localized loss of the protective oxide layer, potential interference of a prolonged consolidation campaign with ongoing plant operation, and insufficient industry experience. At the present time, there is no ongoing research to make rod consolidation a practical option for the nuclear industry. It is FPL's view that rod consolidation technology is insufficiently mature to represent a viable option for the present Turkey Point SFP limitations.

(iii) Spent Fuel Pool Reracking Option

Removal of all existing Turkey Point fuel storage racks, aside from the Cask Area racks, would allow the installation of replacement racks having more advanced design and containing improved neutron absorber material. However, reracking of both Turkey Point spent fuel pools would be a costly undertaking. Due to the design of the spent fuel pool area, the fuel handling building, and overhead crane, in combination with the fuel inventories in both units, the logistics involved with handling fuel, removing contaminated racks and installing new racks present significant challenges. In addition, there would be an enormous amount of radwaste generated from the reracking campaign. Finally, personnel

radiation exposures would be significant due in part to the volume of contaminated racks and their required handling and packaging.

(iv) On-Site Dry Cask Storage Option

Dry cask storage of irradiated fuel is the only practical alternative to the Metamic™ insert installation campaign contemplated for the plant. Dry storage has been successfully implemented at numerous sites and the technology involved is considered to be mature and relatively risk free. Most plants pursuing dry storage have opted for the so-called multi-purpose canister (MPC) technology under general certification (10CFR72, Subpart K). Using this approach, the MPCs are certified for on-site storage as well as for off-site transport. Thus, fuel, once loaded into MPCs, does not have to be handled again.

For Turkey Point style fuel (i.e., Westinghouse 15x15 rod lattice), the currently available MPCs hold up to 32 fuel assemblies in each canister. Dry storage implementation, however, requires a large up front capital outlay, and an extensive set of plant modifications. Among the required modifications are:

- (i) tap-ins to the plant's gaseous waste processing system,
- (ii) making chilled water available to support vacuum drying of the spent fuel cask,
- (iii) piping to return cask water back to the Spent Fuel Pool/Fuel Cask Storage Pool, and
- (iv) upgrade of the cask handling crane.

An important-to-safety concrete pad would be needed to store the loaded casks. The pad requires security fences, exclusion zone monitoring, a diesel generator for emergency power and video surveillance for the duration of fuel storage, which may extend beyond the life of the plant.

Dry storage projects require between four and five years to implement. Because of the magnitude and cost of its undertaking, nuclear power plants seldom resort to dry storage until the maximized in-pool capacity is projected to be insufficient to maintain a prudent wet storage reserve. The presence of Boraflex in Turkey Point's spent fuel racks further challenges in-pool storage projections and capabilities. As a result, loading additional dry storage casks could become necessary as a means to offset storage limitations in the spent fuel pool introduced by Boraflex. These spent fuel pool storage limitations are discussed above as part of the no action option. Finally, as the cost summary in the

following subsection indicates, dry storage is estimated to be an order of magnitude more expensive than the Metamic™ insert option.

### 10.3.1 Alternative Option Cost Summary

An estimate of relative costs in 2005 dollars for the aforementioned options is provided in the following:

|                                       |                               |
|---------------------------------------|-------------------------------|
| Installation of Metamic™ Inserts:     | \$7 million                   |
| No Action:                            | Comparable to Dry Storage     |
| Rod Consolidation of all stored fuel: | \$100 million (estimate)      |
| Spent Fuel Pool Reracking             | \$30 million (for both Units) |
| Dry Storage Metal cask (MPC):         | \$40-60 million               |

The above estimates are consistent with estimates by EPRI and others [10.7.2, 10.7.3].

To summarize, based on the required short time schedule, the continuing degradation of Boraflex, and the costs of technically-viable alternatives, the most acceptable alternative for retaining the on-site licensed spent fuel storage capacity at Turkey Point involves the installation of Metamic™ inserts.

### 10.4 Cost Estimate

The plant modification proposed for the Turkey Point Unit 3 and 4 fuel pools contemplates the use of Metamic™ inserts in the existing Boraflex-poisoned spent fuel racks.

The total capital cost is estimated to be approximately \$3 million. Installation campaign, overhead and on-going surveillance costs applicable to Metamic™ inserts are estimated to be \$4 million.

As described in the preceding section, other fuel storage expansion technologies were evaluated prior to deciding on the use of the Metamic™ solution. The installation of Metamic™ inserts provides cost, ALARA, and schedule advantages over other options.

## 10.5 Resource Commitment

The installation of Metamic™ inserts in the SFP is expected to require the following primary resources per Unit:

Aluminum: 5 tons

Boron Carbide: 7 tons

The requirements for boron carbide and aluminum represent a small fraction of total world output of these metals (less than 0.001%). Therefore, the raw materials for this project will have a miniscule effect on their availability in the world market.

## 10.6 Environmental Considerations

The proposed installation of Metamic™ inserts does not result in any additional heat load burden to the Spent Fuel Pool Cooling and Cleanup System because the inventory of stored spent fuel is not being increased. The maximum bulk pool temperature will be limited to less than 150°F under normal refueling scenarios. Refer to Section 5.0 for a more detailed discussion of the thermal-hydraulic evaluations performed to support the addition of Metamic™ inserts.

The heat load represented by the decay heat of discharged fuel assemblies remains unchanged. Therefore there will be no additional load on the Fuel Building HVAC system capacity. Thus, the change does not necessitate any hardware modifications for the HVAC system. Therefore, the environmental impact resulting from this change is negligible and is less than the environmental impact of any other option evaluated.

## 10.7 References

[10.7.1] OT Position Paper for Review and Acceptance of Spent Fuel Storage and Handling Applications, USNRC (April 1978).

[10.7.2] Electric Power Research Institute, Report No. NF-3580, May 1984.

- [10.7.3] Singh, K.P., "Spent Fuel Storage Options: A Critical Appraisal", Power Generation Technology, Sterling Publishers, pp. 137-140, U.K. (November 1990).